

**DEVELOPMENT OF NOVEL SORBENTS FOR  
SPECIATION OF INORGANIC AND ORGANIC  
SELENIUM PRIOR TO DETERMINATION BY  
ATOMIC SPECTROMETRIC TECHNIQUES**

**A Thesis Submitted to  
the Graduate School of Engineering and Sciences of  
İzmir Institute of Technology  
in Partial Fulfillment of the Requirements for the Degree of**

**MASTER OF SCIENCE  
in Chemistry**

**by  
Merve DEMİRKURT**

**July 2011  
İZMİR**

We approve the thesis of **Merve DEMİRKURT**

---

**Prof. Dr. Ahmet E. EROĞLU**  
Supervisor

---

**Prof. Dr. Emür HENDEN**  
Committee Member

---

**Prof. Dr. F. Nil ERTAŞ**  
Committee Member

---

**Assoc. Prof. Dr. Durmuş ÖZDEMİR**  
Committee Member

---

**Assoc. Prof. Dr. Mustafa M. DEMİR**  
Committee Member

---

**Prof. Dr. Serdar ÖZÇELİK**  
Head of the Department of Chemistry

---

**Prof. Dr. Durmuş Ali Demir**  
Dean of the Graduate School of  
Engineering and Science

## ACKNOWLEDGEMENTS

I would like to acknowledge the help of many people during my study. Firstly I would like to express my thanks to my advisor Prof.Dr. Ahmet E. EROĞLU for his guidance, care and freedom that he provided me throughout the study. One simply could not wish for a better or friendlier supervisor. I am also grateful to my co-advisor Assoc. Prof.Dr. Mehtap EMİRDAĞ EANES and Assist.Prof. Dr. Ali ÇAĞIR for valuable discussions and giving me opportunity to study in their laboratory.

I also would like to thank to other members of the thesis committee, Prof.Dr. Emür HENDEN, Prof.Dr. Nil ERTAŞ, Assoc.Prof.Dr. Durmuş ÖZDEMİR and Assoc.Prof.Dr. Mustafa M. DEMİR for their valuable comments and suggestions. I also thank to Assoc.Prof.Dr. Talal SHAHWAN for his encouragement and support.

I would like to extend my sincere thanks to Dr. Hüseyin ÖZGENER for providing help on elemental analysis, to the research scientists at the Center for Materials Research (IZTECH) for their help on facilities TGA, XRD and SEM, and also to the research scientists at the Environmental Research Centre for ICP-MS analyses. I would like to thank to TÜBİTAK and BAP for financial support.

Thanks to my colleagues and Analytical Chemistry Research Group lab mates for their support and positive input. I deeply thank to my sister Ezel BOYACI who shared her ideas with me all the time. I would also like to thank my other elder sisters, Meral KARACA, Arzu ERDEM, Özge TUNUSOĞLU, Ayşegül ŞEKER ERDOĞAN, Müşerref YERSEL, Semira ÜNAL YEŞİLLER.

Special thanks to all my friends in IZTECH especially Banu ÖNEN, Doğan TAÇ, Taylan MEŞİN, Mithat BOZ and Hüseyin İLGÜ for their moral support and everything. They have made my school life much more enjoyable than it would have otherwise been.

My deepest gratitude goes to my lovely blood-sis Esen DÖNERTAŞ for her encouragement and never ending friendship. School, work, even life would not have been meaningful without her. I am so lucky to have such best friend.

And last, I wish to thank all of my family, Zeytin and my little frog for the support they have given. I dedicate this thesis to my brother Dr. Erkan DEMİRKURT.

## ABSTRACT

### DEVELOPMENT OF NOVEL SORBENTS FOR SPECIATION OF INORGANIC AND ORGANIC SELENIUM PRIOR TO DETERMINATION BY ATOMIC SPECTROMETRIC TECHNIQUES

Selenium is an essential trace element for plants, animals and the human body. However, its possible toxicity at high concentrations necessitates the development of analytical methods for the separation and determination of the several forms of the element in environmental and biological systems.

In the first part of the study, commercially available and newly synthesized ceria ( $\text{CeO}_2$ ) and zirconia ( $\text{ZrO}_2$ ) were used for the sorption and speciation of inorganic selenium. Sorption parameters were investigated for both sorbents for selenite ( $\text{Se(IV)}$ ) and selenate ( $\text{Se(VI)}$ ) and the optimized parameters were determined to be  $25^\circ\text{C}$  for sorption temperature, 50.0 mg for sorbent amount, 30 min for shaking time for 20.0 mL of  $100.0 \mu\text{gL}^{-1}$  of both species. The release of  $\text{Se(IV)}$  and  $\text{Se(VI)}$  from the sorbents was realized using two eluents, 0.10 M NaOH and 0.10 M  $\text{NH}_4\text{Cl}$ , respectively. The accuracy of the proposed methodology was verified with spike recovery tests for various water types spiked with  $10.0 \mu\text{gL}^{-1}$  and  $100.0 \mu\text{gL}^{-1}$   $\text{Se(IV)}$  and  $\text{Se(VI)}$ . Spike recovery values were determined to range between 91% and 97% at  $10.0 \mu\text{gL}^{-1}$  level, and between 97% and 113% at  $100.0 \mu\text{gL}^{-1}$  level, for ceria and zirconia, respectively. Moreover, the sorption efficiencies of the newly synthesized sorbents were compared with those of the commercial sorbents. Ceria and zirconia were shown to be applied in the speciation of inorganic selenium.

Sorption studies with nZVI-modified zirconia have demonstrated that the sorbent can be utilized for the speciation of inorganic and organoselenium; namely,  $\text{Se(IV)}$ ,  $\text{Se(VI)}$ , Seleno-L-cystine and Seleno-DL-methionine.

In the final part of the study, it was shown by column-type equilibration studies that alginate beads modified/immobilized with  $\text{CeO}_2$  or  $\text{ZrO}_2$  through three different synthesis routes can be used for the sorption and speciation of inorganic selenium.

## ÖZET

### İNORGANİK VE ORGANİK SELENYUMUN ATOMİK SPEKTROMETRİK TEKNİKLERLE TAYİNİ ÖNCESİ TÜRLENDİRİLMESİ İÇİN YENİ SORBENTLERİN GELİŞTİRİLMESİ

Selenyum, bitkiler, hayvanlar ve insan vücudu için gerekli bir eser elementtir. Ancak, yüksek derişimlerdeki olası zehirliliđi, çevresel ve biyolojik sistemlerdeki çeşitli formlarının ayrılması ve belirlenmesi için analitik yöntemlerin geliştirilmesini gerektirir.

Çalışmanın birinci bölümünde, ticari ve bu çalışmada sentezlenen serya ( $\text{CeO}_2$ ) ve zirkonya ( $\text{ZrO}_2$ ), inorganik selenyumun sorpsiyonu ve türlendirilmesinde kullanılmıştır. Her iki sorbent için sorpsiyon parametreleri incelenmiş ve 20,0 mL 100,0  $\mu\text{gL}^{-1}$  Se(IV) ve Se(VI) için 25°C sorpsiyon sıcaklığı, 50,0 mg sorbent miktarı, 30 dk çalkalama süresi optimum değerler olarak belirlenmiştir. Se(IV) ve Se(VI), kullanılan sorbentlerden, sırasıyla 0,10 M NaOH ve 0,10 M  $\text{NH}_4\text{Cl}$  ile desorbe edilmiştir. Önerilen metodun kesinliđi çeşitli sulara 10,0  $\mu\text{gL}^{-1}$  ve 100,0  $\mu\text{gL}^{-1}$  seviyelerinde Se(IV) and Se(VI) standart katma/geri alma testleriyle gösterilmiştir. Serya ve zirkonya için elde edilen değerlerin, 10,0  $\mu\text{gL}^{-1}$  seviyesinde % 91 ve % 97, 100,0  $\mu\text{gL}^{-1}$  seviyesinde ise % 97 ve % 113 arasında deđiştii bulunmuştur. Ayrıca, yeni sentezlenen sorbentlerin sorpsiyon verimi ticari sorbentlerin sorpsiyon verimiyle karşılaştırılmıştır. İnorganik selenyumun türlendirilmesi için serya ve zirkonyaya başvurulabileceđi gösterilmiştir.

nZVI ile modifiye zirkonya ile yapılan sorpsiyon çalışmaları, anılan sorbentin inorganik ve organoselenyum, yani Se(IV), Se(VI), Seleno-L-cystine and Seleno-DL-methionine türlendirilmesinde kullanılabileceđini göstermiştir.

Çalışmanın son bölümünde, üç farklı metotla sentezlenen  $\text{CeO}_2$  veya  $\text{ZrO}_2$  ile modifiye/immobilize aljinat küreciklerinin kolon tipi denge çalışmalarında inorganik selenyumun sorpsiyonu ve türlendirilmesinde kullanılabileceđi belirlenmiştir.

# TABLE OF CONTENTS

LIST OF FIGURES .....	vii
LIST OF TABLES.....	xi
CHAPTER 1. INTRODUCTION .....	1
1.1. Significance of Selenium .....	1
1.2. Selenium Species in the Environment and in Biological Systems .....	2
1.3. Bioavailability of Selenium .....	5
1.4. Selenium Determination Methods .....	6
1.5. Speciation of Inorganic and Organic Selenium .....	7
1.6. Solid Phase Extraction .....	9
1.7. Solid Sorbents .....	11
1.7.1. Cerium Oxide .....	11
1.7.2. Zirconium Oxide .....	14
1.7.3. Nanoscaled Zero-Valent Iron (nZVI) .....	15
1.7.4. Alginate .....	17
1.8. Aim of This Work.....	19
CHAPTER 2. EXPERIMENTAL.....	20
2.1. Instrumentation and Apparatus .....	20
2.2. Reagents and Solutions .....	23
2.3. Aqueous Calibration Plot.....	27
2.4. Synthesis of Sorbents.....	27
2.4.1. Synthesis of CeO <sub>2</sub> and ZrO <sub>2</sub> Particles .....	27
2.4.2. Synthesis of Nanoscaled Zero-Valent Iron (nZVI) and nZVI Modified ZrO <sub>2</sub> .....	30
2.4.3. Synthesis Alginate Beads Immobilized with CeO <sub>2</sub> and ZrO <sub>2</sub> Particles.....	31
2.4.3.1. Synthesis of Alginate beads.....	32
2.5. Sorption Studies .....	34
2.5.1. Studies Utilizing Commercially Available CeO <sub>2</sub> and ZrO <sub>2</sub> .....	34

2.5.2. Sorption Studies Using Synthesized CeO <sub>2</sub> and ZrO <sub>2</sub> (Sol-gel and Hydrothermal Methods).....	39
2.5.3. Studies Utilizing nZVI and nZVI-Modified ZrO <sub>2</sub> .....	39
2.5.4. Studies Utilizing Strong Ion Exchanger Amberlite IR-120 Resin ..	40
2.5.5. Sorption studies of Alginate beads immobilized with CeO <sub>2</sub> and ZrO <sub>2</sub> particles .....	40
 CHAPTER 3. RESULTS AND DISCUSSION.....	 41
3.1. Characterization of the Sorbents.....	41
3.1.1. Commercial CeO <sub>2</sub> and ZrO <sub>2</sub> .....	41
3.1.2. Synthesized CeO <sub>2</sub> and ZrO <sub>2</sub> .....	42
3.1.3. Nanoscaled Zero-Valent Iron and (nZVI) Modified ZrO <sub>2</sub> .....	45
3.1.4. CeO <sub>2</sub> and ZrO <sub>2</sub> Modified Alginate Beads.....	47
3.2. Calibration Plots.....	55
3.2.1. Calibration Curves for Se(IV) ,Se(VI), SeCys and SeMet Using ICP-MS .....	55
3.2.2. Calibration Curves for Se(IV) Using HGAAS .....	56
3.3. Sorption and Speciation Studies .....	57
3.3.1. Studies with Commercial CeO <sub>2</sub> and ZrO <sub>2</sub> .....	57
3.3.2. Sorption Studies of Sol-gel and Hydrothermal Synthesized CeO <sub>2</sub> and ZrO <sub>2</sub> .....	75
3.3.3. Sorption Studies Utilizing ZVI and nZVI-Modified ZrO <sub>2</sub> .....	76
3.4. Sorption Studies Utilizing Cation Exchanger Resin (IR-120).....	79
3.5. Sorption studies CeO <sub>2</sub> and ZrO <sub>2</sub> alginate beads .....	80
 CHAPTER 4. CONCLUSION .....	 85
 REFERENCES .....	 85

# LIST OF FIGURES

<b>Figure</b>	<b>Page</b>
Figure 1.1. pe-pH diagram of selenium at 25 °C. ....	4
Figure 1.2. Schematic illustration of the SPE modes .....	10
Figure 1.3. SEM image of three-dimensional (3D) flowerlike CeO <sub>2</sub> micro/nanocomposite structure. ....	13
Figure 1.4. High-magnification (b) SEM image and (c). TEM image of the CeO <sub>2</sub> . ....	13
Figure 1.5. The core-shell structure of nZVI. ....	16
Figure 1.6. The structure of sodium alginate. ....	17
Figure 1.7. Schematic representation of the "egg-box" model of alginate gel. ....	18
Figure 2.1. Segmented Flow Injection HGAAS system used in selenium determinations. ....	21
Figure 2.2. Schematic representation of an autoclave with its parts. ....	22
Figure 2.3. Apparatus used in the synthesis of the sorbents. ....	28
Figure 2.4. Block diagram of the procedure used during the synthesis. ....	29
Figure 2.5. Apparatus used in the synthesis of ZVI-modified ZrO <sub>2</sub> . ....	31
Figure 2.6. Pathway of the synthesis, (a) Method A (b) Method B (c) Method C. ....	32
Figure 3.1. Typical SEM images of Ceria (a) and Zirconia (b). ....	41
Figure 3.2. Effect of pH on zeta potential of (a) CeO <sub>2</sub> and (b) ZrO <sub>2</sub> . ....	42
Figure 3.3. Typical SEM images of CeO <sub>2</sub> obtained through (a) sol-gel synthesis and (b) hydrothermal synthesis. ....	43
Figure 3.4. Typical SEM images of ZrO <sub>2</sub> obtained through (a) sol-gel synthesis and (b) hydrothermal synthesis. ....	44
Figure 3.5. XRD patterns of CeO <sub>2</sub> . ....	44
Figure 3.6. XRD pattern of ZrO <sub>2</sub> . ....	45
Figure 3.7. SEM images and XRD pattern of (a) nZVI, (b) ZrO <sub>2</sub> ve (c) nZVI-ZrO <sub>2</sub> . ....	46
Figure 3.8. Effect of pH on zeta potential of (a) nZVI and (b) nZVI-ZrO <sub>2</sub> . ....	47
Figure 3.9. SEM images of CeO <sub>2</sub> -based alginate beads obtained by (a) Method A, (b) Method B, and (c) Method C. ....	48
Figure 3.10. XRD graphs of CeO <sub>2</sub> -based alginate beads obtained by (a) Method A, (b) Method B, and (c) Method C. ....	49



Figure 3.11. SEM images of ZrO <sub>2</sub> -based alginate beads obtained by (a) Method A, (b) Method B, and (c) Method C.....	50
Figure 3.12. XRD graphs of ZrO <sub>2</sub> -based alginate beads obtained by (a) Method A, (b) Method B, and (c) Method C.....	51
Figure 3.13. Infrared spectra of CeO <sub>2</sub> -based sorbents.....	53
Figure 3.14. Infrared spectra of ZrO <sub>2</sub> -based sorbents.....	53
Figure 3.15. TGA curves of CeO <sub>2</sub> -based sorbents.....	54
Figure 3.16. TGA curves of ZrO <sub>2</sub> -based sorbents.....	55
Figure 3.17. Calibration plots of Se(IV), Se(VI), SeCys and SeMet.....	56
Figure 3.18. Calibration plot of Se(IV).....	56
Figure 3.19. Distribution diagram of (a) Se(IV) and (b) Se(VI) in aqueous solutions...	59
Figure 3.20. Effect of solution pH on the sorption of (●) Se(IV), (▼) Se(VI), (■) SeCys, (◆) SeMet for (a) CeO <sub>2</sub> and (b) ZrO <sub>2</sub> .....	60
Figure 3.21. Effect of solution pH on the sorption of (a) Se(IV) ,(b) Se(VI), (c) SeCys and (d) SeMet for (●) CeO <sub>2</sub> and (▼) ZrO <sub>2</sub> .....	61
Figure 3.22. Effect of shaking time on the sorption of (●) Se(IV) and (▼) Se(VI) (a) CeO <sub>2</sub> and (b) ZrO <sub>2</sub> .....	63
Figure 3.23. Effect of sorbent amount on the sorption of (●) Se(IV) and (▼) Se(VI) for (a) CeO <sub>2</sub> and (b) ZrO <sub>2</sub> .....	65
Figure 3.24. Effect of sorption temperature on the sorption of (●) Se(IV) and (▼) Se(VI) for (a) CeO <sub>2</sub> and (b) ZrO <sub>2</sub> .....	67
Figure 3.25. Percent sorption of (a) CeO <sub>2</sub> and (b) ZrO <sub>2</sub> for ten loadings.....	70
Figure.3.26. Effect of solution pH on the sorption of (●) Se(IV), (▼) Se(VI), (■)SeCys and (◆) SeMet for nZVI.....	77
Figure 3.27. Effect of solution pH on the sorption of (●) Se(IV), (▼) Se(VI), (■) SeCys and (◆) SeMet for ZrO <sub>2</sub> .....	77
Figure 3.28. Effect of solution pH on the sorption of (●) Se(IV), (▼) Se(VI), (■) SeCys and (◆) SeMet for nZVI-ZrO <sub>2</sub> .....	78
Figure 3.29. The effect of pH on the sorption of (●) Se(IV), (▼) Se(VI), (■)SeCys and SeMet(◆) with Amberlite IR-120 resin.....	80

Figure 3.30. The effect of pH on (a) Se(IV) and (b) Se(VI) with CeO<sub>2</sub>-based-alginate sorbent and (c) Se(IV) and (d) Se(VI) with ZrO<sub>2</sub>-based-alginate sorbent obtained by Method A . pH 2.0 (●), pH 3.0 (▼), pH 4.0 (■), pH 5.0 (◆), pH 6.0(▲), pH 7.0 (●) pH 8.0 (●)..... 82

Figure 3.31. The effect of pH on (a) Se(IV) and (b) Se(VI) with CeO<sub>2</sub>-based-alginate sorbent and (c) Se(IV) and (d) Se(VI) with ZrO<sub>2</sub>-based-alginate sorbent obtained by Method B . pH 2.0 (●), pH 3.0 (▼), pH 4.0 (■), pH 5.0 (◆), pH 6.0(▲), pH 7.0 ,(●) pH 8.0 (●)..... 83

Figure 3.32. The effect of pH on (a) Se(IV) and (b) Se(VI) with CeO<sub>2</sub>-based-alginate sorbent and (c) Se(IV) and (d) Se(VI) with ZrO<sub>2</sub>-based-alginate sorbent obtained by Method B . pH 2.0 (●), pH 3.0 (▼), pH 4.0 (■), pH 5.0 (◆), pH 6.0(▲), pH 7.0 (●) pH 8.0 (●)..... 84

## LIST OF TABLES

<b><u>Table</u></b>	<b><u>Page</u></b>
Table 1.1. Structures of some of the most relevant Se-compounds.....	3
Table 1.2. pKa values of selenium compounds. ....	5
Table 1.3. Some important physical and chemical characteristics of CeO <sub>2</sub> . ....	12
Table 1.4. Some important physical and chemical characteristics of ZrO <sub>2</sub> . ....	14
Table 2.1. HGAAS operating parameters. ....	21
Table 2.2. ICP-MS operating parameters. ....	21
Table 2.3. Reagent used through the study. ....	24
Table 2.3. Studied parameters and range. ....	34
Table 2.4. Desorption Eluents for CeO <sub>2</sub> and ZrO <sub>2</sub> . ....	38
Table 3.1. Elemental Analysis Results of Synthesized Sorbents.....	52
Table 3.2. Thermodynamic parameter of CeO <sub>2</sub> and ZrO <sub>2</sub> . ....	66
Table 3.3. Effect of initial Se(IV) concentration on the sorption efficiency for CeO <sub>2</sub> and ZrO <sub>2</sub> . ....	68
Table 3.4. Effect of initial Se(VI) concentration on the sorption efficiency for CeO <sub>2</sub> and ZrO <sub>2</sub> . ....	69
Table 3.5. Percent recovery of various desorbing matrices for Se(IV). ....	72
Table 3.6. Percent recovery of various desorbing matrices for Se(VI). ....	73
Table 3.7. Percent sorption of spiked selenite and selenate in ultrapure bottled and tap water for CeO <sub>2</sub> and ZrO <sub>2</sub> . ....	74
Table 3.8. Recovery of Se(IV) and Se(VI). ....	74
Table 3.9. Recovery of Se (IV) and Se(VI). ....	75
Table 3.10. Sorption results obtained with the commercial and the synthesized CeO <sub>2</sub> for Se(IV)/Se(VI). ....	76
Table 3.11. Percent Recovery of Se (IV), Se(VI) and SeCys. ....	78

# CHAPTER 1

## INTRODUCTION

### 1.1. Significance of Selenium

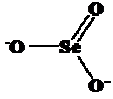
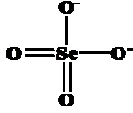
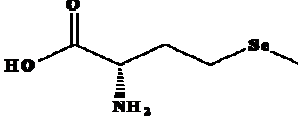
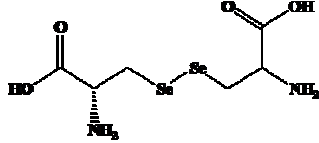
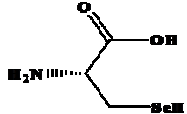
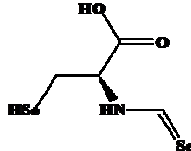
Selenium is an essential element due to its important role in life processes. It can cause toxicity or deficiency symptoms depending on its concentration. It is regarded as essential below  $40\text{mg}\cdot\text{g}^{-1}$ , but it is toxic above  $4000\text{mg}\cdot\text{g}^{-1}$  (Shunxing et al., 2002).

Several studies have shown that consumption of plants with high Se concentration causes chronic poisoning called alkali disease in livestock (Levander and Burk, 1994). Chronic toxicity of selenium can cause some symptoms such as hair and nail loss and brittleness, gastrointestinal problems, skin rash, garlic breath odor, and nervous system abnormalities (Yang et al., 1983). On the other hand, the biological roles of Se for human and animal has gained importance as result of many studies. In 1979, Keshan Disease Research Group (1979) has found the disease called Keshan caused by the low selenium content in the some area of China. Keshan disease can cause degeneration in cardiac muscle and affects children and women prior to menopause. (Neve et al., 1987; Ortuño et al. 1996). The significance of selenium was only discovered in 1973 by the identification of glutathione peroxidase which has been recognized as very potent antioxidant protecting the body from damage due to oxidation by free radicals (Rotruck et al., 1973). Also many studies have shown that selenium has a detoxification mechanism for animals which are poisoned by heavy metals such as mercury, lead, silver but the mechanism has not been completely explained (Frost 1983; Cuvin-Aralar and Furness 1991; Ellingsen et al. 1993; Levander and Burk, 1994).

## 1.2. Selenium Species in the Environment and in Biological Systems

Selenium is nonmetal and member of chalogens with an atomic number of 34 and an average atomic weight of 78.96. The place of Selenium in the periodic table is between sulfur and tellurium, whose chemistry resembles but differs significantly in some properties. In environmental and biological systems, selenium can exist in inorganic (as elemental selenium; selenite,  $\text{SeO}_3^{2-}$ ; selenate,  $\text{SeO}_4^{2-}$ ; selenides, e.g.  $\text{HgSe}$ ) and organic forms (selenoaminoacids, methylated forms and very complex selenoproteins)(Polatajko et al., 2006). Table 1.1 contains the structures of some of Se-compounds. Inorganic selenium species can be transformed into volatile compounds such as dimethyldiselenide and dimethylselenide as a result of detoxification mechanism(Dauchy et al., 1994). Hydrogen selenide is the most toxic form among all selenium compounds (Agency for Toxic Substances and Disease Registry 1996). In natural waters, inorganic selenium species such as Se(IV) and Se(VI) are predominant. Generally, selenium has been found in soils in the forms of elemental selenium, selenides, selenites, selenates(Pyrzynska, 2002). Organic forms can exist in yeast, broccoli, garlic, onion, mushrooms, wheat, and soybeans. Animals, especially fish, have higher selenium content than plants (Ari et al. 1991; Benemariya 1992; Diaz-Alarcón et al. 1995; Diaz-Alarcon et al. 1996b), and determination of protein content is important in order to decide the selenium amount in food. The highest selenium accumulation is found in marine products, especially in shrimps (Hershey et al. 1988; Zhang et al. 1993; Diaz-Alarcon et al. 1994). Selenium content in vegetables strongly depends on the concentration in soil. In acidic soils, selenium is not available for plants because the less absorbable and insoluble form of selenite is predominant. In alkaline soils, on the other hand, it is easily absorbed by plants because selenite is oxidized to selenate (Gondi et al. 1992). Selenite and selenate absorbed by plants can be converted into organoselenium by replacing sulfur in the amino acids (Simonoff and Simonoff 1991; Favier 1993). Depending on the vegetal species, they can transform inorganic selenium into organic selenium species. Extensively consumed vegetables such as broccoli, radish and garlic have the capability to convert inorganic selenium into selenomethylselenocysteine and glutamyl selenomethylselenocysteine (garlic). Brazil nuts and mushrooms are also important sources of selenium in the diet and selenium is mainly found as selenomethionine.

Table 1.1. Structures of some of the most relevant Se-compounds.

Se-species	Structure
Selenite	
Selenate	
Selenomethionine	
Selenocystine	
Selenocysteine	
Selenomethylselenocysteine	

Inorganic selenium species are generally found in four oxidation states, -2 ( $\text{H}_2\text{Se}$ ), 0 (elemental selenium), +4 ( $\text{SeO}_3^{2-}$ ), and +6 ( $\text{SeO}_4^{2-}$ ) depending on the pH and the redox potential of the solution. For prediction of dominant forms of selenium, pE-pH stability field diagram of selenium can be used. Figure 1.1 demonstrates that acidic and reducing conditions reduce inorganic selenites to elemental selenium, whereas alkaline and oxidizing conditions favor the formation of selenates. The pK value of  $\text{H}_2\text{SeO}_4$  (selenic acid) can be estimated by thermodynamic calculations and it is negative. Thus this form of selenium is most likely not present under natural conditions. The second dissociation of selenic acid needs to be taken into consideration and is

reported to be ranging from 1.66 to 2.05 (Seby et al. 2001). Also pKa values of inorganic selenium species were given in Table 1.2.

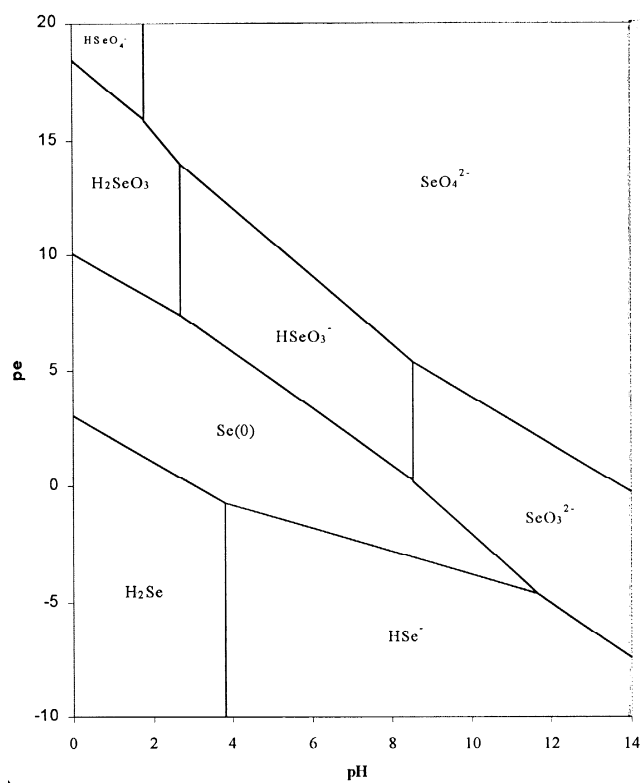


Figure 1.1. pe-pH diagram of selenium at 25 °C.  
(Source: Seby et al. 2001)

Organoselenium compounds play an important role in a number of chemical and biological processes. Similarly, organoselenium species were affected by pH and redox conditions. SeMet has two pKa values at pH ~ 2 and the other at pH ~ 9 corresponding to COOH and NH<sub>3</sub><sup>+</sup> groups and an isoelectric point at 5.75. SeCys has four pKa values, two at pH ~ 2 and two at pH ~ 8 (Table 1). These compounds are in the zwitterionic form, in the range of pH 2-10. In this form, NH<sub>3</sub><sup>+</sup> behaves as proton-donor group and COO<sup>-</sup> behaves as proton-acceptor group. Therefore, in the neutral solution these compounds provide enough concentration of an unprotonated amino group in the range of pH 2-10.

Table 1.2. pK<sub>a</sub> values of selenium compounds.

Compound	pK <sub>a</sub>	Oxidation state of selenium
Selenomethionine	2.2, 9.3	-2
Selenocystine	1.7, 2.3, 7.9, 9.8	-2
H <sub>2</sub> SeO <sub>4</sub>	1.92	+6
H <sub>2</sub> SeO <sub>3</sub>	2.46, 7.31	+4

### 1.3. Bioavailability of Selenium

Selenium (Se) is an essential nutrient of great importance to human health as mentioned in the previous section whose concentrations can cause deficiency or toxicity. The determination of the total content of selenium in food is still used to know but not enough because it is necessary to know the bioavailability of the Se or the amount absorbed, used and converted into biologically available forms in the organism (Cabañero et al. 2007). The bioavailability of selenium is influenced by chemical form. Organoselenium compounds are present in foods mainly as selenomethionine (SeMet), selenocystine and Se-(methyl)selenocystine while inorganic selenium exists less frequently and in very low amounts in food. Organic forms have greater bioavailability than inorganic forms (Dumont et al. 2006).

The most important selenium sources in diet are wheat and meat. Se-Cysteine and Se-Methionine are mostly found in meat. Especially Se-Met is an essential selenoamino acid and known to be highly bioavailable (Dumont et al. 2006). Selenium content of fish is high but it is not highly bioavailable because selenium complexes with Hg and other metals (Pappa et al. 2006). Finley et al. (2004) stated that the chemical forms of selenium species also change among foods. For instance, bioavailability of broccoli is low, despite of containing methylated forms of selenium. On the other hand, the bioavailabilities of red meats such as pork or beef for selenoprotein synthesis are high which can accumulate high selenium. The Food and Nutrition Board of the United States Research Council has recommended dietary limits for a healthy adult man as 70 µg Se/day and for a healthy adult woman as 55 µg Se/day (Navarro-Alarcon and Lopez-Martinez, 2000).



## 1.4. Selenium Determination Methods

There are various instrumental techniques to determine selenium concentration in different samples. Electrothermal atomic absorption spectrometry (ETAAS) was used by Izgi et al. (2005) to determine the concentration of selenium in garlic and onions after the application of a preconcentration step with 3,3-diaminobenzidine (DAB) reagent on the activated carbon. Saygi et al. (2006) used graphite furnace atomic absorption spectrometry (GFAAS) for the determination and speciation of Se(IV) and Se(VI) in environmental samples after the solid phase extraction process of Se(IV)-ammonium pyrrolidine dithiocarbamate (APDC) chelate on Diaion HP-2MG. Valencia et al. (1999) developed a method based on the oxidation of potassium iodide by Se(IV) in acidic conditions and the formation of complex of resulting  $I_3^-$  with Rhodamine B (RB) fixed on a dextran type lipophilic gel. To determine Se(IV) in natural waters solid-phase spectrophotometry was used.

Another method using spectrophotometry was proposed by Chand and Prasad (2009) for the determination of Se(IV), Se(VI) and total inorganic selenium in water. It was based on the catalytic effect of Se(IV) on the reduction of bromate by hydrazine dihydrochloride, the decolorization of methyl orange (MO) by the generated bromine, and the monitoring of the absorbance spectrophotometrically at 507 nm as a function of time. In the study of Zhao et al. (2010), All forms of selenium compounds in biological samples were decomposed to selenite by using low volume microwave digestion procedure and the selenium content of the samples was determined by hydride generation atomic fluorescence spectrometry (HG-AFS), or voltammetry. Panigati et al. (2007) employed differential pulse cathodic stripping voltammetry (DPCSV) on the hanging drop mercury electrode (HDME) in the presence of Cu(II) to determine the total selenium content in rice. A mixture of wet acid/dry ashing with Mg(II) salts were used to carry out the digestion in open vessel. Dedkova et al. (2009) proposed a method to determine the selenium content by using diffuse reflectance spectroscopy which has depend on complexation reactions between Se(IV) and organic reagents on solid phase of polyacrylonitrile filled with AV-17 anion\_exchanger. Zhang et al. (2009) used nano-titanium dioxide particles for the removal of Se(IV) and Se(VI) from aqueous solutions and UV-VIS spectrometry was used for determination of selenium by using 1.0 mL 6.0 mol L<sup>-1</sup> HCl, 3.0 mL 0.05% malachite green, 3.0 mL 10% KI and 3.0 mL 10% Arabic

gum solution. Leggli et al. 2008 have used surfactant/oil/water as a sample pre-treatment system and determined trace level of selenium in whole hen eggs by graphite furnace absorption spectrometry (GFAAS). Zhang et al. (2010) proposed a newly effective method for determination of total arsenic (As), total bismuth (Bi), total tellurium (Te) and total selenium (Se) in tea leaves which is the simultaneous multi-channel hydride generation atomic fluorescence spectrometry (HG-AFS). Bakir et al. 2003 used instrumental neutron activation analysis (INAA) for selenium concentration in blood and tumour tissues of breast cancer patients and healthy volunteers in Syria.

Hydride generation atomic absorption spectrometry (HGAAS) is widely used selenium determination technique. Maleki et al. (2005) introduced a HGAAS method for the determination of traces of selenium at  $\text{ng mL}^{-1}$  concentration ranges by using a solid reagent of tartaric acid and sodium tetrahydroborate. In most of studies, inductively coupled plasma atomic emission spectrometry (ICP-AES) and hydride generation-inductively coupled plasma atomic emission spectrometry (HG-ICP-AES) were also used as selenium determination techniques (Harwood et al. 1997, Stripeikis et al. 2000). In order to detect very low concentrations ( $\mu\text{g L}^{-1}$ ) of selenium with a proper linear dynamic range, inductively coupled plasma mass spectrometry (ICP-MS) is one of the most efficient methods (Kápolna et al. 2006, Miekeley et al. 2005). Liu (2009) developed a method for the determination of ultra-trace amounts of inorganic selenium species in aqueous systems and used IC-ICP-MS as the detection system based on nano- $\text{Al}_2\text{O}_3$  solid phase extraction technique.

## **1.5. Speciation of Inorganic and Organic Selenium**

As mentioned section 1.4, most analytical measurements deal with the determination of total concentration of selenium in sample but it was realised that this analytical information was insufficient. Biochemical and toxicological research has demonstrated that, the chemical form or the oxidation state of selenium that is found in the environment, is crucial for living organisms. Therefore, it is necessary to determine not only the total concentration of the selenium but also its individual chemical and physical form.

Over years, quite a large number of articles have been published related to the speciation of inorganic and organic selenium. In the study of Tao et al. (2008), albumin,

globulin, protamine and glutelin were extracted from selenium (Se)-rich rice and the content of Se in these protein extracts was determined by inductively coupled plasma mass spectrometer (ICP-MS). In another study, speciation of selenium in selenium-enriched green onions (*Allium fistulosum*) was performed. Reversed-phase ion-pairing high performance liquid chromatography (RP-IP-HPLC) and size-exclusion chromatography inductively coupled mass spectrometry (SEC-ICP-MS) for Se-cystine, methylselenocysteine, Se-methionine, and inorganic selenium species (Kápolna et al., 2006). The speciation of selenocystine (SeCys), selenomethionine (SeMet), selenoethionine (SeEt) and Se(IV) was performed by using on-line coupling of reversed phase high-performance liquid chromatography (HPLC) and atomic fluorescence spectrometry (AFS) with hydride generation (HG) as sample introduction system (Ipolyi et al. 2000). A simpler and cleaner chromatographic separation was developed by Vilano et al. in 1998. In this study, liquid chromatography–UV irradiation–hydride generation–quartz cell atomic absorption spectrometry was introduced for speciation of inorganic and organic selenium species. UV irradiation was used for conversion of all selenium species to selenite without any additional reagent.

A electrodeposition–electrothermal AAS method for speciation analysis of selenocysteine and Se(IV) in environmental water and agricultural soil samples has been developed by Najavi et al (2010). An uncontrolled applied potential (1.8 V) on a mercury coated electrode was applied for the selective reduction of selenium species. In acidic media (1.0 M HCl solution) the only Se(IV) and selenocysteine electrodeposited. Su et al (2008) used a novel hyphenated technique, HPLC-UV/nano-TiO<sub>2</sub>-CL for determination of selenocystine and selenomethionine based on UV decomposition of these species.

Goeslaret al.(1997) investigated the retention behavior of selenous acid, selenic acid, selenocystine, selenohomocystine, selenomethionine, selenoethionine, trimethylselenonium iodide, and dimethyl (3-amino-3-carboxy-1-propyl) selenonium iodide on a Supelcosil LC-SCX cation-exchange column and inductively coupled plasma mass spectrometry (ICP-MS) was used for determination of these selenium species. Another technique, Capillary electrophoresis inductively coupled plasma mass spectrometry (CE-ICP-MS), has been also applied to separate of selenomethionine, selenite, selenate and selenocysteine in nuts (Kannamkumarath et al. 2005).

Pedersen and Larsen (1997) have presented a speciation procedure for Se(IV), Se(VI), SeMet, SeCysin plants (white clover). HPLC-ICP-MS and HPLC-FAAS have been used for four selenium species. Ionosphere-C column was used as stationary phase and aqueous solution of 2.0 mM pyridine formiate and 3.0 % MeOH at pH 2.9 were used as the mobile phase. Duan and Hu (2009) have applied online speciation procedure for the separation and determination of selenomethionine (SeMet) and selenocystine (SeCys2) by using Cu(II) loaded nanometer-sized Al<sub>2</sub>O<sub>3</sub> coupled to inductively coupled plasma mass spectrometry (ICP-MS).

## **1.6. Solid Phase Extraction**

Many separation and preconcentration methods can be found in literature for various purposes. For example, liquid-liquid extraction (solvent extraction), electro-deposition, ion exchange, membrane filtration.

Solid-phase extraction (SPE) is one of the most common techniques used for extraction and pre-concentration of analytes in liquid samples because of many advantages such as high enrichment factor, high recovery, rapid phase separation, low cost, low consumption of solvents. Solid phase extraction (SPE) is a non-equilibrium process and is based on the extraction of the desired species on a sorbent, and then elution of the retained species using a suitable solvent. There are basically two type of SPE; namely, the batch and the column modes. When SPE is performed on a batch type, solid sorbent is weighed and put into the sample liquid solution. To obtain efficient mass transfer of the solutes, large surface area is provided by the particles in solid phase. After shaking process, two phases easily can be separated by filtration (Figure 1.2 (a)). In column type SPE, the column is loaded with the sample solution for the sorption of the analyte by the solid phase(Figure 1.2 (b)).A higher percentage of extraction is expected in SPE column compares to batch type extractions.The concentration of analyte in the effluent (non-sorbed fraction) is determined and used for the calculation of the percentage sorption. The analyte (retained by the sorbent) is eluated by using, generally, a smaller volume of a proper eluent. The analyte concentration in the eluate gives the percentage elution. Finally, total recovery calculations can be made according to Equation 1.1.

$$\text{Total Recovery} = \frac{[\text{analyte}]_{\text{eluate}}}{[\text{analyte}]_{\text{sample}}} \times 100 \quad (1.1)$$

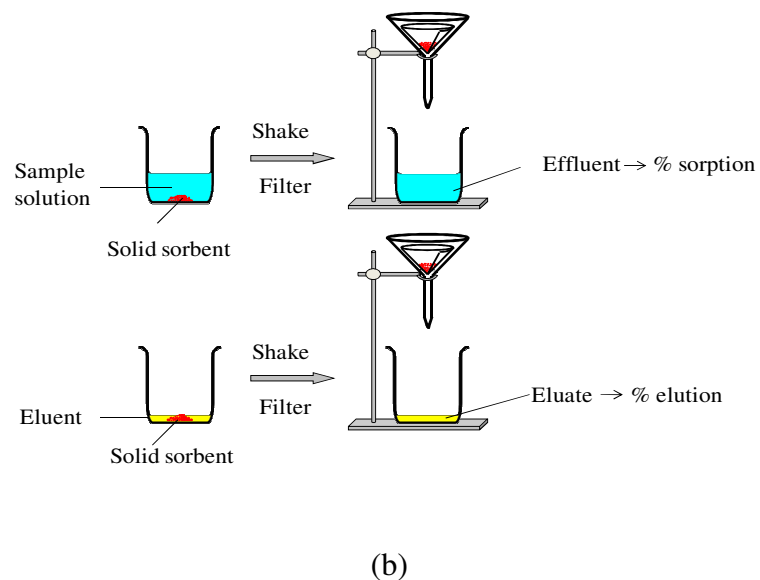
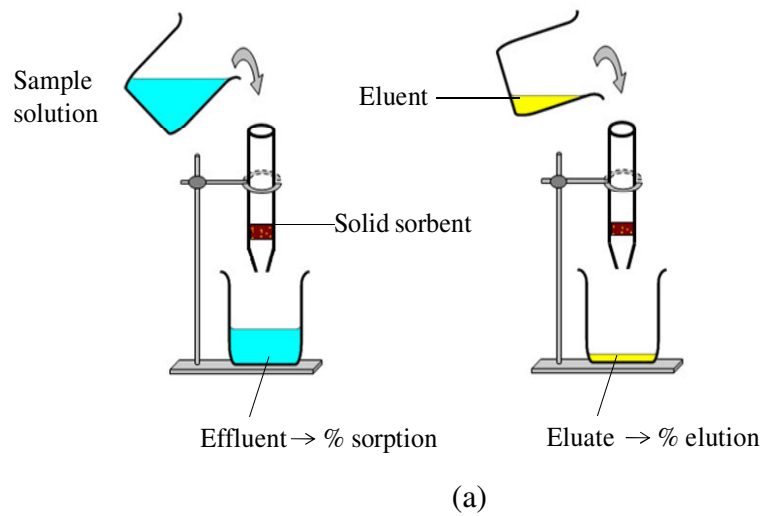


Figure 1.2. Schematic illustration of the SPE modes (a) column type, (b) batch type.

SPE has both advantages and disadvantages over the other methods mentioned above. In addition, the target species can be fixed in a more stable chemical form on the solid surface. A special care must be given to the possible plugging problem that can be caused by the concentration, type, and size of the particulates in the sample, pore size of the sorbent and surface area of the sorbent bed. There is also a potential for the association of analyte with particulate and colloidal matter contamination in the sample.

To avoid these problems sample particulate matter should be removed by filtration prior to SPE analysis.

## **1.7. Solid Sorbents**

By recent developments in nanoscience and nanotechnology, nanosorbents have widely used for remediation of environmental problems. Nanosorbents have many advantages such as low cost, high adsorption capacities and fast adsorption rates for heavy metal ions. The synthesis of non-siliceous mesoporous materials such as metal oxides has gained attention by the discovery of mesoporous silica material. For example, semiconductor nanomaterials, such as,  $\text{Fe}_2\text{O}_3$ ,  $\text{TiO}_2$ , and  $\text{Cu}_2\text{O}$ ,  $\text{SnO}_2$  have been used for removal of organic and inorganic pollutants from water. To develop ideal nanomaterials for removal of pollutant from water is the one of ultimate aim of nanoscience and nanotechnology (Hu et al., 2008). In this study, cerium oxide, zirconium oxide, nano-scale zerovalent iron (nZVI), nZVI-modified zirconium oxide and cerium oxide or zirconium oxide immobilized alginate were used for the sorption and speciation of Se(IV), Se(VI), Seleno-L-Cystine and Seleno-DL-Methionine.

### **1.7.1. Cerium Oxide**

Cerium oxide, an important rare-earth material, and known as ceria or cerium dioxide, has a chemical formula of  $\text{CeO}_2$  and it is a pale yellow powder. Some important physical and chemical characteristics of cerium oxide are shown on Table 1.3. Cerium is thermodynamically unstable metal and in the presence of oxygen it can easily reduced to  $\text{CeO}_2$  and  $\text{Ce}_2\text{O}_3$ . Generally, pressure and temperature are the major factors on the final stoichiometry.

Table 1.3. Some important physical and chemical characteristics of CeO<sub>2</sub>.

Chemical Name	<b>Cerium Oxide</b>
Formula	CeO <sub>2</sub>
Molecular weight	172.12 g/mol
Physical State	Solid, cubic, face-centered crystals Solid as white, yellow or tan powder
Density	7.65 g/cm <sup>3</sup>
Boiling Point	3500 °C
Melting Point	2400 °C
Water Solubility	Insoluble
Refractive Index	2.0
Hardness	5-6

There are various techniques for production of cerium oxide nanoparticles, mainly, wet-chemical synthesis techniques such as chemical precipitation, sol-gel, microemulsion (reverse micelles), sonochemical and hydrothermal/solvothermal syntheses. Zhou et al. (2002) produced approximately 4 nm CeO<sub>2</sub> nanoparticles by precipitation method, Mai, et al. (2005) obtained CeO<sub>2</sub>nanorods, nanopolyhedras via hydrothermal preparation, Sathyamurthy et al. (2005) successfully synthesized CeO<sub>2</sub>nanoparticles with an average size of 3.7 nm by microemulsion method and Wang et al. (2002) used both sonochemical and microwave assisted method to fabricate CeO<sub>2</sub> nanoparticles.

Ceria has unique properties, including oxygen storage capacity and oxygen ion conductivity. Because of these characteristics, ceria has been widely used for catalyst, fuel cell, sensor, UV shielding, and luminescence. Also many report demonstrated that the prepared ceria materials could be used as a sorbent for removal of inorganic pollutants. In the study of Zhong et al. (2006) three-dimensional (3D) flowerlike ceria micro/nanocomposite structure was synthesized with a simple and economical route based sol-gel process(Figure 1.4) and used as a sorbent for the removal of As (V) and Cr(VI) in wastewater treatment.

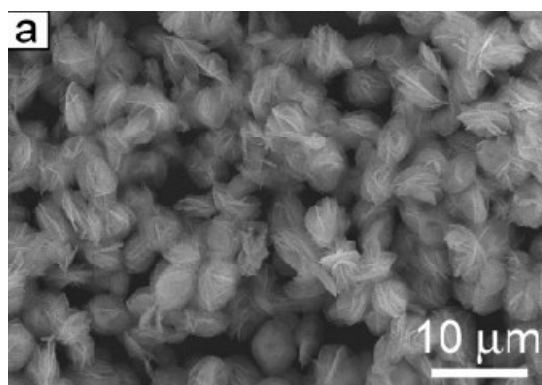


Figure 1.3. SEM image of three-dimensional (3D) flowerlike  $\text{CeO}_2$  micro/nanocomposite structure. (Source: Zhang et al., 2006)

In 2007, Ozturk and Kavak investigated to removal of boron from aqueous solutions using cerium oxide as sorbent. In another study, ceria hollow nanospheres were synthesized with microwaveassisted aqueous hydrothermal method (Figure 1.5). These ceria hollow nanospheres have showed an excellent adsorption capacity for heavy metal ions, for As(V) and Cr(VI) (Cao et al. 2010).

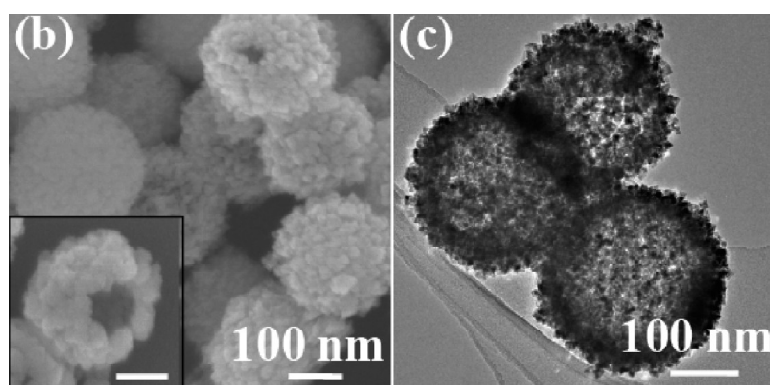


Figure 1.4. High-magnification (b) SEM image and (c). TEM image of the  $\text{CeO}_2$ . (Source: Cao et al., 2010)

Recillas et al. (2010)  $\text{CeO}_2$  nanoparticles (6.5nm mean size) have been synthesized and used as adsorbent for the removal of chromium (VI) from pure water solutions. In 2009, Xiao et al., explored a nonaqueous sol-gel method to synthesize hierarchical  $\text{CeO}_2$  nanocrystal microspheres by reacting cerium nitrate hydrate with benzyl alcohol at a temperature as low as 120 °C for the first time. The resulting hierarchical  $\text{CeO}_2$  nanocrystal microspheres could effectively remove heavy metal ions (Cr(VI) and organic dye (RhB) from simulated wastewater at neutral pH. An interesting



study was performed by Deng et al. in 2010 which the novel Ce–Ti hybrid oxide adsorbent obtained by the hydrolysis with subsequent precipitation exhibited high sorption capacity for As(V).

### 1.7.2. Zirconium Oxide

Zirconium dioxide ( $ZrO_2$ ), which is also referred to as zirconium oxide or zirconia, is mainly used in ceramic materials. Some important physical and chemical characteristics of zirconium oxide are shown on Table 1.4. Zirconium oxide can present three crystalline structures: tetragonal (t- $ZrO_2$ ), cubic (c- $ZrO_2$ ) and monoclinic (m- $ZrO_2$ ). The crystallization of  $ZrO_2$  and conclude that the first structure to crystallize is the tetragonal form which occurs between 300 and 500 °C followed by its transformation to the monoclinic form which occurs between 900 and 1000 °C. The monoclinic structure is a thermodynamically stable phase.

Table 1.4. Some important physical and chemical characteristics of  $ZrO_2$ .

<b>Chemical Name</b>	<b>Zirconium Oxide</b>
<b>Formula</b>	$ZrO_2$
<b>Molecular weight</b>	123.218 g/mol
<b>Physical State</b>	Cubic, tetragonal, monoclinic Solid as white powder
<b>Density</b>	5.68 g/cm <sup>3</sup>
<b>Boiling Point</b>	2715°C
<b>Melting Point</b>	4300°C
<b>Water Solubility</b>	Insoluble
<b>Refractive Index</b>	2.13
<b>Hardness</b>	5-6

As mentioned cerium oxide synthesis, Various chemistry-based novel synthesis methods have been used for the preparation of zirconia powders including co-precipitation, hydrothermal, sol gel, sonochemical method, microemulsion and thermal decomposition processing. Recently, Vatansever et al. (2010) produced approximately 50 nm Yttria stabilized  $ZrO_2$  nanoparticles by reverse microemulsion method, Piticescu

et al. (2001) obtained  $ZrO_2$  with crystallite sizes in the range 6–22 nm by hydrothermal preparation, Matos et al. (2009) successfully synthesized  $ZrO_2$  nanoparticles with an average size of 40 nm by sol-gel method.

The advanced applications of zirconia nanopowders are including transparent optical devices, electrochemical capacitor electrodes, oxygen sensors, fuel cells and catalysts including photocatalysts (Srdic and Omorjan, 2001; Kongwudthiti et al., 2003). Zirconia catalyzes the hydrogenation of olefins, isomerization of olefins and epoxides and the dehydrations of alcohols. Also zirconia can be used as sorbent because zirconium is a rather harmless element, and its oxide has resistance against the attack of acids and alkali solution. Bortun et al. (2009) was prepared mesoporous hydrous zirconium oxide from a zirconium salt granular precursor and the use of hydrous zirconium oxide for As (V) was investigated. In the another work silica modified with zirconium oxide as a solid phase sorbent, coupled to a HG AAS system that allows the determination of total inorganic arsenic present in steel samples was described by Macarovscha et al. 2006. In the study of Suzuki et al. (2001) adsorption properties for oxoanions of Se(IV), Se(VI), As(III), As(V), and methyl derivatives of As(V) have been examined by the porous polymer beads loaded with monoclinic hydrous zirconium oxide (Zr-resin).

### 1.7.3. Nanoscaled Zero-Valent Iron (nZVI)

Iron in elemental form is very reactive and it is immediately oxidized in atmospheric conditions. So it exists in the form of magnetite ( $Fe_3O_4$ ), hematite (natural ore) ( $Fe_2O_3$ ), limonite. Several studies demonstrated that zero-valent iron is effective at stabilization or destruction of a host of pollutants by its highly reducing character. Nanoscaled zero-valent iron can be synthesized by several methods (Sun, et al. 2006, Nurmi, et al. 2005, Li, et al. 2006). The most widely used method for environmental purposes is the borohydrate reduction of Fe(II) or Fe(III) ions in aqueous media. The method presented by Wang and Zhang consists of dropwise addition of sodium borohydride ( $NaBH_4$ ) to a solution of Fe(II) or Fe(III) (Wang and Zhang 1997).

One of the proposed mechanisms for the reaction is:



Figure 1.6 shows the core-shell structure of nZVI suggested by Li and Zhang in 2007. The authors studied nZVI structure before and after contacting with various metals and proposed three possible types of metal uptake on nZVI surface.

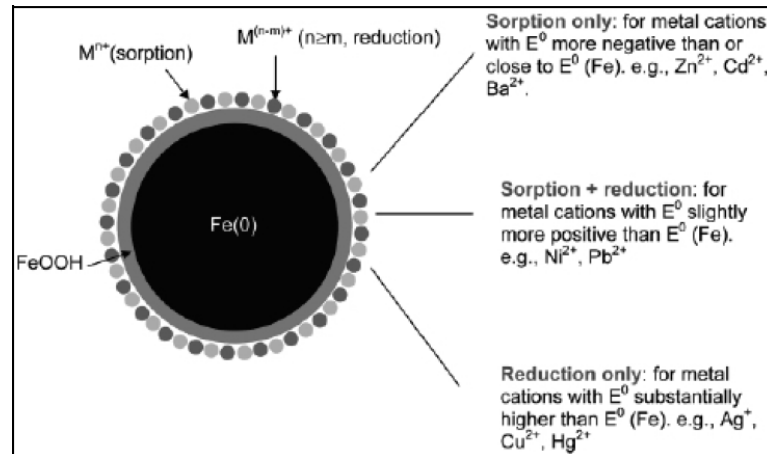


Figure 1.5. The core-shell structure of nZVI.  
(Source: Li and Zhang,2007)

There are some restrictions on the usage of nZVI in real remediation applications. Firstly, iron nanoparticles have positive surface charges within the natural pH range and they tend to repel each other strongly and it is very hard to keep them stable. Secondly, colloidal properties of nZVI, particles tend to precipitate and they cannot be driven for more than a few meters by the migration of water and probably cannot reach the contaminated zone. Another problem, valid for all methods, is the storage of iron nanoparticles for along time without oxidizing since thermodynamically zero-valent iron tends to react with oxygen. To overcome these problems, iron nanoparticles can be modified, supported or mixed with a filling material.

Biterna et al. (2007) investigated the efficiency of zero valent iron (ZVI) to remove arsenate from water. In the work of Mondal's group in 2004, The removal of selenate from aqueous solution using nanosized particles of Fe and bimetallic NiFe was performed.

### 1.7.4. Alginate

Alginate, a polyanionic linear copolymer of 1,4-linked- $\alpha$ -l-guluronic acid and  $\beta$ -d-mannuronic acid residues found in brown seaweeds, has been known as an excellent polysaccharide for gel bead system because of its unique features such as biocompatibility, biodegradability, immunogenicity, and non-toxicity. Use of sodium alginate is especially widespread. The structure of sodium alginate was given in Figure 1.7.

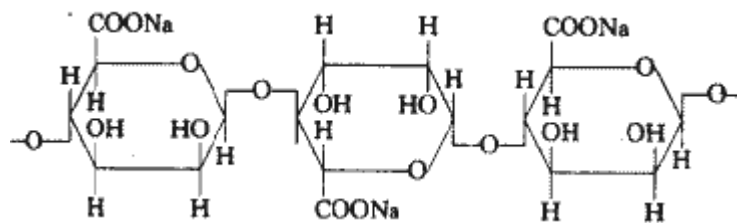


Figure 1.6. The structure of sodium alginate.  
(Source :McHugh et al; 1987).

Alginate gelation takes place when divalent cations (usually  $\text{Ca}^{2+}$ ,  $\text{Ba}^{2+}$ ,  $\text{Sr}^{2+}$ ), interact ionically with blocks of guluronic acid residues and three-dimensional network formed which is described by egg-box model shown in Fig 1.8. The divalent cations bind to the  $\alpha$ -L-guluronic acid blocks. Each alginate chain dimerizes to form junctions with many other chains and as a result gel networks are formed. Depending on the amount of calcium present in the system, these inter-chain associations can be either temporary or permanent. Low levels of calcium tend to formation of temporary interactions, giving rise to highly viscous solutions. At higher calcium levels, permanent associations of the chains are obtained.

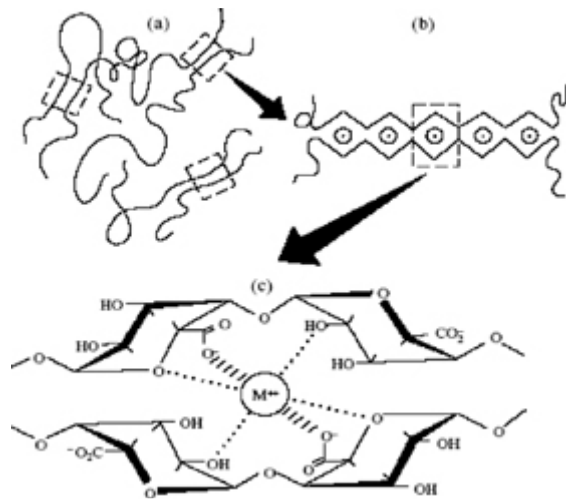


Figure 1.7. Schematic representation of the "egg-box" model of alginate gel.  
(Source: McHugh et al; 1987).

Alginate is biopolymers that are finding widespread applications in food and pharmaceutical industry. Alginate especially is used extensively in food industry as a thickener, emulsifier and as a stabilizer. In recent year alginate has used for enviromental applications. In the work of Escudero et al. (2008) a mixture of mainly Fe(III) and Ni(II) (hydr)oxides, has been entrapped in calcium alginate and investigated for As(III) and As(V) sorption. In another work, firstly the powder of zirconium mesostructure (ZM) was prepared with the template of surfactant and than immobilized into calcium alginate for practical application and the resulting material was tested to evaluate the phosphate removal efficiency (Yeon et al., 2008).

In 2001, Chen and Wang were prepared new type of Ca-alginate based ion-exchange resin for removal of zinc and copper. In another study, the adsorption performance of copper on calcium alginate encapsulated magnetic sorbent was investigated (Lim et al., 2009). Bezbaruah et al. (2008) successfully entrapped zero-valent iron in biopolymer, calcium (Ca)-alginate beads and used these sorbents for removal of nitrate ions in groundwater.

## **1.8. Aim of This Work**

The purpose of this study is to prepare a novel sorbent for the speciation of both inorganic (selenite and selenate) and organic selenium (seleno-L-cystine and seleno-L-methionine) prior to determination by atomic spectrometric techniques. For this purpose, various materials, such as commercial and synthesized  $ZrO_2$  and  $CeO_2$ , nanoscale zero valent iron (nZVI),  $ZrO_2$  modified with nZVI, and alginate beads modified separately with  $ZrO_2$  and  $CeO_2$  were investigated for their sorption behavior towards selenium species. The sorption performance of the sorbents in terms of solution pH, reaction temperature, shaking time, sorbent amount, and initial concentration of selenium species were examined through batch type sorption studies. Column type sorption was also tried for alginate-based sorbents. Characterization of the sorbents was realized before the sorption studies.

## CHAPTER 2

### EXPERIMENTAL

#### 2.1. Instrumentation and Apparatus

A Thermo Elemental Solaar M6 Series atomic absorption spectrometer (Cambridge, UK) with an air-acetylene burner was used in selenium determinations for heavy matrix solutions such as the eluates after desorption studies (Figure 2.1). A selenium hollow cathode lamp at the wavelength of 196.0 nm and a deuterium lamp were employed as the source line and for background correction, respectively. In HGAAS, the quartz tube atomizer was 10.0 cm long, 8.0 mm in internal diameter and 10.0 mm in external diameter with a 4.0 mm bore inlet tube fused at the middle for sample introduction. The quartz tube was heated externally with air-acetylene flame and nitrogen was used as the carrier gas. Operating parameters for the HGAAS system are given in Table 2.1.

Agilent 7500ce Series (Tokyo, Japan) inductively coupled plasma mass spectrometer (ICP-MS) equipped with a high solid nebulizer, a Peltier-cooled spray chamber (2 °C), and an octopole collision/reaction cell with helium gas pressurization was used throughout the study for selenium determination. Although the most abundant isotope of selenium is  $^{80}\text{Se}$  (49.60%), it could not be used in ICP-MS measurements because of the spectral interference of  $^{40}\text{Ar}^{40}\text{Ar}$ . Therefore, as an initial check, measurements were made with the three isotopes, namely,  $^{78}\text{Se}$ ,  $^{80}\text{Se}$ , and  $^{82}\text{Se}$ . Counts at  $m/z = 80$  were enormously high which necessitated the use of collision cell. However, the signals from  $^{78}\text{Se}$  and  $^{82}\text{Se}$  counts were similar and sufficient; therefore, the measurements were done at  $m/z = 78$  ( $^{78}\text{Se}$ , natural abundance of 23.50%). Operating parameters for ICP-MS system are given in Table 2.2.

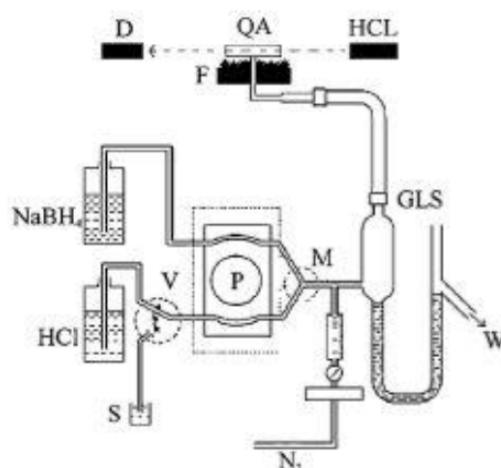


Figure 2.1. Segmented Flow Injection HGAAS system used in selenium determinations. D: deuterium lamp, QA: quartz atomizer, HCL: hollow cathode lamp, F: flame, GLS: gas-liquid separator, W: waste, P: peristaltic pump, V: threeway valve and S: sample (Source: Yersel et al. 2005)

Table 2.1. HGAAS operating parameters.

Carrier gas (N <sub>2</sub> ) flow rate	200.0 mL min <sup>-1</sup>
HCl flow rate	6.1 mL min <sup>-1</sup>
HCl concentration	3.0% (v/v)
NaBH <sub>4</sub> concentration	1.0% (w/v) stabilized with 0.10 % (w/v) NaOH
NaBH <sub>4</sub> flow rate	3.0 mL min <sup>-1</sup>
Sample flow rate	7.0-8.0 mL min <sup>-1</sup>

Table 2.2. ICP-MS operating parameters.

Forward power	1500 W
Reflected power	1 W
Coolant gas flow rate	15 mL min <sup>-1</sup>
Auxiliary flow rate	0.90 mL min <sup>-1</sup>
Sample uptake time	25 sec
Integration time	100 msec



In batch sorption studies, GFL 1083 water bath shaker (Burgwedel, Germany) equipped with microprocessor thermostate was used to provide efficient mixing. All pH adjustments and measurements were done using Denver pH/ion meter (Colorado, USA) with a pH/ATC plastic-body electrode using various concentrations of HNO<sub>3</sub>, NH<sub>3</sub>, HCl, and NaOH. During repetitive loading studies Hettich EBA 12 centrifuge (Tuttlingen, Germany) was used to separate the sorbent for reuse.

During the hydrothermal synthesis of CeO<sub>2</sub> and ZrO<sub>2</sub> particles, 23 mL Teflon lined reaction autoclaves (Parr Instruments – model 4749) were used during the hydrothermal treatment. After adding the precursor materials to the Teflon liner, it was placed in an autoclave covered first corrosion and rupture disks. Then, the spring with upper and lower pressure plates were placed. Finally, with a screw cup was firmly closed (Figure 2.2). Several techniques were applied for the characterization of the sorbents. X-Ray powder diffraction analysis was carried out using a Philips X' Pert Pro diffractometer. Each sorbent was mounted on a holder then introduced for analysis. XRD was carried out using a Cu K $\alpha$  radiation ( $\lambda=1.54 \text{ \AA}$ ) source. Philips XL-30S FEG type instrument was employed for SEM characterization to obtain information about morphology and size of the crystals. Thermal properties of sorbents were analysed with Perkin Elmer Pyris Diamond TG/DTA (Boston, MA, USA). Point of zero charge of ZrO<sub>2</sub> and CeO<sub>2</sub> were determined with Zeta-Sizer (Staunton, USA). Surface area measurements were performed with Micromeritics Gemini V Series Surface Area Analyzer (Norcross, USA).



Figure 2.2. Schematic representation of an autoclave with its parts.

## 2.2. Reagents and Solutions

All the chemicals were of analytical reagent grade. Ultrapure water (18.2 M $\Omega$ , Millipore, and Billerica, MA, USA) was used throughout the study. Glassware and plastic containers were soaked in 10% (v/v) nitric acid overnight and washed with distilled water before use. Table 2.3 shows the reagents and their concentrations used through the study.

Standard Se(IV) stock solution (1000.0 mg/L) was prepared by dissolving 0.833 g of Na<sub>2</sub>SeO<sub>3</sub> · 5H<sub>2</sub>O in 1.0% (v/v) HNO<sub>3</sub> and diluted to 250.0 mL with ultrapure water and kept in refrigerator at 4 °C .

Standard Se(VI) stock solution (1000.0 mgL<sup>-1</sup>) was prepared by dissolving 0.598 g of Na<sub>2</sub>SeO<sub>4</sub> in ultrapure water and diluted to 250.0 mL with ultrapure water kept in refrigerator at 4 °C.

Standard Seleno-DL-Methionine stock solution (547.5 mgL<sup>-1</sup>) was prepared by dissolving 0.068 g of seleno-DL-methionine in 3.0% (v/v) HCl and diluted to 50.0 mL with ultrapure water kept in refrigerator at -20 °C .

Standard Seleno-L-Cystine stock solution (1490 mgL<sup>-1</sup>) was prepared by dissolving 0.3156 g of seleno-L-cystine in 3.0% (v/v) HCl and diluted to 100.0 mL with ultrapure water kept in refrigerator at 4 °C .

Sodium borohydride solution of 1.0% (w/v) was prepared for a daily usage from fine granular product and stabilized by 0.10% (w/v) NaOH in water and also 3.0% (v/v) HCl solution was prepared for HGAAS determination

Calibration standards with lower concentrations were prepared daily by appropriate dilution of the stock standard.

pH adjustments were done by using 1.0M, 0.1M, 0.01M of HCl and NaOH solutions and HNO<sub>3</sub> and NH<sub>3</sub> solutions for HGAAS and ICP-MS determinations, respectively.

Table 2.3.Reagent used through the study.

Reagent	Concentration used	Company	Cas no.	Purpose of use
Na <sub>2</sub> SeO <sub>3</sub> 5H <sub>2</sub> O		Merck	[26970-82-1]	Preparation of Se(IV) stock solution for sorption study
Na <sub>2</sub> SeO <sub>4</sub>		Fluka	[13410-01-0]	Preparation of Se(VI) stock solution for sorption study
Seleno-DL-Methionine		Sigma	[2578-28-1]	Preparation of SeMet stock solution for sorption study
Seleno-L-Cystine		Sigma	[3211-76-5]	Preparation of SeCys stock solution for sorption study
Cerium(IV) oxide, powder		Sigma	[1306-38-3]	Sorption of Se(IV)/Se(VI) in speciation study
Zirconium(IV) oxide,powder		Riedel-de Haen	[1311-23-4]	Sorption of Se(IV)/Se(VI) in speciation study
Cerium(III) nitrate hexahydrate	0.5 M	Merck	[10294-41-4]	Synthesis of CeO <sub>2</sub>
Alginic Acid, sodium salt	2 % (m/v)	Aldrich	[9005-38-3]	Synthesis of alginate beads
Amberlite IR-120, H <sup>+</sup> form		Fluka	[39389-20-3]	Sorption of Se(IV),Se(VI), SeCys and SeMet
Zirconium(IV) chloride	0.5 M	Merck	[10026-11-6]	Synthesis of ZrO <sub>2</sub>
Urea		Sigma	[57-13-6]	Sol-gel Synthesis of CeO <sub>2</sub>

(cont. on next page)

Table 2.3. (Cont.)

Reagent	Concentration used	Company	Cas no.	Purpose of use
Potassium iodate	0.2% (m/v) in 1.0 M HCl	Merck	[7758-05-6]	Desorption of Se(IV) from CeO <sub>2</sub> and ZrO <sub>2</sub>
Cetyltrimethylammoniumbromide, CTAB		Alfa Aesar	[57-09-0]	Sol-gel and Hydrothermal Synthesis of CeO <sub>2</sub> and ZrO <sub>2</sub>
CaCl <sub>2</sub> anhydrous, beads	0.15 M	Sigma-Aldrich	[10042-52-4]	Synthesis of alginate beads
Sodium borohydride, NaBH <sub>4</sub> (granular)	3%(w/v)	Aldrich	[16940-66-29]	Synthesis of nZVI and nZVI modified ZrO <sub>2</sub>
FeCl <sub>2</sub> .4H <sub>2</sub> O	1.0 M	Sigma	[13478-10-9]	Synthesis of nZVI and nZVI modified ZrO <sub>2</sub>
HNO <sub>3</sub>		Merck	[7697-37-2]	Acidification
HCl	6.0 M	Merck	[7647-01-0]	Reduction of Se(VI) to Se(IV)
NH <sub>3</sub>	2.0 M	Merck	[7664-41-7]	Synthesis of CeO <sub>2</sub> and ZrO <sub>2</sub>
NH <sub>4</sub> Cl	0.1 M	Sigma	[12125-02-9]	Desorption of Se(IV) and Se(VI) from CeO <sub>2</sub> and ZrO <sub>2</sub>
K <sub>2</sub> HPO <sub>4</sub>	0.1 M	Sigma-Aldrich	[7758-11-4]	Desorption of Se(IV) from CeO <sub>2</sub> and ZrO <sub>2</sub>
HCl	1.0 M	Merck	[7647-01-0]	Desorption of Se(IV) from CeO <sub>2</sub> and ZrO <sub>2</sub>

(cont. on next page)

Table 2.3. (Cont.)

Reagent	Concentration used	Company	Cas no.	Purpose of use
HCl	0.1 M	Merck	[7647-01-0]	Desorption of SeCys and SeMet from Amberlite IR-120
NH <sub>3</sub>	0.1 M	Merck	[7664-41-7]	Desorption of Se(IV) and Se(VI) from CeO <sub>2</sub> and ZrO <sub>2</sub>
NH <sub>3</sub>	0.5 M	Merck	[7664-41-7]	Desorption of Se(IV) and Se(VI) from CeO <sub>2</sub> and ZrO <sub>2</sub>
Acetic acid (Glacial)	0.1 M	Riedel-de Haen	[64-19-7]	Desorption of Se(IV) from CeO <sub>2</sub> and ZrO <sub>2</sub>
NaOH (pellets)	0.1 M	Sigma-Aldrich	[1310-73-2]	Desorption of Se(IV) and Se(VI) from CeO <sub>2</sub> and ZrO <sub>2</sub>
NaOH (pellets)	0.1 M	Sigma-Aldrich	[1310-73-2]	Desorption of Se(IV), Se(VI) and SeCys from nZVI and nZVI Modified ZrO <sub>2</sub>
NaOH (pellets)	0.5 M	Sigma-Aldrich	[1310-73-2]	Desorption of Se(IV) and Se(VI) from CeO <sub>2</sub> and ZrO <sub>2</sub>
Absolute Ethanol		Sigma	[64-17-5]	Synthesis of nZVI and nZVI modified ZrO <sub>2</sub>
Absolute Ethanol		Sigma	[64-17-5]	Washing of nZVI and nZVI modified ZrO <sub>2</sub>

### **2.3. Aqueous Calibration Plot**

Standard solutions from  $0.0050 \text{ mgL}^{-1}$  to  $0.10 \text{ mgL}^{-1}$  were prepared from  $1000.0 \text{ mgL}^{-1}$  Se(IV), Se(VI),  $1490.0 \text{ mgL}^{-1}$  Seleno-L-Cystine and  $547.5 \text{ mgL}^{-1}$  Seleno-DL-Methionine respectively with simple dilution. All standards contained 1.0% (v/v)  $\text{HNO}_3$  and measured with ICP-MS. For the desorption study of Se(IV), HGAAS was used as the detection method. Standard solutions from  $0.0050 \text{ mgL}^{-1}$  to  $0.050 \text{ mgL}^{-1}$  were prepared from  $1000.0 \text{ mg L}^{-1}$  Se(IV). For the desorption of Se(IV), NaOH was used and for observing selenium signal, reduction step was needed in which 5% HCl was used for both standards and samples. For determination of Se(VI) 0.10 M of  $\text{NH}_4\text{Cl}$  solution was used. Selenium signal was obtained for Se(VI) by reducing to Se(IV) by adding 6 M HCl into the sample solutions and standards and heating for 30 minutes at  $80^\circ\text{C}$ . In addition the limit of detection (LOD) based on 3s (3 times the standard deviation above the blank value) and limit of quantification (LOQ) based on 10s were also evaluated for both detection methods.

### **2.4. Synthesis of Sorbents**

Different types of sorbents were synthesized for both batch type and column type sorption.

#### **2.4.1. Synthesis of $\text{CeO}_2$ and $\text{ZrO}_2$ Particles**

Two different methods were used for synthesis of  $\text{CeO}_2$  and  $\text{ZrO}_2$  particles which were sol-gel and hydrothermal synthesis.

##### **2.4.1.1. Sol-gel Synthesis**

In the synthesis of  $\text{CeO}_2$  by sol-gel method (Zhong et al., 2006), 3.0 g of  $\text{Ce}(\text{NO}_3)_3 \cdot 6\text{H}_2\text{O}$  were dissolved in 250.0 ml ethyleneglycol, 6.0 g CTAB and 2.2 g urea were added into reaction mixtures. Constant reflux was obtained at  $180^\circ\text{C}$  temperature

for 12 hours. After that, particles were washed with ultra pure water to neutralize the surface of ceria. The pH of the solution was controlled with pH paper regularly to check if it becomes neutral. And then it was dried in oven at 120 °C for 24 hours. Calcination was done to remove CTAB at 500 °C.

ZrO<sub>2</sub> was synthesized by dissolving 3.0 g ZrCl<sub>4</sub> in 150.0 ml water/ethanol mixture 6.0 g CTAB and 12.5% NH<sub>3</sub> solution were added to reaction mixture. Constant reflux was obtained at 110°C temperature for 12 hours. After washing and centrifuge, the precipitate was dried in oven at 50°C. Calcination was done to remove CTAB at 500 °C. The apparatus used in the synthesis is illustrated in Figure 2.3.

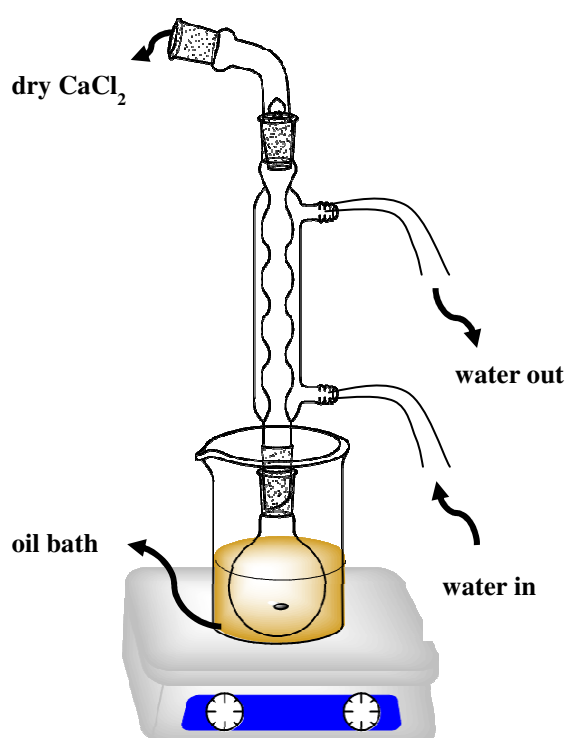


Figure 2.3. Apparatus used in the synthesis of the sorbents.

#### 2.4.1.2. Hydrothermal Synthesis

In a typical synthesis that is illustrated in Figure 2.4, 0.5 g Ce(NO<sub>3</sub>)<sub>3</sub> .6H<sub>2</sub>O and 1.5 g CTAB were dissolved in a 3.0 mL of water and 5.0 % (v/v) ammonia solution was added. Pale yellow amorphous CeO<sub>2</sub> was precipitated and after 30 minutes stirring at room temperature, mixed slurry was transferred into 23.0 mL autoclave and hydrothermal synthesis technique was applied for 160 °C for 16 hours in oven.

Autoclaves were allowed to cool slowly to room temperature and product was washed with water and dried at 60°C. Calcination was done to remove CTAB at 500 °C.

Hydrothermal synthesis was applied to synthesis of ZrO<sub>2</sub> particles, 0.5 g ZrCl<sub>4</sub> and 1.5 g CTAB were dissolved in a 3.0 mL of water and 5.0 % (v/v) ammonia solution was added. White amorphous ZrO<sub>2</sub> was precipitated and same procedure was done.

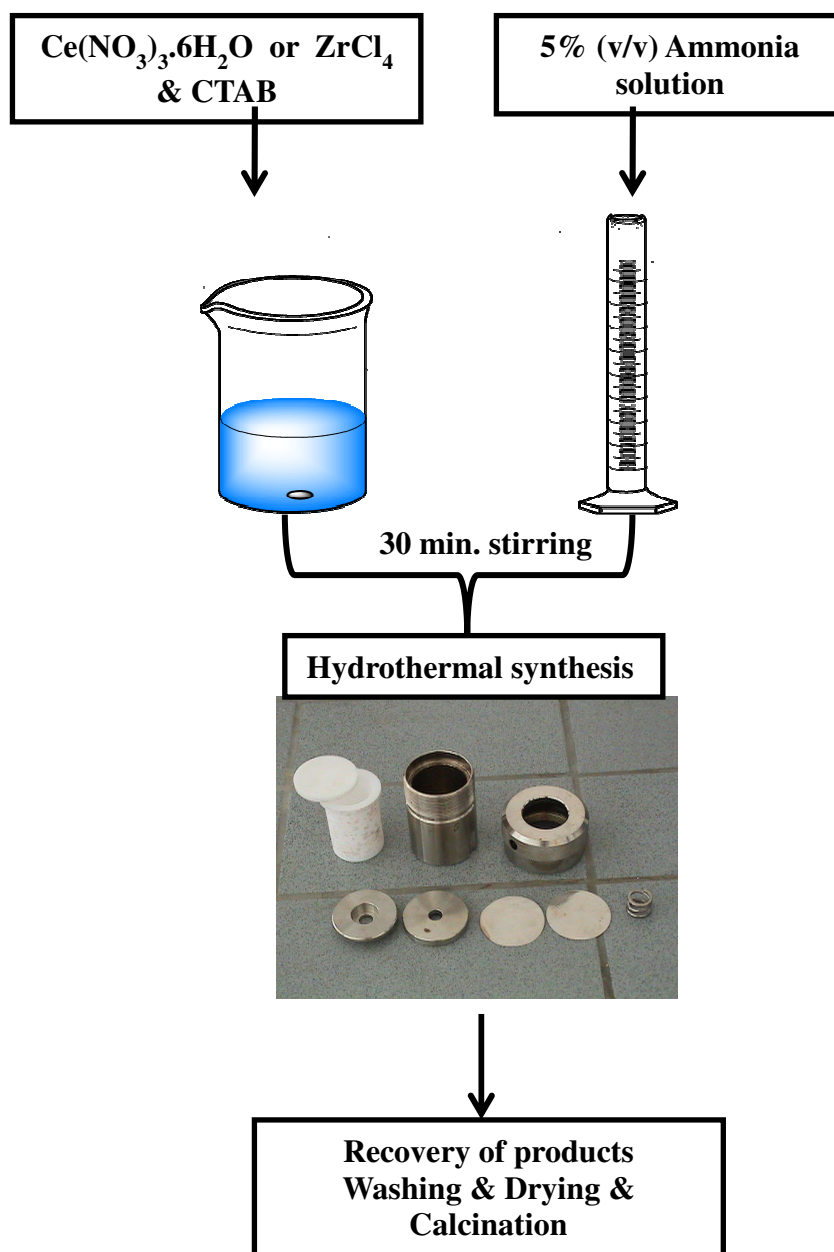


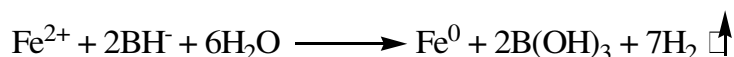
Figure 2.4. Block diagram of the procedure used during the synthesis.



## 2.4.2. Synthesis of Nanoscaled Zero-Valent Iron (nZVI) and nZVI Modified ZrO<sub>2</sub>

### 2.4.2.1. Nanoscaled Zero-Valent Iron (nZVI)

The synthesis of nZVI used in this work was done using borohydride reduction of Fe(II) (Zhang et al 2001). For this purpose, 5.34 g FeCl<sub>2</sub>.4H<sub>2</sub>O was dissolved in a 4/1 (v/v) ethanol/water mixture (24.0 ml ethanol + 6.0 ml deionized water) and stirred on a magnetic stirrer. On the other hand, 3.00 g NaBH<sub>4</sub> was dissolved in 100.0 ml of deionized water. The borohydride solution was poured in a burette, and then added dropwise to the Fe<sup>2+</sup> solution, while still stirring on magnetic stirrer. Black solid particles immediately appeared after the first drop of sodium borohydride solution. After adding the whole borohydride solution, the mixture was left for further 10 minutes of stirring. The redox reaction can be represented by :



To separate the black iron nanoparticles from the liquid phase, vacuum filtration Technique was used. Two sheets of blue band Whatman filter papers were used infiltration. At this point, solid particles were washed with absolute ethanol to remove all of the water. Synthesized nanoparticles were finally dried in oven at 50 °C overnight. Drying in evacuated ovens must be avoided because this would cause Fe nanoparticles to spontaneously ignite upon exposure to air.

### 2.4.2.2. Nanoscaled Zero-Valent Iron (nZVI) Modified ZrO<sub>2</sub>

To synthesis of nZVI modified zirconia particles, iron(II) chloride tetrahydrate (FeCl<sub>2</sub>. 4H<sub>2</sub>O) and sodium borohydride (NaBH<sub>4</sub>) were used for iron(II) and borohydride sources respectively. 5.34 g FeCl<sub>2</sub>.4H<sub>2</sub>O was dissolved in a 4/1 (v/v) ethanol/water mixture (24.0 ml ethanol + 6.0 ml deionized water). Then 3.0 g ZrO<sub>2</sub> was added to this solution and the mixture was held on a magnetic stirrer to be mixed for 24 hours. After that process, mixed slurry was washed with water to remove excess Fe<sup>2+</sup> solution. After

removal of excess  $\text{Fe}^{2+}$ , 3.0 % (m/v)  $\text{NaBH}_4$  solution was added into treated sorbent drop by drop. After adding the first drop of sodium borohydride solution Black solid particles were observed. After the addition of the borohydride solution was completed, the mixture was left for excess 10 minutes of stirring. Apparatus used in synthesis of nZVI modified zirconia is given in Figure 2.5. To separate the black iron nanoparticles from the liquid phase, vacuum filtration was used. Two sheets of blue band Whatman filter papers were used in filtration. At this stage, solid particles were washed absolute ethanol to remove all of the water. Last step of the synthesis is to dry the synthesized nanoparticles in oven at  $50^\circ\text{C}$  overnight.

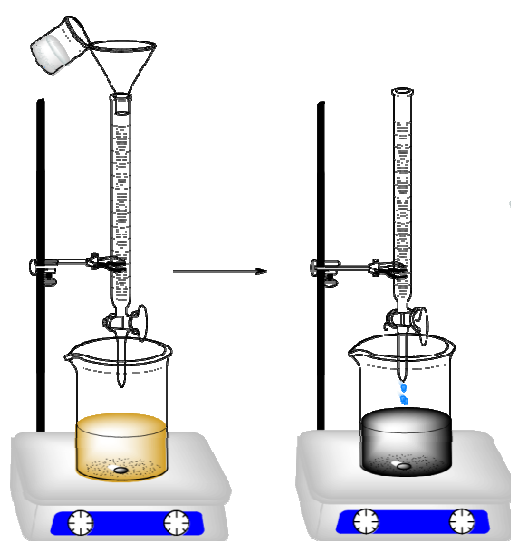


Figure 2.5. Apparatus used in the synthesis of ZVI-modified  $\text{ZrO}_2$ .

### 2.4.3. Synthesis Alginate Beads Immobilized with $\text{CeO}_2$ and $\text{ZrO}_2$ Particles

In order to use in column type studies, alginate beads were synthesized and modified with  $\text{CeO}_2$  and  $\text{ZrO}_2$ . These synthesis were done with three different ways, namely, A,B,C. Pathway of these synthesis is illustrated in Figure 2.6

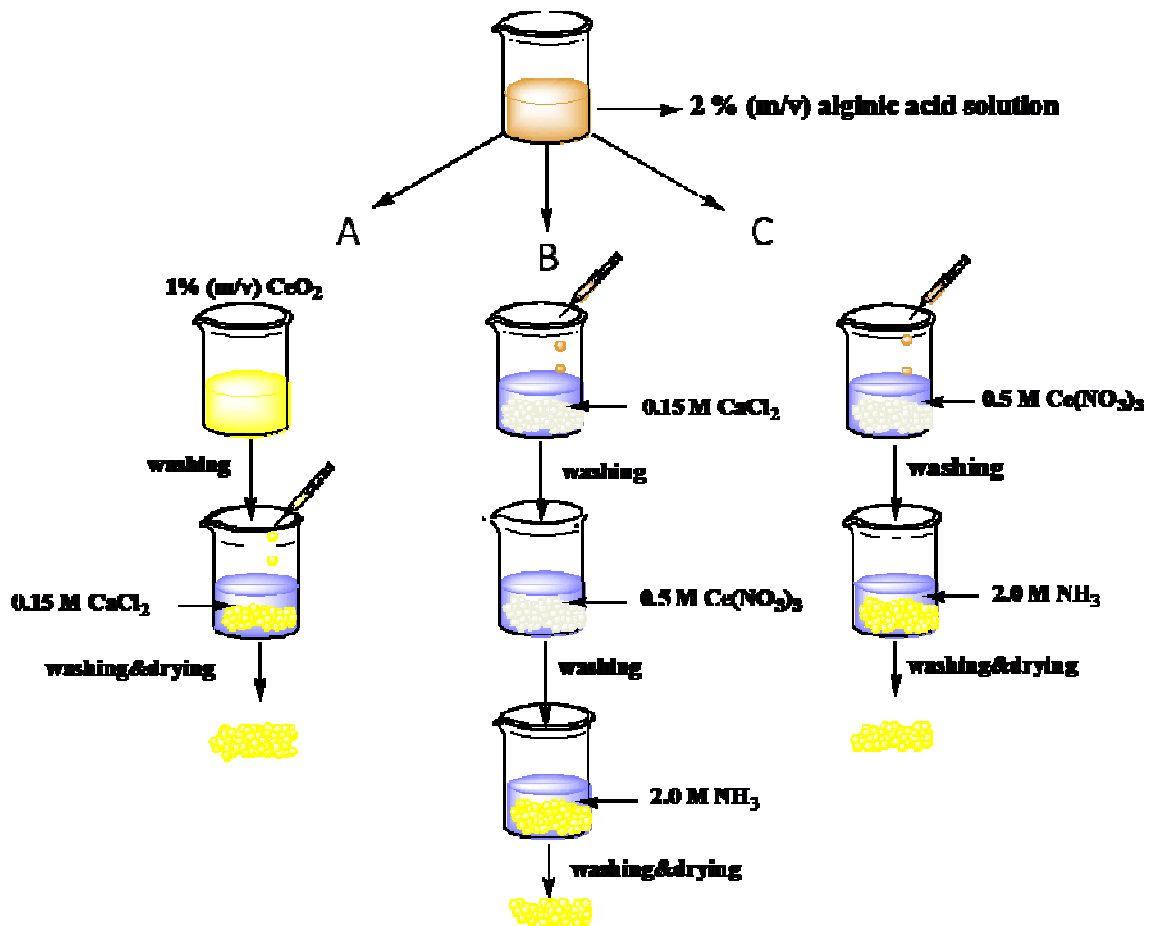


Figure 2.6. Pathway of the synthesis, (a) Method A (b) Method B (c) Method C.

### 2.4.3.1. Synthesis of Alginate beads

To synthesis only calcium alginate beads, 1.00 g of sodium alginate was dissolved in 50.0 mL ultrapure water (UPW) at room temperature. The alginate–water mixture was stirred until dissolution was completed (20–30 min) and left at room temperature for 30 min. The mixture was added into a 0.15 M aqueous solution of  $\text{CaCl}_2$  at room temperature using a syringe. As soon as the alginate drops came in contact with the  $\text{CaCl}_2$  solution, Ca-alginate gel beads were formed. The gel beads were retained in  $\text{CaCl}_2$  solution for 12h for hardening and then washed with UPW.

### **2.4.3.2 Method A**

In the method A, One gram of sodium alginate was dissolved in 50.0 mL ultrapure water (UPW) at room temperature. The alginate solution (2.0%, w/v) was gently mixed with 1.0 g of commercial CeO<sub>2</sub> and ZrO<sub>2</sub>, respectively. The mixed slurries were dropped into 0.15 M aqueous solution of CaCl<sub>2</sub> using a syringe. As soon as the alginate drops came in contact with the CaCl<sub>2</sub> solution, Ca-alginate gel beads were formed. To ensure that almost all ZrO<sub>2</sub> and CeO<sub>2</sub> were entrapped the alginate solution with ZrO<sub>2</sub> and CeO<sub>2</sub> mixture was continuously stirred with a glass rod. The leftover ZrO<sub>2</sub> and CeO<sub>2</sub> were washed with UPW. The gel beads were retained in CaCl<sub>2</sub> solution for 24 h for hardening and then washed with UPW. Materials as a result of this synthesis are named as CeO<sub>2</sub>-Ca-alginate hybrid sorbent and ZrO<sub>2</sub>-Ca-alginate hybrid sorbent.

### **2.4.3.3. Method B**

In the second method, synthesised calcium-alginate beads were mixed with 0.5 M Ce(NO<sub>3</sub>)<sub>3</sub>·6H<sub>2</sub>O and ZrCl<sub>4</sub> solutions over a night, respectively. After that, excess ions were removed by washing them with ultrapure water. To obtain ZrO<sub>2</sub> and CeO<sub>2</sub> modified particles, beads were retained in 2.0 M NH<sub>3</sub> solution for 24 hour. Finally synthesized CeO<sub>2</sub> doped yellow alginate beads and ZrO<sub>2</sub> doped white alginate beads were dried in oven at 50 °C for 24 h. Materials as a result of this synthesis is named as Ca-alginate beads immobilized with CeO<sub>2</sub> and Ca-alginate beads immobilized with ZrO<sub>2</sub>

### **2.4.3.4. Method C**

In method C, 2 % (w/v) sodium alginate solution in ultra pure water was prepared same as previous sections but alginate beads were formed at 0.5 M Ce(NO<sub>3</sub>)<sub>3</sub> and ZrCl<sub>4</sub> solutions instead of 0.15 M aqueous solution of CaCl<sub>2</sub>, by dropping. Ce-alginate gel beads and Zr-alginate gel beads were obtained. These beads were retained in the solution for 24 hour for hardening and then washed with ultrapure water. Hardened beads were taken into 2.0 M aqueous solution of ammonia for 24 h. Finally,

yellow(ceria) and white(zirconia) beads were dried in oven at 50 °C for 24 h. Novel sorbents as a result of this synthesis is named as CeO<sub>2</sub>+Alginate beads and ZrO<sub>2</sub>-Alginate beads.

## 2.5. Sorption Studies

Sorption studies were performed for all the sorbents prepared through batch process and column process. Standard solutions in 5.0, 10.0, 25.0, 50.0 and 100.0 µgL<sup>-1</sup> concentrations were prepared. Before ICP-MS determination, all samples and standard solutions were acidified with the addition of appropriate amount of concentrated HNO<sub>3</sub> to produce 1.0% (v/v) HNO<sub>3</sub> in the final solution. The percentage of selenium sorption was calculated using equation 2.1, where C<sub>i</sub> is the initial and C<sub>f</sub> is the final concentration in the solution.

$$\text{Sorption \%} = \frac{C_i - C_f}{C_i} \times 100\% \quad (2.1)$$

### 2.5.1. Studies Utilizing Commercially Available CeO<sub>2</sub> and ZrO<sub>2</sub>

In this study, commercially available CeO<sub>2</sub> ve ZrO<sub>2</sub> were used as sorbent for the sorption of Se(IV), Se(VI), Seleno-L-methionine ve Seleno-L-cystine. The studied parameters and range were given in Table 2.3.

Table 2.3. Studied parameters and range.

	Range
Solution pH	1,0, 2,0, 3,0, 4,0, 5,0, 6,0, 8,0, 10,0, 11,0, 12,0
Amount of sorbent (mg)	5,0, 10,0, 25,0, 50,0 ve 100,0
Shaking Time (min)	1, 5, 15, 30, 60 ve 120
Temperature (°C)	25, 50, 75
Initial concentration (mg/L)	0,1, 1,0, 10,0, 50,0 ve 100,0

Solution pH is one of the most important parameters on the sorption of Se species by the sorbents. In order to investigate the effect of pH on the sorption of

Se(IV), Se(VI), SeCys and SeMet,  $100 \mu\text{gL}^{-1}$  standard solutions were prepared. Dilute  $\text{HNO}_3$  and  $\text{NH}_3$  were used to adjust the pH at 1.0, 2.0, 3.0, 4.0, 5.0, 6.0, 7.0, 8.0, 9.0, 10.0, 11.0, and 12.0. From each of these solutions 20.0 mL were taken into centrifuge tube which 50.0 mg of  $\text{CeO}_2$  and  $\text{ZrO}_2$  were added, respectively. The mixture was first shaken for 1-2 minutes manually and then for 30.0 minutes on the thermostated water bath shaker at  $25^\circ\text{C}$ . After the solid and the liquid phases were separated by filtration and the remaining selenium species were determined with ICP-MS. Rest of these experiments for this section only applied to inorganic selenium species because organoselenium species did not retain on the surface of ceria and zirconia.

### **2.5.1.2. Effect of Shaking Time**

Effect of shaking time on the sorption of Se(IV) and Se(VI) by  $\text{CeO}_2$  and  $\text{ZrO}_2$  were investigated for time intervals of 1, 5, 15, 30, 60 and 120 min. Other parameters were kept constant at  $100.0 \mu\text{gL}^{-1}$  selenium concentration, 20.0 ml solution volume, 50.0 mg sorbent amount and  $25^\circ\text{C}$  sorption temperature. Sorption experiments were carried out at the pH 2.0 that was chosen for both Se (IV) and Se (VI).

### **2.5.1.3. Effect of Sorbent Amount (Solid/Liquid Ratio)**

The effect of sorbent amount was investigated for both ceria and zirconia with the use of 5.0, 10.0, 25.0, 50.0, and 100.0 mg while the other parameters were fixed at  $100.0 \mu\text{gL}^{-1}$  selenium concentration, 30 min shaking time, 20.0 mL solution volume, and  $25.0^\circ\text{C}$  sorption temperature. Experiments were carried out at pH 2.0.

### **2.5.1.4. Effect of Reaction Temperature**

The sorption efficiency of a sorbent towards a particular sorbate may change with the reaction temperature. Therefore, effect of the temperature on the sorption of selenium was investigated for both  $\text{CeO}_2$  and  $\text{ZrO}_2$  at  $25^\circ\text{C}$ ,  $50^\circ\text{C}$  and  $75^\circ\text{C}$  and the other parameters were fixed at  $100.0 \mu\text{gL}^{-1}$  selenium concentration, 20.0 mL solution volume, 50.0 mg sorbent amount and pH 2.0. The thermodynamic parameters of

sorption ( $\Delta G^\circ$ ,  $\Delta S^\circ$  and  $\Delta H^\circ$ ) were also investigated as The results of these experiments were also used to investigate the thermodynamic parameters of sorption utilizing the well-known equations 2.2, 2.3 and 2.4 (Atkins and de Paula 2002; Yersel et al2005):

$$\Delta G^\circ = -RT \ln R_d \quad (2.2)$$

$$\Delta H^\circ = R \ln \frac{R_d(T_2)}{R_d(T_1)} \left( \frac{1}{T_1} - \frac{1}{T_2} \right)^{-1} \quad (2.3)$$

$$\Delta S = \frac{\Delta H^\circ - \Delta G^\circ}{T} \quad (2.4)$$

$R_d$  (mL g<sup>-1</sup>) is the ratio of selenium ions distributed between solid (sorbent) and liquid phase at equilibrium and is defined by the Equation 2.5.

$$R_d = \frac{C_{solid}}{C_{liquid}} \quad (2.5)$$

$C_{solid}$  is the concentration of selenium in sorbent (mg g<sup>-1</sup>) and  $C_{liquid}$  is the concentration of selenium ions in solution after sorption (mg L<sup>-1</sup>).

### 2.5.1.5. Initial Concentration

The sorption efficiency of CeO<sub>2</sub> and ZrO<sub>2</sub> were also investigated for initial Se(IV) and Se(VI) concentrations of 0.010, 0.10, 1.0, 10.0, 50.0 and 100 mgL<sup>-1</sup>. For this purpose, 20.0 mL of these solutions (at pH 2.0) were taken and 50.0 mg of sorbent was added to each of them. Then the mixtures were shaken for 30.0 minutes on the shaker at 25.0 °C. After filtration, the filtrates were analyzed with ICP-MS.

### **2.5.1.6. Repetitive Loading**

Sequential (10 times) sorption of Se(IV) and Se(VI) standard solutions by commercial CeO<sub>2</sub> and ZrO<sub>2</sub> was investigated at 100.0 µgL<sup>-1</sup> concentrations. Solution volume, shaking time, solution pH, sorbent amount and reaction temperature were 20.0 mL, 30 min, pH=2.0, 50.0 mg, and 25°C, respectively. After shaking, the solution was centrifuged for 5 minutes at 6000 rpm, and the remaining solutions were analyzed by ICP-MS for selenium determination.

### **2.5.1.7. Desorption Studies**

Desorption of Se(IV) and Se(VI) species from CeO<sub>2</sub> and ZrO<sub>2</sub> were investigated for various eluents. Desorption matrices have been chosen according to the desorbing solution in which sorbent is dissolved or not. Desorption eluents were given in table 2.4. Standards for drawing calibration curve were prepared in the same matrix of each desorption solutions. Both ICP-MS and HGAAS were used. For selenium determination especially for heavy matrices with Se (IV) solution, HGAAS was used. Before HGAAS both samples and standards were acidified with concentrated HCl to produce 1.0% (v/v) of HCl in the final solution. For reduction of Se (IV) standards and solutions, HCl was added to produce 5% (w/v) in the solution. Selenium signal was obtained for Se (VI) by reducing to Se(IV) by adding 6.0 M HCl into the sample solutions and standards and heating for 30 minutes at 80 °C.



Table 2.4. Desorption Eluents for CeO<sub>2</sub> and ZrO<sub>2</sub>.

Eluent
0.2% (m/v) KIO <sub>3</sub> in 1.0 M HCl
1.0 M HCl
1.0 M HNO <sub>3</sub>
1.0 M CH <sub>3</sub> COOH
0.1 M KH <sub>2</sub> PO <sub>4</sub>
0.1 M NH <sub>3</sub>
0.5 M NH <sub>3</sub>
0.1 NaOH
0.5 M NaOH
0.1 M NH <sub>4</sub> Cl

### 2.5.1.8. Method Validation and Spike Recovery Experiments

The sorption efficiency of sorbents was investigated using the spiked samples of distilled, bottled drinking and tap water. This was realized by spiking 20.0 mL aliquots of ultrapure, bottled drinking, and tap water samples with 100.0 µg L<sup>-1</sup>Se (IV) and Se (VI) solutions and applying the batch process for both CeO<sub>2</sub> and ZrO<sub>2</sub> sorbents. Selenium ion concentration, solution volume, shaking time, solution pH, sorbent amount and reaction temperature were 100.0 µg L<sup>-1</sup>, 20.0 mL, 30 min, pH 2.0, 50.0 mg, and 25 °C, respectively.

Selenate ions did not retain on the surface of sorbents so the sorption and desorption studies were performed by reduction of Se(VI) to Se(IV). From the total selenium, selenate ion concentration can be calculated. Selenium ion concentration, solution volume, shaking time, solution pH, sorbent amount and reaction temperature

were  $100.0 \mu\text{gL}^{-1}$  and  $10.0 \mu\text{gL}^{-1}$ , 20.0 mL, 30 min, pH 2.0, 50.0 mg, and 25 °C, respectively.

### **2.5.2. Sorption Studies Using Synthesized $\text{CeO}_2$ and $\text{ZrO}_2$ (Sol-gel and Hydrothermal Methods)**

Synthesized  $\text{CeO}_2$  and  $\text{ZrO}_2$  were used as sorbent for inorganic selenium species. Optimum parameters were obtained from previously done experiments which Selenium ion concentration, solution volume, shaking time, solution pH, sorbent amount and reaction temperature were  $100.0 \mu\text{gL}^{-1}$ , 20.0 mL, 30 min, pH 2.0 and pH 8.0, 50.0 mg, and 25 °C, respectively.

### **2.5.3. Studies Utilizing nZVI and nZVI-Modified $\text{ZrO}_2$**

Sorption studies were performed for all the sorbents prepared; namely, zerovalent iron and zerovalent iron modified zirconia through batch process for both inorganic and organic selenium species. The sorption parameters were as follows;  $100 \mu\text{gL}^{-1}$  concentration of Se(IV), Se(VI), seleno-L-cystine and seleno-L-methionine, shaking time of 30 min, solution volume of 20.0 ml, sorption temperature of 25 °C, the solution pH of 4.0, 5.0, 6.0, 7.0, 8.0, 9.0 and 10.0. Filtrated solutions were analyzed in ICP-MS.

After sorption studies, desorption procedure only applied to Se(IV), Se (VI), seleno-L-cystine. For preliminary studies, 0.1 M NaOH was used as eluent for all sorbents. Prior to desorption studies, the sorption of three selenium species was performed at pH 8.0 where the maximum sorption was obtained for Se(IV), Se(VI), seleno-L-Cystine. The sorption parameters were as follows;  $100 \mu\text{g L}^{-1}$  concentration of Se(IV), Se(VI) and seleno-L-cystine shaking time of 30 min, solution volume of 20.0 ml, sorption temperature of 25 °C.

#### **2.5.4. Studies Utilizing Strong Ion Exchanger Amberlite IR-120 Resin**

Sorption studies were performed commercial strong ion exchanger amberlite IRA-120 through column process for both inorganic and organic selenium species. The sorption parameters were as follows; 100  $\mu\text{g L}^{-1}$  concentration of Se(IV), Se(VI), seleno-L-Cystine and seleno-L-Methionine, shaking time of 30 min, solution volume of 20.0 mL, sorption temperature of 25 °C, the solution pH of 2.0, 4.0, 6.0, 8.0 and 10.0. Filtrated solutions were analyzed in ICP-MS.

Desorption studies only were performed for organic selenium species because inorganic selenium species did not retain on IR-120 resin. This commercial resin can be regenerated with HCl or H<sub>2</sub>SO<sub>4</sub> so as preliminary study 0.1 M HCl was used as eluent. Prior to desorption studies, the sorption parameters were as follows; 100  $\mu\text{g L}^{-1}$  concentration of seleno-L-cystine and seleno-L-methionine shaking time of 30 min, solution volume of 20.0 mL, sorption temperature of 25 °C. Selenium solutions were prepared at pH 8.0 where the high sorption capacity was observed.

#### **2.5.5. Sorption studies of Alginate beads immobilized with CeO<sub>2</sub> and ZrO<sub>2</sub> particles**

The main purpose of CeO<sub>2</sub> and ZrO<sub>2</sub> particles immobilization to alginate matrix is to use in column-type studies is mentioned in previous synthesis section. Mini-columns were prepared with CeO<sub>2</sub> and ZrO<sub>2</sub> immobilized alginate beads which were synthesized by three different methods. To this end, tip of the glass pipette was sealed with the help of small sponge and beads held in water as column filling material were filled into glass pipette with 5.0 cm height. Column type sorptions were performed with 50.0 mL of 100.0  $\mu\text{g L}^{-1}$  Se(IV) or Se(VI) solutions. With the help of peristaltic pump, the solutions were passed through the column by the rate of 1.0 mL/dk and collected as 5.0-mililiter fractions. The pH of both Se(IV) and Se(VI) was adjust to 2.0, 3.0, 4.0, 5.0, 6.0, 7.0 ve 8.0.

## CHAPTER 3

### RESULTS AND DISCUSSION

#### 3.1. Characterization of the Sorbents

Characterization of the sorbents was carried out using scanning electron microscopy (SEM), X-Ray Diffraction (XRD), thermo gravimetric analysis (TGA), elemental analysis, infrared spectrometry and through the measurements of zeta potential.

##### 3.1.1. Commercial $\text{CeO}_2$ and $\text{ZrO}_2$

The surfaces of synthesized and commercial sorbents were investigated using scanning electron microscopy (SEM). Related images of  $\text{CeO}_2$  and  $\text{ZrO}_2$  particles are given in Figure 3.1. It can be mentioned that the morphology of these particles depends on the synthesis conditions. Both materials appear to be composed of agglomerated particles.

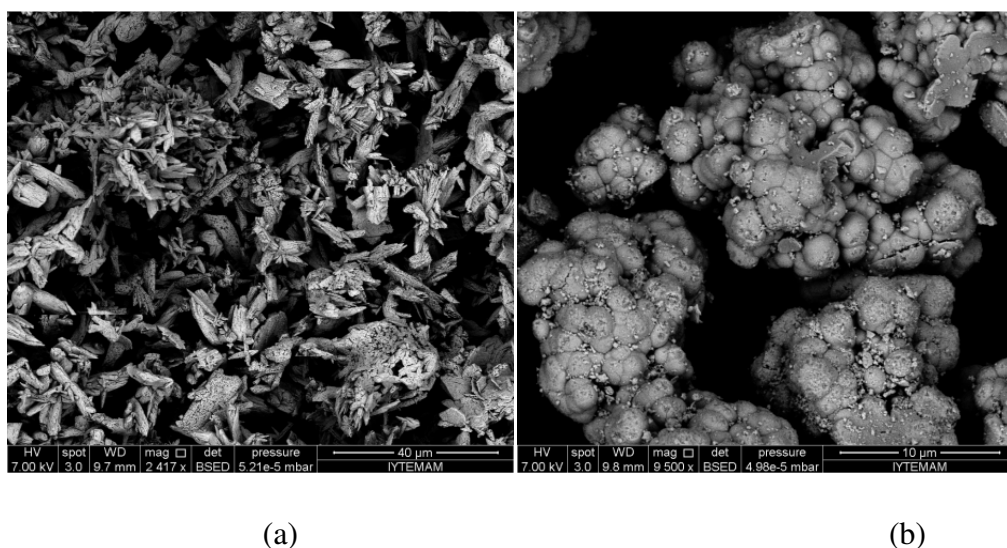


Figure 3.1. Typical SEM images of Ceria(a) and Zirconia (b).

Zeta potential of  $\text{ZrO}_2$  and  $\text{CeO}_2$  as a function of pH were determined in a way that a small portion of  $\text{ZrO}_2$  or  $\text{CeO}_2$  was added into distilled water and the mixture was shaken in ultrasonic bath for 30 minutes at room temperature. The average of 3 measurements was considered to represent the zeta potential (Figure 3.2). The magnitude of electrostatic interaction between the surfaces and the metal ions is a function of zeta potential. From the point of zero charge (pzc) value, the sign of surface charge is estimated, e.g., metal oxides are positively charged at  $\text{pH} < \text{pH}_{\text{pzc}}$  and negatively charged at  $\text{pH} > \text{pH}_{\text{pzc}}$ , and this helps in understanding the sorption phenomenon. It can clearly be seen that the two curves have similar characteristics in terms of zeta potential. In the case of  $\text{CeO}_2$ , the zeta potential value crosses pH axis at 2.4. The aqueous phase becomes slightly acidic (since it receives protons) whilst the ceria surface becomes positive. Similarly, zeta potential of zirconia increases as pH is lowered and it crosses pH axis at 2.8.

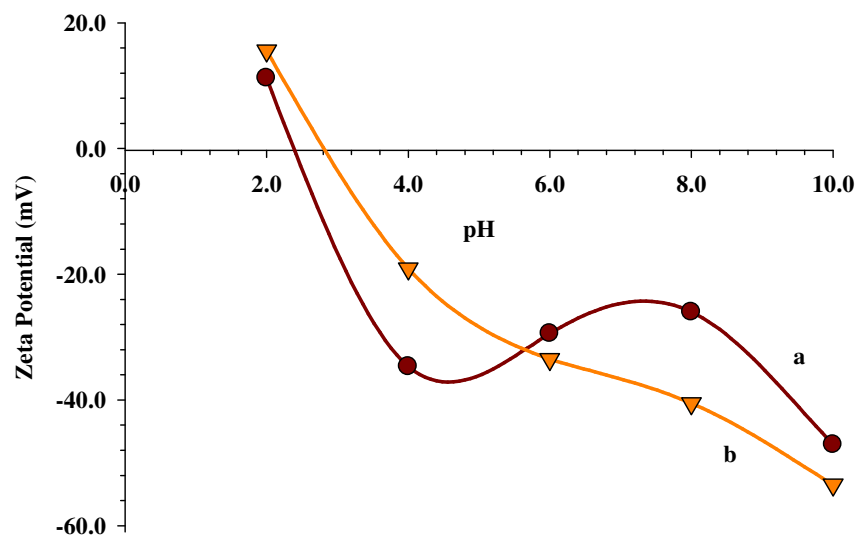


Figure 3.2. Effect of pH on zeta potential of (a)  $\text{CeO}_2$  and (b)  $\text{ZrO}_2$ .

### 3.1.2. Synthesized $\text{CeO}_2$ and $\text{ZrO}_2$

In the sol-gel synthesis of ceria particles, CTAB was used as both surfactant and shape-directing agent. However, the synthesized particles have 3D flower-like morphology (Figure 3.3(a)), possibly due to particle crystallization, electrostatic

association with the aggregates, van der Waals force, and hydrophobic interaction, Hydrogen bond formation may have also contributed to the final structure.

The SEM image of ceria obtained by hydrothermal method at 160 °C for 16 h (Figure 3.3(b)) indicates that nearly dispersed nanospheres with average diameter of 60 nm were produced. Hydrothermal synthesis conditions, such as temperature, time and use of surfactant play a very important role in the growth of various nanostructures. Therefore, different morphologies can be obtained by changing these parameters.

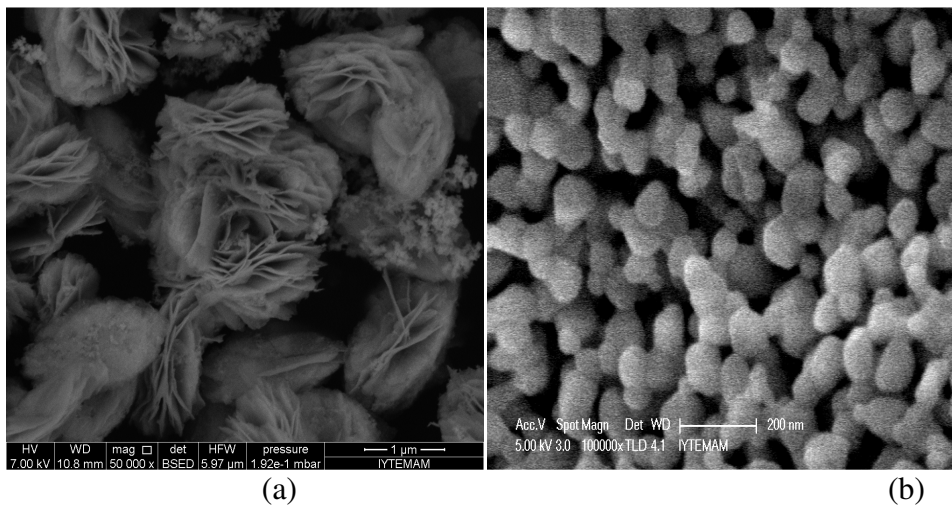


Figure 3.3. Typical SEM images of CeO<sub>2</sub> obtained through (a) sol-gel synthesis and (b) hydrothermal synthesis.

ZrO<sub>2</sub> nanoparticles with different morphologies can be obtained by reflux synthesis and hydrothermal processing. Figure 3.4(a) reveals that zirconia particles prepared by sol-gel method have nanosized particles which were not observed clearly because high magnification SEM images could not have been taken. On the other hand, as shown in Figure 3.4(b) a large number of spherelike ZrO<sub>2</sub> nanoparticles can be obtained through hydrothermal synthesis. It is verified that the sphere-like ZrO<sub>2</sub> nanoparticles represent an aggregation by interaction of van der Waals.

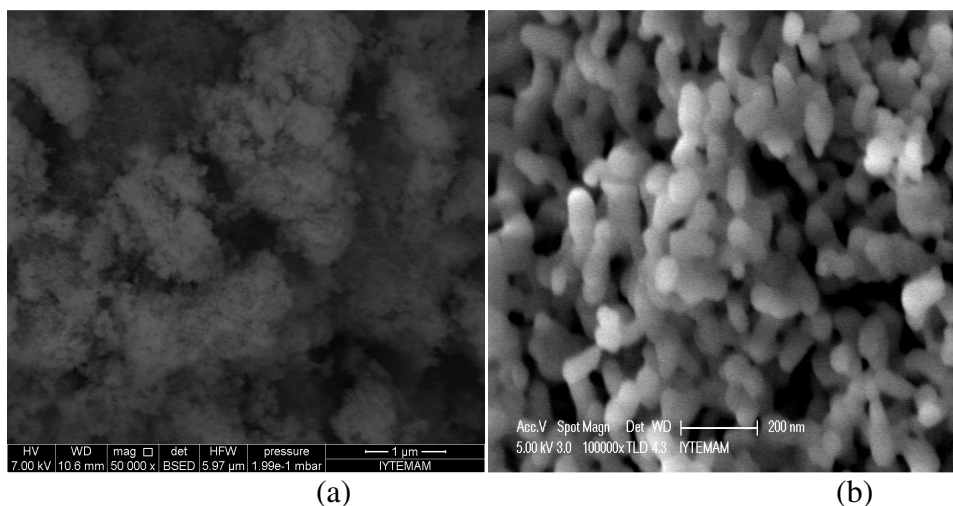


Figure 3.4. Typical SEM images of ZrO<sub>2</sub> obtained through (a) sol-gel synthesis and (b) hydrothermal synthesis.

The powder XRD patterns of CeO<sub>2</sub> were obtained by hydrothermal and sol-gel methods are given in Figure 3.5. Ceria prepared by sol gel route shows a strong low-angle reflection. All the diffraction peaks agreed well with the standard values, indicating that cerium oxide was successfully prepared via the employed procedures.

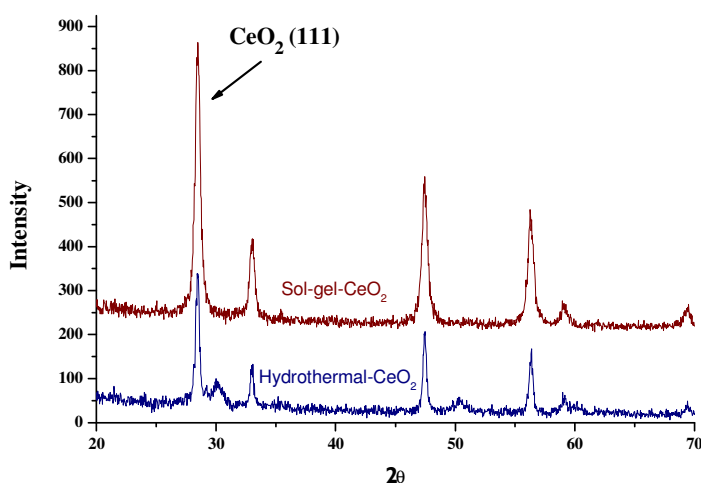


Figure 3.5. XRD patterns of CeO<sub>2</sub>. (Hydrothermal and Sol-gel Synthesis)

Figure 3.6 shows the XRD patterns of ZrO<sub>2</sub> nanopowders synthesized by hydrothermal and sol gel methods. In the XRD pattern of hydrothermally synthesized ZrO<sub>2</sub>, monoclinic structure is well defined. As a result of sol-gel synthesis, cubic structure of ZrO<sub>2</sub> was obtained. All the diffraction peaks agreed well with the standard

values in the literature, indicating that zirconium oxidesynthesis was successful. Different morphologies can be obtained by the different synthesis methods.

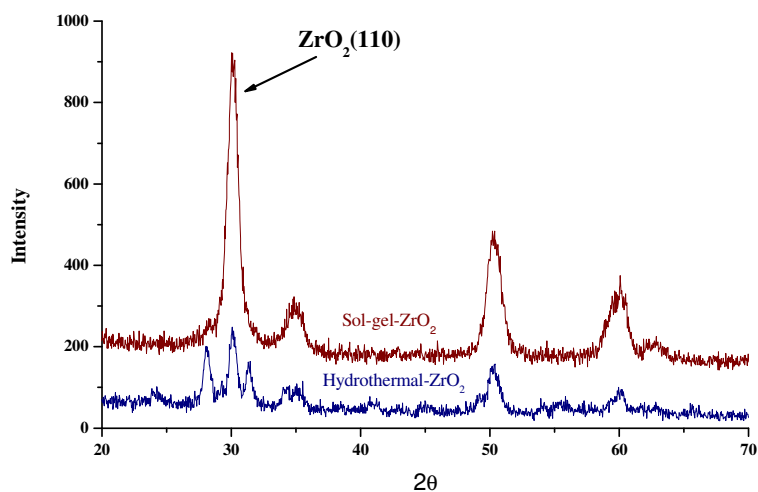
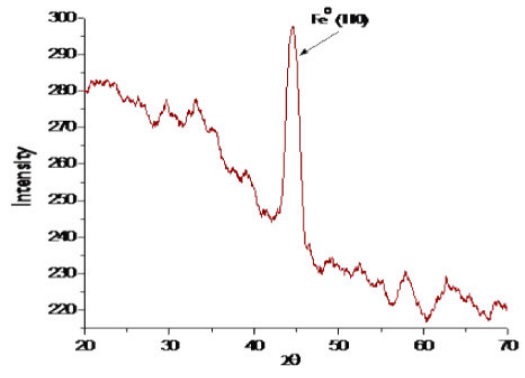
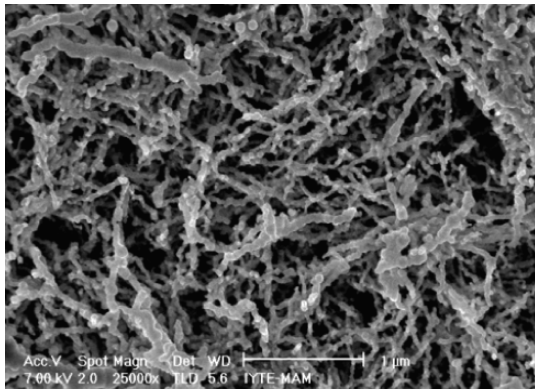


Figure 3.6. XRD pattern of ZrO<sub>2</sub>. (Hydrothermal and Sol-gel Synthesis)

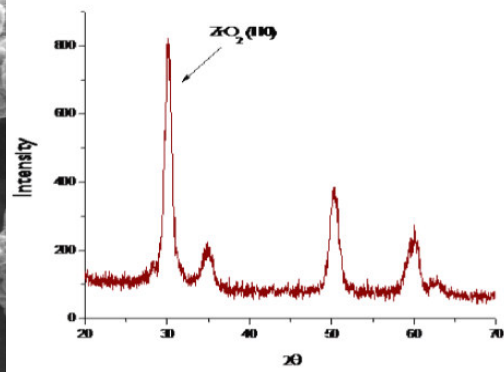
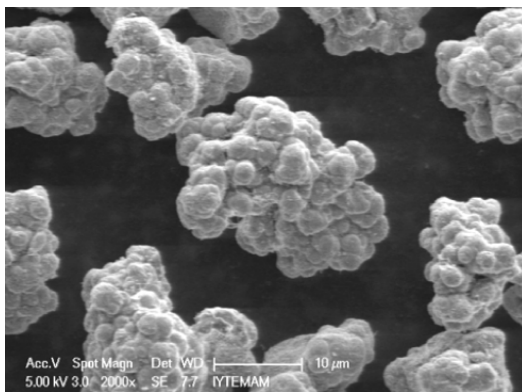
### 3.1.3. Nanoscaled Zero-Valent Iron and (nZVI) Modified ZrO<sub>2</sub>

To obtain larger surface area and immobilize the zero-valent iron, commercial zirconia and zero-valent iron were used. Although they are called “zero-valent iron nanoparticles”, it should be noted that the spherical iron particles form chain-like structures the length of which might be larger than a micron. SEM images and XRD pattern of synthesized iron nanoparticles are presented in Figure 3.7(a). The characteristic diffraction peak at  $2\theta$  angle of  $44.7^\circ$  belongs to zero-valent iron in the sorbent material Zirconia has agglomerated particles and Also specific diffraction peak of commercial zirconia is observed on the XRD pattern. (Figure 3.7(b)). A SEM image and XRD pattern of nZVI-ZrO<sub>2</sub> is presented in Figure 3.7(c). Chainlike aggregates of iron nanoparticles still exist but unlike pure nZVI, separated iron nanospheres can also be observed. The dispersion of nZVI does not look uniform. The XRD diffraction pattern indicates the presence of nZVI on zirconia. The diffraction line near  $44.7^\circ$  belongs to ZVI as in the case of pure nZVI. The other lines in the figure originate from the crystal structure of zirconia (basically 110 line).

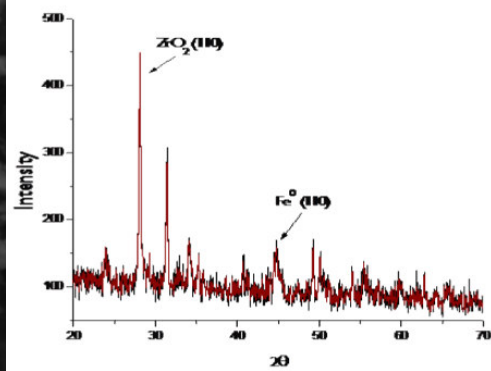
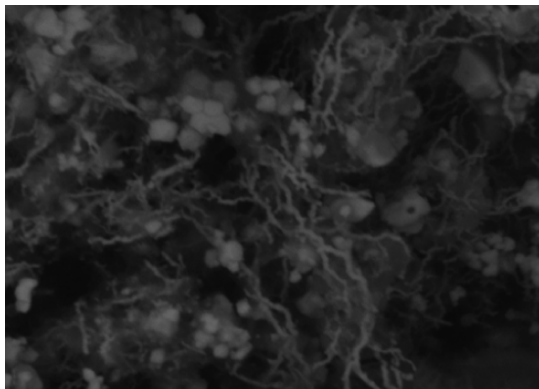




(a)



(b)



(c)

Figure 3.7. SEM images and XRD pattern of (a) nZVI, (b) ZrO<sub>2</sub> ve (c) nZVI-ZrO<sub>2</sub>.

To determine the point zero charge of iron nanoparticles and hybrid material, their zeta potential at various pH media were examined. The results are provided in Figure 3.8(a). The point zero charge (PZC), where the surface charge of iron nanoparticles is zero, arises nearly at pH 6.6. This is relatively a high PZC and means that within natural pH range, nZVI particles have negative surface charges. Point zero charge (PZC) of nZVI-ZrO<sub>2</sub> sample was determined by measuring the zeta potentials at various pH. The trend is given in Figure 3.8(b) and the PZC was determined as pH ~6.4. point zero charge of pure zirconia is found in previous section as pH 2.8.

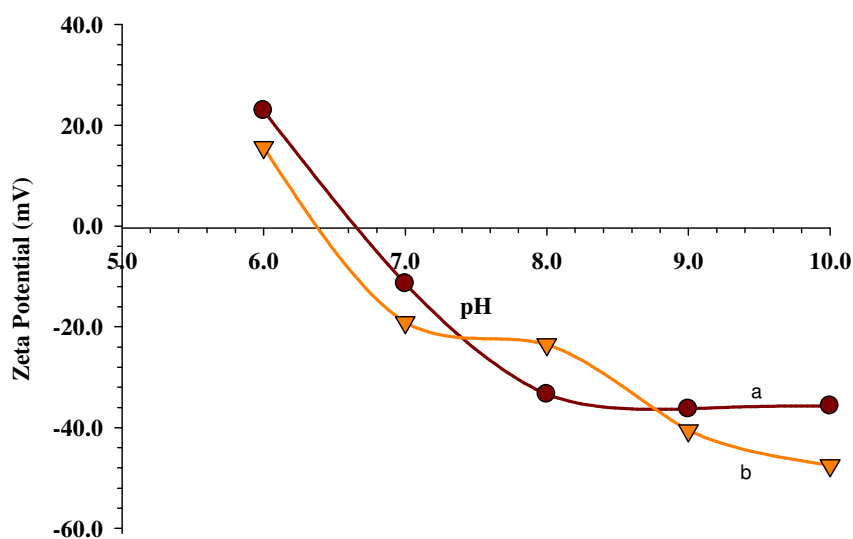
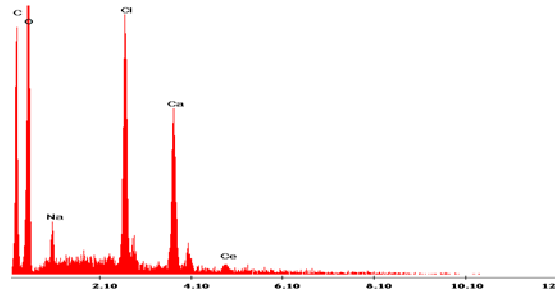
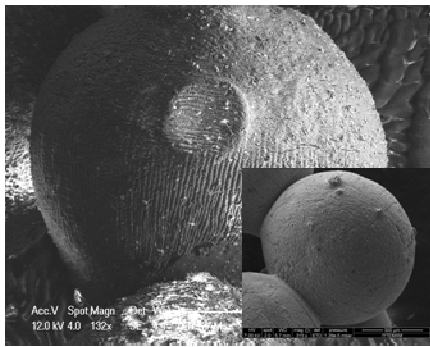


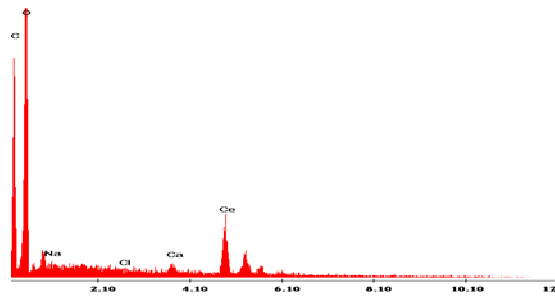
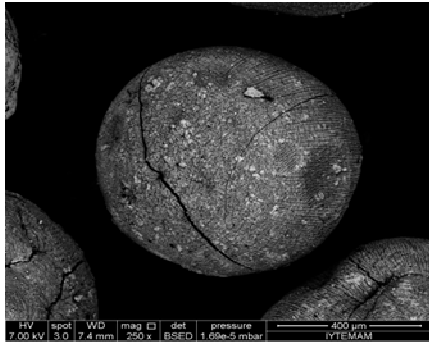
Figure 3.8. Effect of pH on zeta potential of (a) nZVI and (b) nZVI-ZrO<sub>2</sub>.

### 3.1.4. CeO<sub>2</sub> and ZrO<sub>2</sub> Modified Alginate Beads

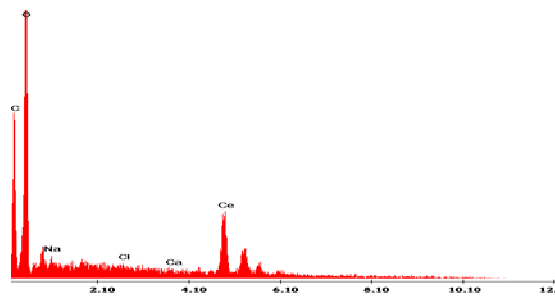
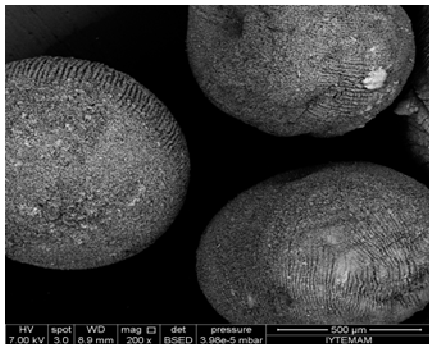
Characterization of the alginate-based sorbents prepared by three different procedures (Section 2.4.3) was first performed by scanning electron microscopy to gain information about the morphology of the alginate beads. Also, the diameter of the beads was approximately the same, around 800  $\mu\text{m}$ , for all structures. Method A is based on the entrapment of commercial cerium oxide powder into sodium alginate matrix. From the SEM images given in Figure 3.9 (a) it is hard to differentiate any changes in the morphology of the prepared beads but XRD results verified that entrapment of cerium oxide powder into alginate matrix successfully was achieved (Figure 3.10(a)).



(a)



(b)



(c)

Figure 3.9. SEM images of  $\text{CeO}_2$ -based alginate beads obtained by (a) Method A, (b) Method B, and (c) Method C. (Inserted figure in (a) is calcium-alginate bead used as blank.)

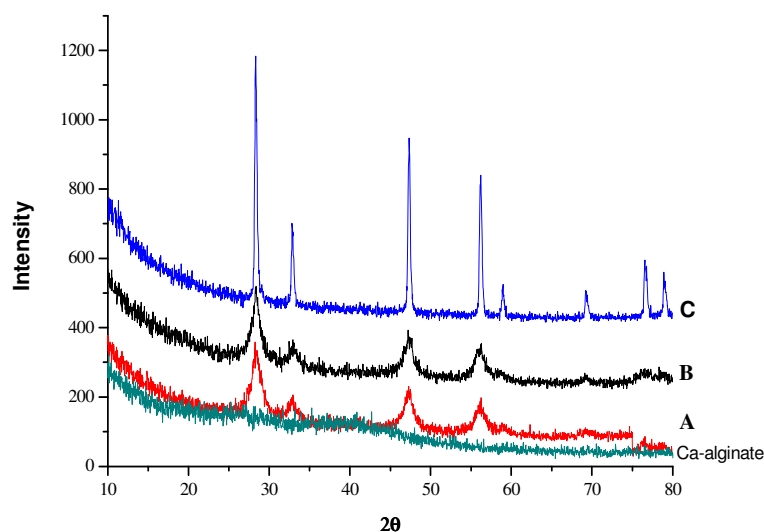
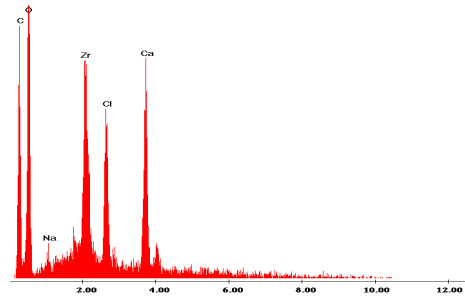
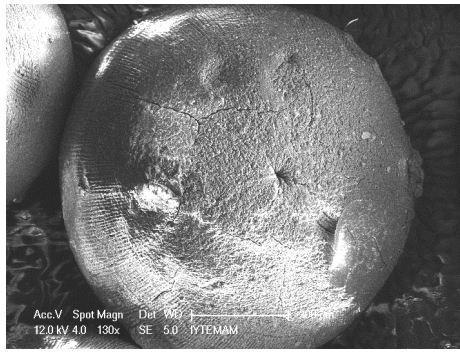


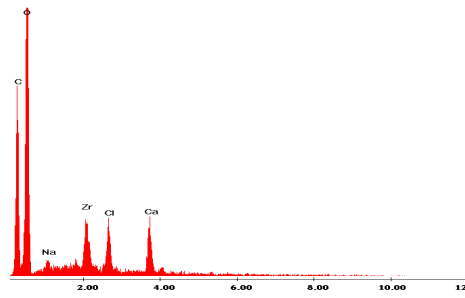
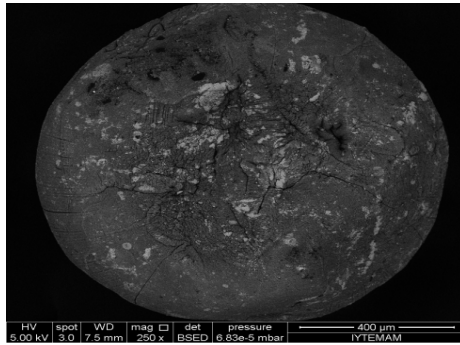
Figure 3.10. XRD graphs of  $\text{CeO}_2$ -based alginate beads obtained by (a) Method A, (b) Method B, and (c) Method C. (Inserted figure in graph is calcium-alginate bead used as blank.)

Figure 3.9(b) shows that the Ca-alginate beads immobilized with  $\text{CeO}_2$  (Method B) are spherical in shape and uniform in size with a mean diameter of about  $800 \mu\text{m}$ . When the SEM image (Figure 3.9(b)) and the XRD pattern (Figure 3.10(b)) of Ca-alginate beads immobilized with  $\text{CeO}_2$  are considered together, it can be mentioned that a relatively homogeneous surface was obtained and the characteristic peaks of  $\text{CeO}_2$  broaden due to the presence of Ca-alginate in the structure. The white spots seen on the figures belong to  $\text{CeO}_2$  crystals. EDX analysis also showed that high level of C, O, Cl and Ca are present in synthesized beads (Method B) with low content of cerium (Figure 3.9(b)).

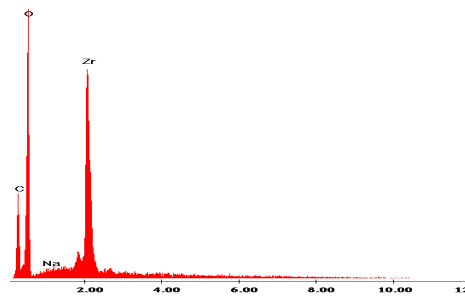
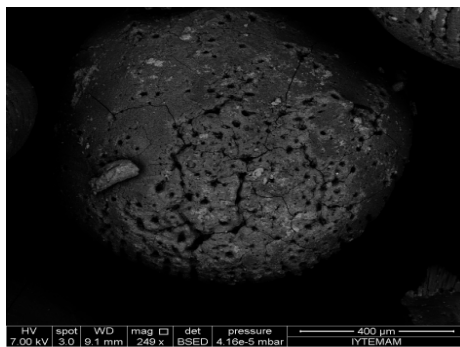
In Method C, Na-alginate was added, drop-by-drop, to  $\text{Ce}(\text{NO}_3)_3 \cdot 6\text{H}_2\text{O}$  instead of  $\text{CaCl}_2$  solutions. As can be seen in Figure 3.9(c), a quite homogeneous surface was obtained in the case  $\text{Ce}(\text{NO}_3)_3 \cdot 6\text{H}_2\text{O}$  and very clear characteristic XRD peaks seen in Figure 3.10(c) can still be demonstrating the presence of  $\text{CeO}_2$  in the structure. Moreover, EDX results confirmed the presence of C, O and Ce at high level in prepared material.



(a)



(b)



(c)

Figure 3.11. SEM images of  $ZrO_2$ -based alginate beads obtained by (a) Method A, (b) Method B, and (c) Method C. (Inserted figure in (a) is calcium-alginate bead used as blank.)

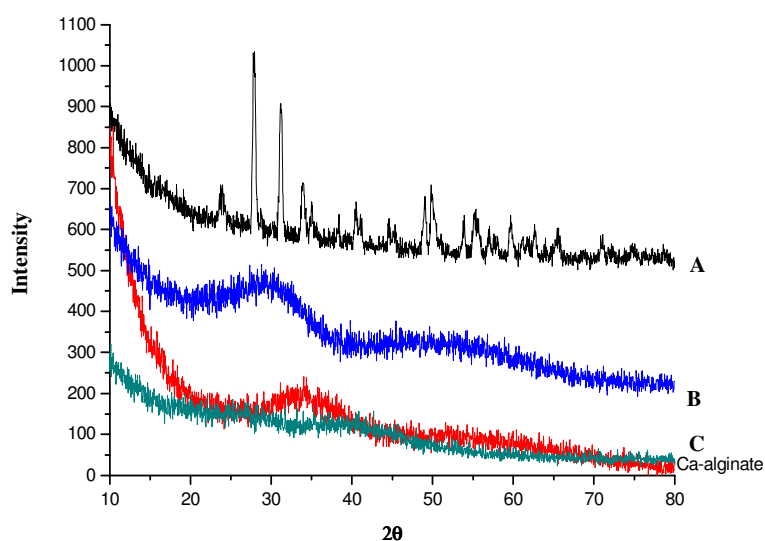


Figure 3.12. XRD graphs of  $ZrO_2$ -based alginate beads obtained by (a) Method A, (b) Method B, and (c) Method C. (Inserted figure in graph is calcium-alginate bead used as blank.)

SEM image was obtained for Ca-alginate beads immobilized with  $ZrO_2$  as shown in Figure 3.11(b), no obvious peaks appeared in the corresponding XRD spectrum (Figure 3.12(b)). This was the indication of amorphous phase obtained using Method B (Section 2.4.3). In EDX spectrum of these beads, high level of C, O and low level of Ca, Na and Zr were observed. (Figure 3.11(b)).

On the other hand, the surface of the beads obtained with  $ZrCl_4$  was heterogeneous and contained white spots on various locations (Figure 3.11(c)). Also EDX analysis gave information about composition of the synthesized beads, which contain C, O and Zr at high level. In addition, the presence of an amorphous phase was indicated on the XRD spectrum (Figure 3.12(c)).

Elemental analysis was applied to indicate the percentages of C and H in the synthesized sorbents (Table 3.1). As can be seen from the results, the presence of Zr or because the decrease in the percentages of C and H in synthesized alginate beads compared to sodium alginate.

Table 3.1. Elemental Analysis Results of Synthesized Sorbents.

		<b>C%</b>	<b>H%</b>
<b>Method A</b>	CeO <sub>2</sub> -Alginate	15.01	2.72
	ZrO <sub>2</sub> -Alginate	11.5	3.33
<b>Method B</b>	CeO <sub>2</sub> -Alginate	19.29	3.29
	ZrO <sub>2</sub> -Alginate	17.34	3.89
<b>Method C</b>	CeO <sub>2</sub> -Alginate	15.83	3.84
	ZrO <sub>2</sub> -Alginate	20.75	3.44
	Sodium Alginate	29.82	4.77

Infrared spectra of sodium alginate, zirconium oxide, cerium oxide, and alginate beads containing CeO<sub>2</sub> or ZrO<sub>2</sub> were recorded by FTIR (Figure 3.13 and Figure 3.14). As reported by Sartori et al. (1997), peak shifts, change in peak shapes and the appearance of new peaks in the spectra can be as a consequence of rapid ion exchange process between sodium and calcium ions. For example, the characteristic COO<sup>-</sup> stretching peak of sodium alginate at ~1608 cm<sup>-1</sup> which can be taken as reference is shifted to 1595 cm<sup>-1</sup> for CeO<sub>2</sub> synthesized through Method A. A similar shift applies also to the peak at 1420 cm<sup>-1</sup>. In addition, a new peak appeared at around 2300 cm<sup>-1</sup> for CeO<sub>2</sub> synthesized through Method C. The disappearance of the shoulder at 1665 cm<sup>-1</sup> for sodium alginate may be another evidence of the change of the structure as a result of the modification procedures.

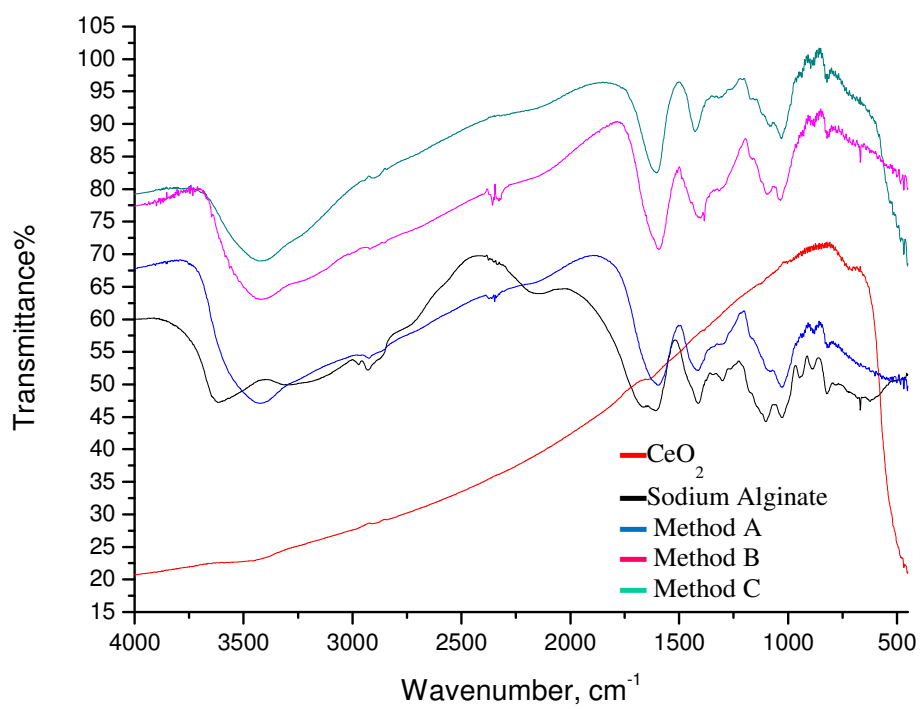


Figure 3.13. Infrared spectra of CeO<sub>2</sub>-based sorbents.

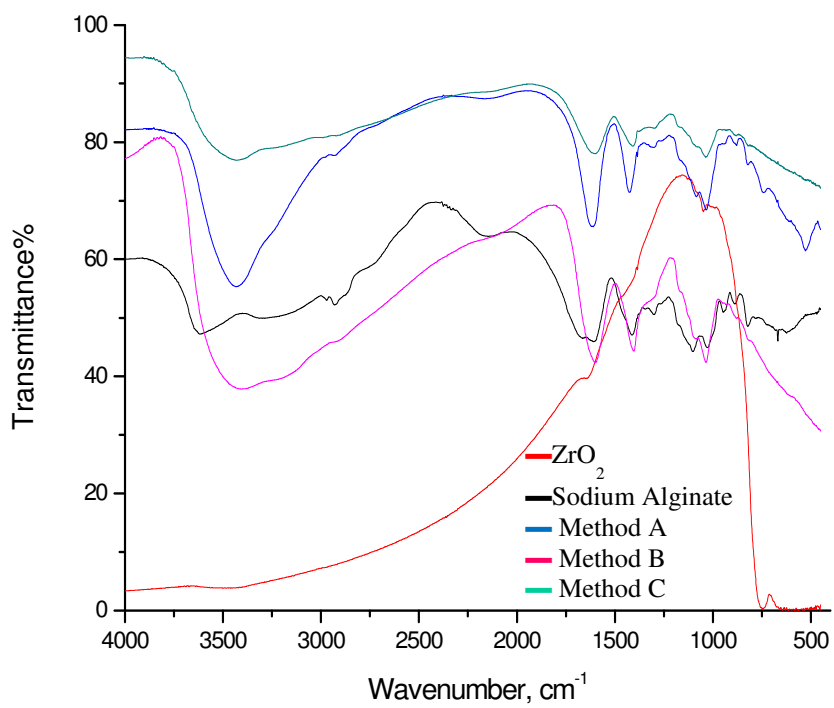


Figure 3.14. Infrared spectra of ZrO<sub>2</sub>-based sorbents.



Thermal behavior of alginic acid and its sodium salt was investigated as a function of temperature under nitrogen atmosphere. The TGA curves given in Figure 3.15 demonstrate that the material has lost weight due to dehydration process; first around 100 °C as a consequence of removal of adsorbed water and around 200 °C from the removal of hydrate in the structure. The difference in the TGA curves of the synthesized materials and that of sodium alginate after 200 °C can simply be explained by the presence of cerium oxide in the structure. These findings are in accordance with the results of similar studies in literature (Saores et al., 2004). Similar thermal behaviors can be seen in the case of  $ZrO_2$ , with only difference that, Method C produces a more stable structure with  $CeO_2$  versus temperature compared to  $ZrO_2$  (Figure 3.16).

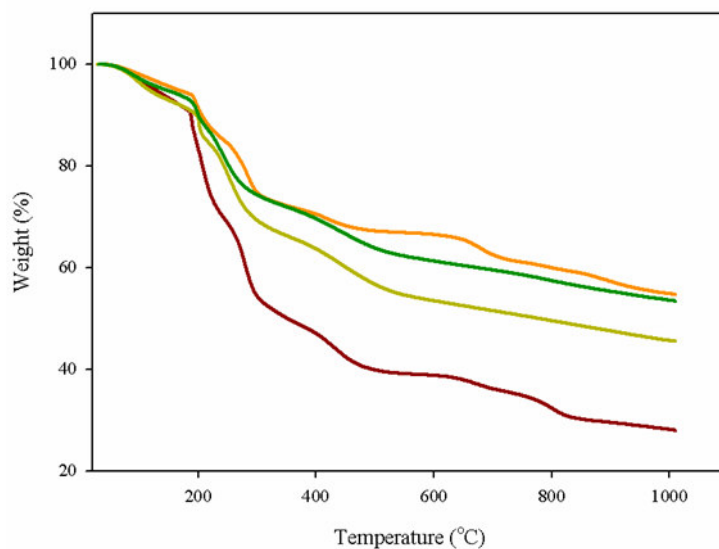


Figure 3.15. TGA curves of  $CeO_2$ -based sorbents.

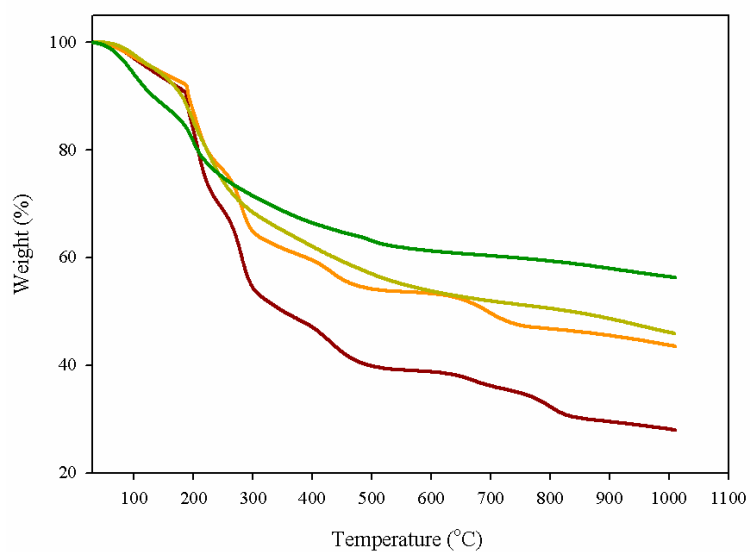


Figure 3.16. TGA curves of ZrO<sub>2</sub>-based sorbents.

## 3.2. Calibration Plots

### 3.2.1. Calibration Curves for Se(IV) ,Se(VI), SeCys and SeMet Using ICP-MS

Plots of signal versus concentration constructed for Se(IV) and Se(VI) using ICP-MS can be seen in Figure 3.17. The limit of detection (LOD) based on 3s was calculated as 0.016  $\mu\text{g L}^{-1}$  and limit of quantification (LOQ) based on 10s was 0.052  $\mu\text{g L}^{-1}$

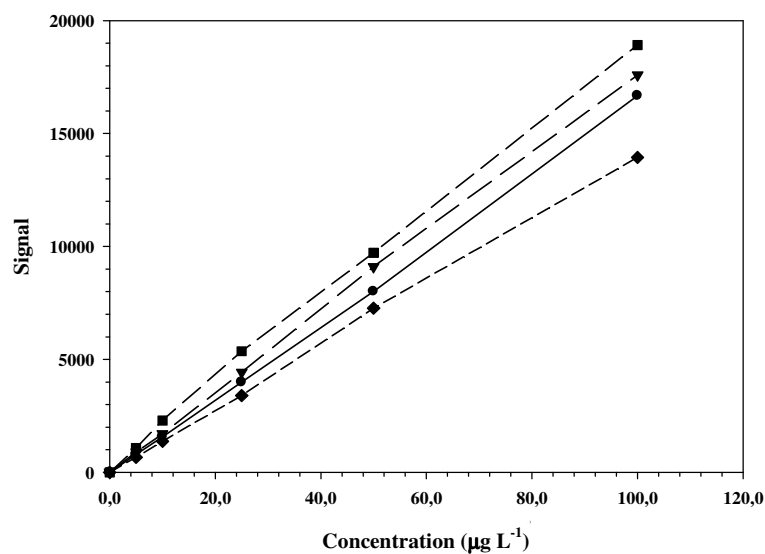


Figure 3.17. Calibration plots of Se(IV), Se(VI), SeCys and SeMet. (●) Se(IV) ( $y= 166.5x-103.4$ ,  $R^2=0.9998$ ), (▼) Se(VI) ( $y= 176.7x + 21.89$ ,  $R^2=0.9998$ ), (■) SeCys ( $y=187.6 + 287.4$ ,  $R^2=0.9997$ ) and (◆) SeMet ( $y=140.3x + 4.39$ ,  $R^2=0.9996$ )

### 3.2.2. Calibration Curves for Se(IV) Using HGAAS

Plot of absorbance versus concentration constructed for Se(IV) using HGAAS can be seen in Figure 3.18. The limit of detection (LOD) based on 3s was calculated as  $0.297 \mu\text{g L}^{-1}$  and limit of quantification (LOQ) based on 10s was  $0.991 \mu\text{g L}^{-1}$ .

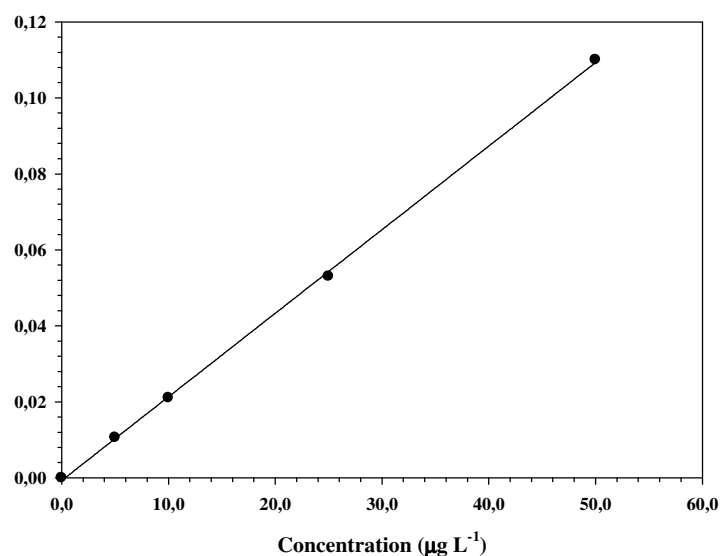


Figure 3.18. Calibration plot of Se(IV). ( $y=0.0022x-0.0007$ ,  $R^2=0.9997$ )

### 3.3. Sorption and Speciation Studies

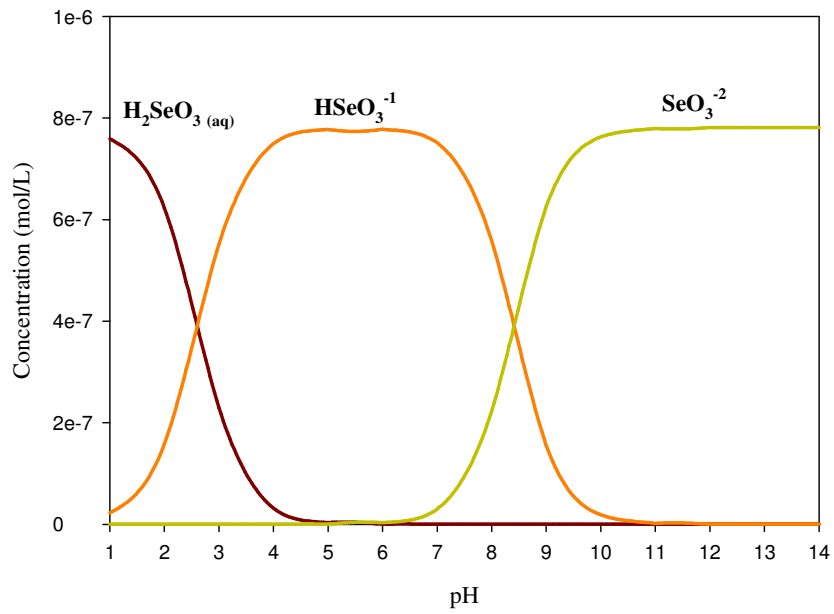
Selenium is sensitive to redox conditions and the pH of the natural matrices. As can be seen from Figure 1.1 acidic and reducing conditions reduce inorganic selenites to elemental selenium, whereas alkaline and oxidizing conditions favor the formation of selenates. The solution pH both determines the form of the analyte in the solution and may also change the surface properties of the sorbent. The form of the analyte can be estimated from the distribution diagrams. The distribution diagrams for Se(IV) and Se(VI) are shown in Figure 3.19. Depending on the solution pH, Se(IV) can be in three different forms in aqueous solutions; namely,  $\text{H}_2\text{SeO}_3$  is predominant in pHs lower than 2,  $\text{HSeO}_3^-$  between pH 2.0 and 8.0, and  $\text{SeO}_3^{2-}$  above pH 8 (Figure 3.19(a)). When Se(VI) is considered,  $\text{SeO}_4^{2-}$  and  $\text{HSeO}_4^-$  are the predominant forms above and below pH 2, respectively (Figure 3.19(b)). SeMet have two pKa values at pH ~2 and the other at pH ~9 corresponding to  $-\text{COOH}$  and  $-\text{NH}_3^+$  groups, respectively, and SeCys has four pKa values, two at pH ~ 2 and two at pH ~8. These compounds are in the zwitterionic form, in the range of pH 2.0-10.0. In this form, both  $-\text{NH}_3^+$  and  $-\text{COO}^-$  groups are exceptional proton-donor and proton-acceptor groups, respectively. Therefore it is very important to consider both the pH and the redox conditions of the sample solutions since these factors determine the form of the species.

#### 3.3.1. Studies with Commercial $\text{CeO}_2$ and $\text{ZrO}_2$

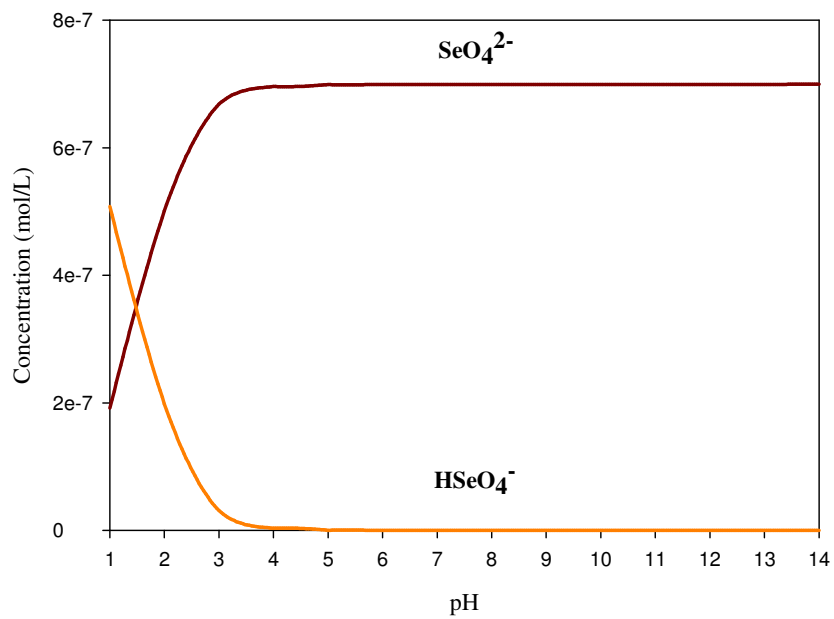
##### 3.3.1.1. Effect of Solution pH

The effect of solution pH on the sorption of Se(IV), Se(VI), SeCys and SeMet and efficiency of each sorbent in the sorption of both species is shown in Figure 3.20. Commercial ceria sorbent showed strong sorption capacity for both species from pH 1.0 to pH 5.0 (> 95.0%) and, whereas the sorption of Se(VI) was diminishing after the pH 5.0 and reaching approximately zero at pH 8.0. For Se(IV) species, sharp decreasing was observed at pH 9.0. Not fully explained behavior was observed above pHs 8.0 and 9.0 for Se(IV) and Se(VI), respectively (Figure 3.20(a)). The sorption mechanism can

be explained by the electrostatic interaction between  $\text{CeO}_2$  surface and the negatively charged forms of  $\text{Se(VI)}$  and  $\text{Se(IV)}$ . Below pH 2.4, cerium dioxide has strong positive charge on surface that's cause to retain selenium species on it because of PZC of  $\text{CeO}_2$ . Also the other mechanism can be a complex reaction of ceriumdioxide and selenium compounds which can result in insoluble precipitate (Shi et al., 2009). After the pH 2.4 retention mechanism of  $\text{Se(IV)}$  can be explained by this insoluble complex compound of selenium oxoanions and  $\text{CeO}_2$ . Figure 3.20(b) shows that  $\text{ZrO}_2$  is very effective in the sorption of  $\text{Se(IV)}$  and  $\text{Se(VI)}$  at pH 2.0 (> 95.0%). Fluctuation was observed at pH 7.0 in the sorption of selenium species. According to PZC of  $\text{ZrO}_2$ , positive charges on the surface of zirconia are dominant at lower pH 2.8 so an electrostatic interaction between on zirconia surface and the negatively charged forms of  $\text{Se(IV)}$  and  $\text{Se(VI)}$ . The sorption behaviour of  $\text{ZrO}_2$  resembled to  $\text{CeO}_2$ , on the other hand  $\text{CeO}_2$  showed more stable performance kineticly. Sorption studies have revealed that quantitative sorption can be obtained using commercial ceria and zirconia for both  $\text{Se(IV)}$  and  $\text{Se(VI)}$  species at pH 2.0.  $\text{CeO}_2$  have displayed higher than 95.0% sorption for  $\text{Se(IV)}$  at pH 8.0 while the sorption for  $\text{Se(VI)}$  was less than 10%, speciation of  $\text{Se(IV)}$  and  $\text{Se(VI)}$  can be done. Organic selenium species did not retain on the surface of both sorben

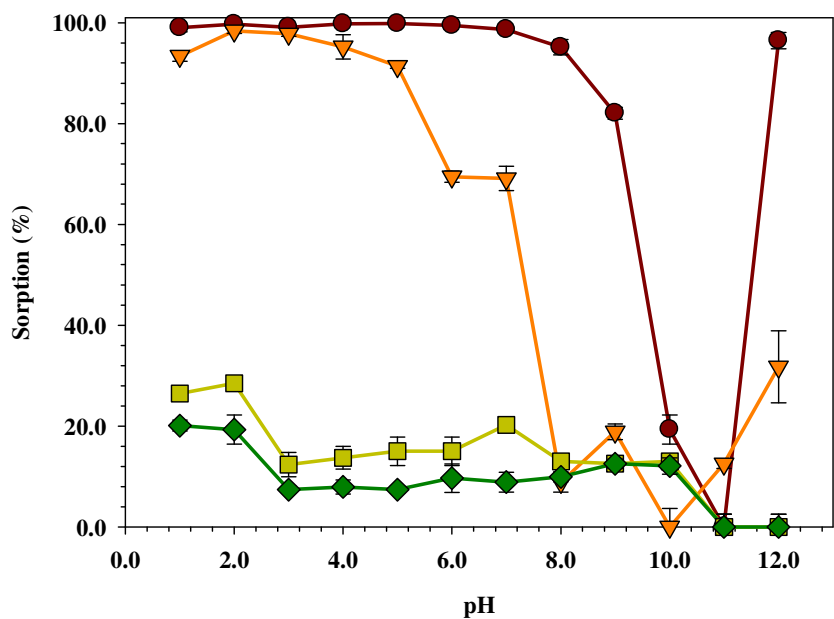


(a)

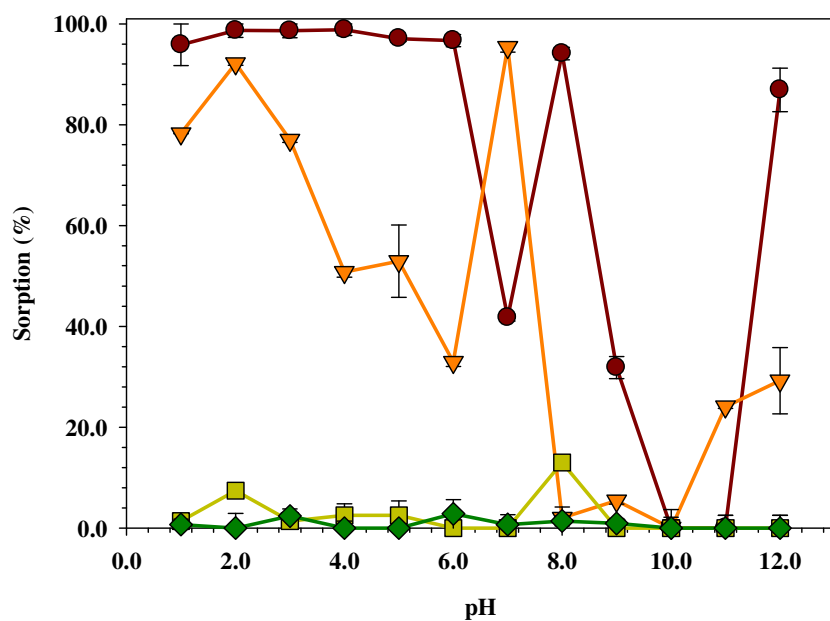


(b)

Figure 3.19. Distribution diagram of (a) Se(IV) and (b) Se(VI) in aqueous solutions. (Source: MINTEQ program)



(a)



(b)

Figure 3.20. Effect of solution pH on the sorption of (●) Se(IV), (▼) Se(VI), (■) SeCys, (◆) SeMet for (a) CeO<sub>2</sub> and (b) ZrO<sub>2</sub>. (20.0 mL and 100.0 μg L<sup>-1</sup> Se(IV), Se(VI), SeCys, SeMet solution, 30 min shaking time, 50.0 mg sorbent, 25.0 °C reaction temperature)

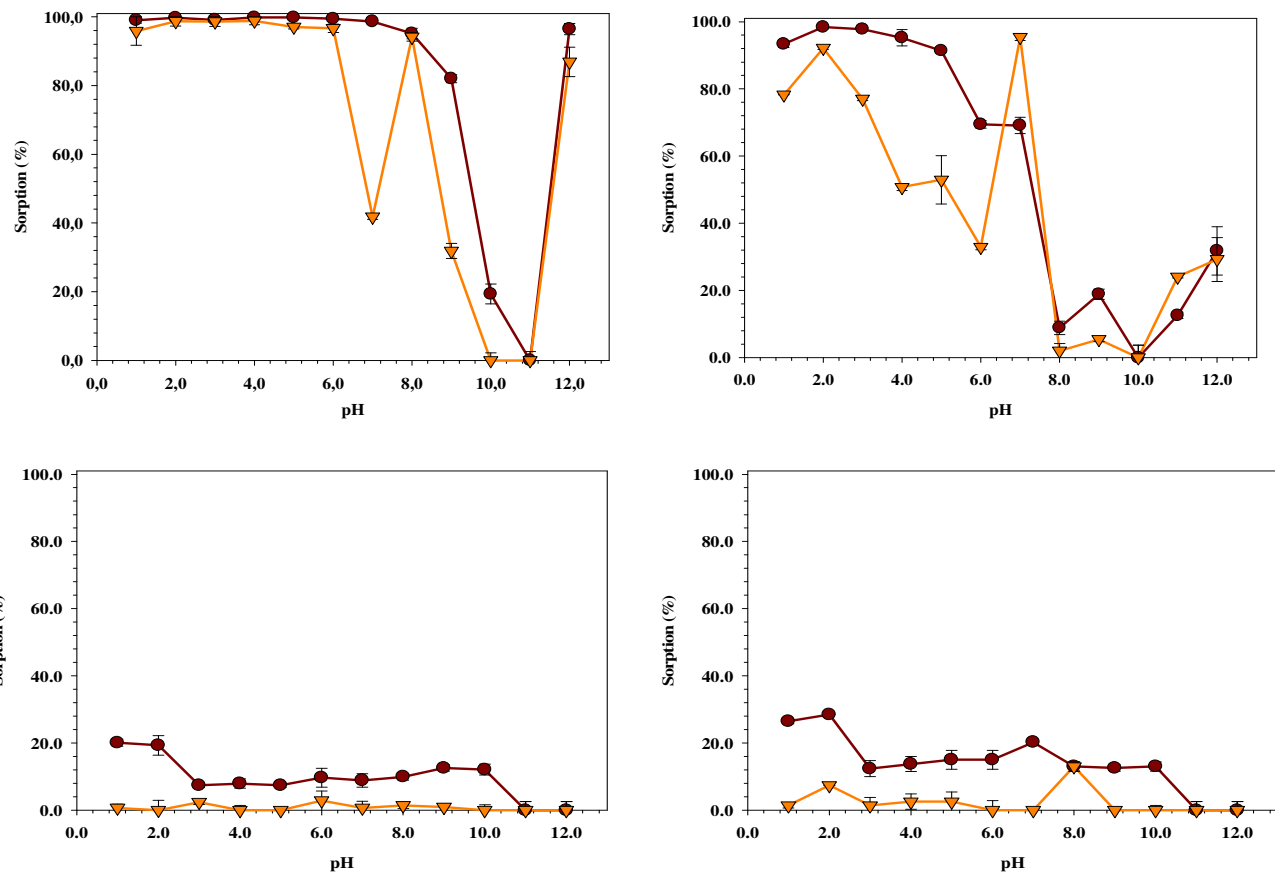
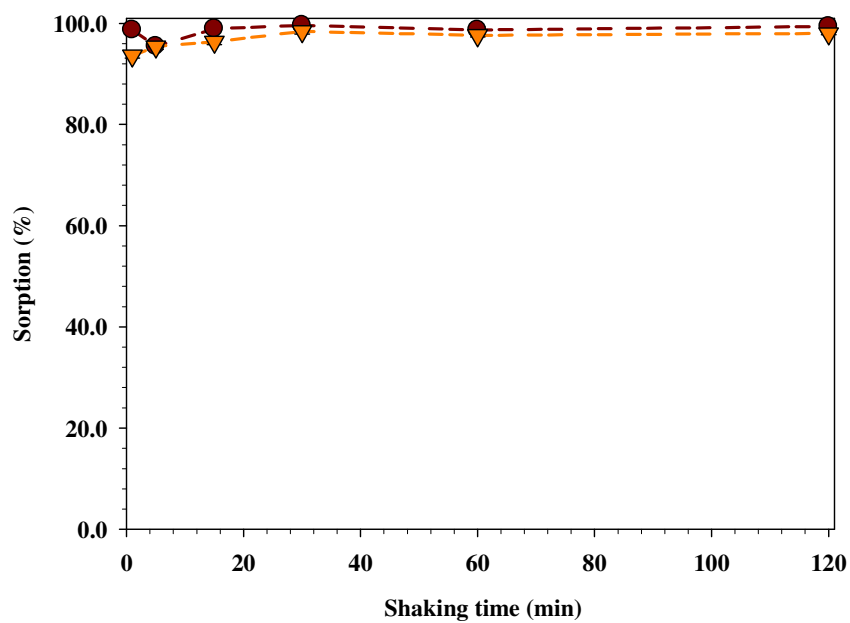


Figure 3.21. Effect of solution pH on the sorption of (a) Se(IV) ,(b) Se(VI), (c) SeCys and (d) SeMet for (●) CeO<sub>2</sub> and (▼) ZrO<sub>2</sub>. (20.0 mL and 100.0 μgL<sup>-1</sup> Se(IV) ,Se(VI), SeCys, SeMet solution, 30 min shaking time, 50.0 mg sorbent, 25.0 °C reaction temperature).

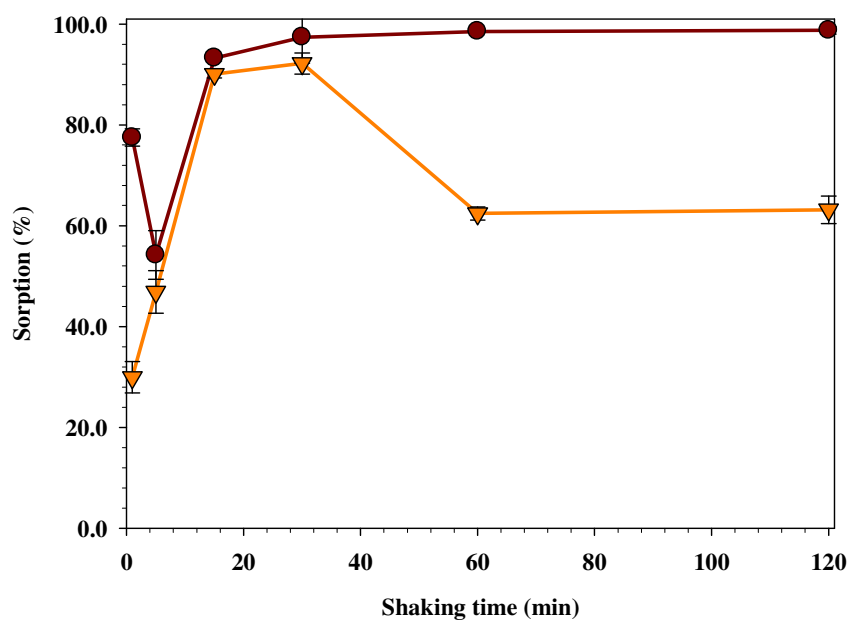


### 3.3.1.2. Effect of Shaking Time

Batch sorption time was investigated for 1, 5, 15, 30, 60 and 120 minutes at pH 2.0 for both  $\text{CeO}_2$  and  $\text{ZrO}_2$  as illustrated in Figure 1.3. The sorption behaviour of  $\text{CeO}_2$  showed that there is an sorption (>95.0%) even in 1 min for both Se(IV) and Se(VI) and the maximum sorption is obtained in 30 min.(Figure 3.22(a)) In further experiment, a shaking time of 30 min was chosen for both selenium compound to obtain high efficiency in sorption. The effect of shaking time on the sorption of both Se(IV) and Se(VI) was investigated for  $\text{ZrO}_2$ . The result is given in figure 3.22(b). It can be said that zirconia reaches high sorption capacity in 30 min for both selenium species. After shaking time of 30 min, decreasing in the sorption of Se(VI) was observed while the sorption of Se(IV) retained stable in any time.



(a)

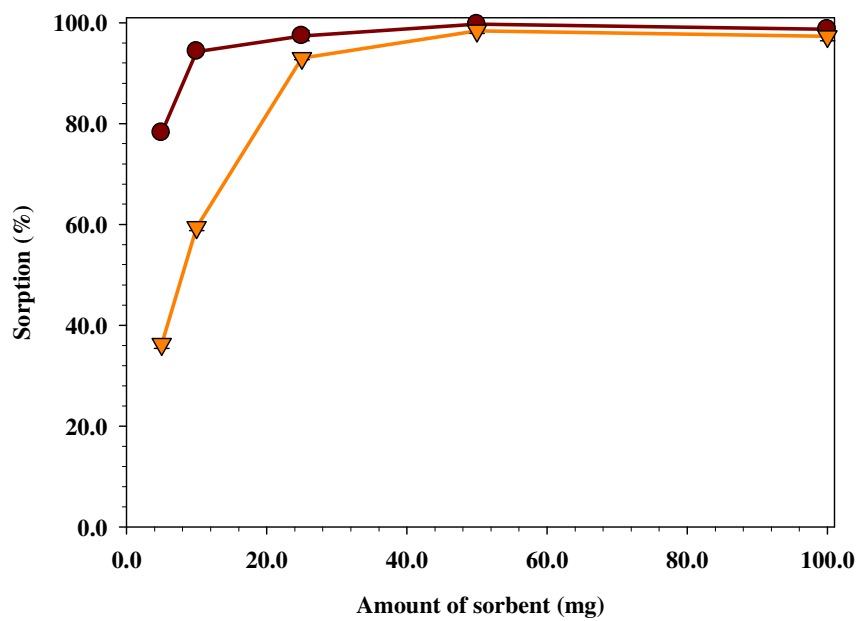


(b)

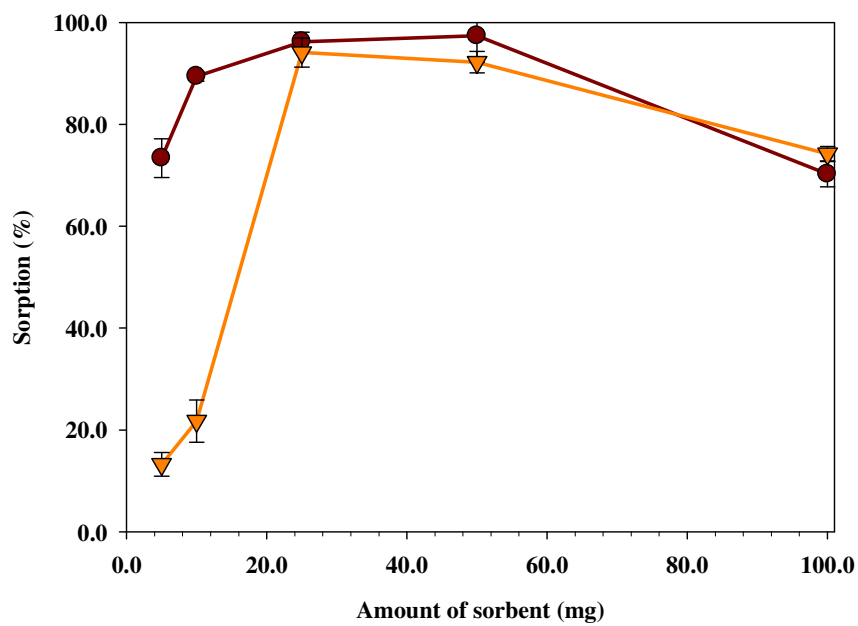
Figure 3.22. Effect of shaking time on the sorption of (●) Se(IV) and (▼) Se(VI) (a) CeO<sub>2</sub> and (b) ZrO<sub>2</sub>. (20.0 mL and 100.0 μgL<sup>-1</sup> Se(IV), Se(VI) solution, pH 2.0, 50.0 mg sorbent, 25.0 °C reaction temperature)

### 3.3.1.3. Effect of Sorbent Amount

To determine the required amount of sorbents for the maximum sorption of selenium species, the sorption studies were done for 5.0, 10.0, 25.0, 50.0, 100.0 mg sorbent amounts. The selenium sorption behaviour with amount of  $\text{CeO}_2$  and  $\text{ZrO}_2$  is given in the Figure 3.23. Similar sorption results were obtained with both selenium species for  $\text{CeO}_2$ . It can be observed that 10.0 mg of ceria is enough to give quantitative sorption (95.0%), given in Figure 3.23(a). For  $\text{ZrO}_2$ , a minimum amount of 25.0 mg was necessary for effective sorption of both selenium species and the sorption performance was decreasing with the increase in the amount of zirconia (Figure 3.23(b)). The results have showed that the more kinetically-favored interaction of Se(IV) and Se(VI) with ceria than zirconia and this observation is also indicative of large capacity of ceria for selenium sorption. . To guarantee the quantitative sorption 50.0 mg sorbents of  $\text{ZrO}_2$  and  $\text{CeO}_2$  were used for both selenium species at pH 2.0.



(a)



(b)

Figure 3.23. Effect of sorbent amount on the sorption of (●) Se(IV) and (▼) Se(VI) for (a) CeO<sub>2</sub> and (b) ZrO<sub>2</sub>. (20.0 mL and 100.0 μg L<sup>-1</sup> Se(IV), Se(VI), solution, at pH 2.0, 30 min shaking time, 25.0 °C reaction temperature)

### 3.3.1.4. Effect of Reaction Temperature

Temperature effect on the sorption of selenium was studied at 25, 50 and 70 °C. The sorption behaviours of ZrO<sub>2</sub> and CeO<sub>2</sub> as a function of temperature are given in the Figure 3.24. As shown in Figure 3.24(a), ceria have shown no change with the increase in temperature for Se(IV) and Se(VI) whereas the sorption capacity of zirconia for Se(VI) decreased which demonstrating the exothermic nature of sorption and this results show importance of control of the sorption temperature (Figure 3.24 (b)), because of this reason further experiments were carried out a constant temperature 25.0 °C.

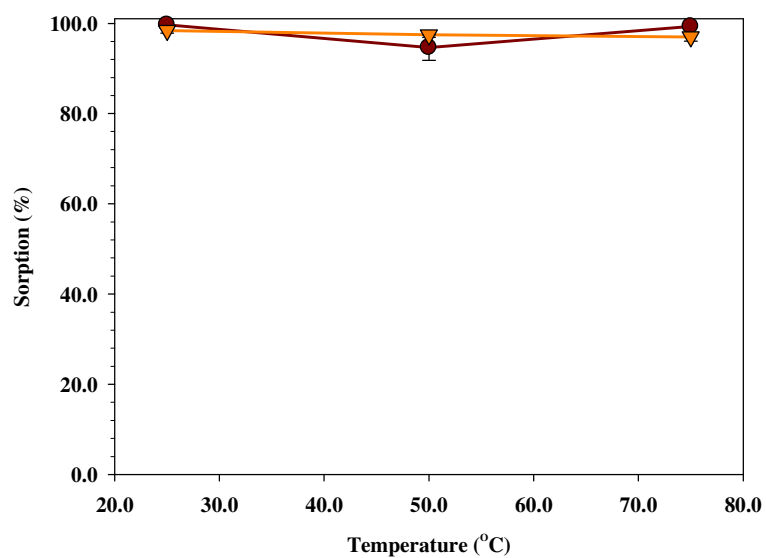
In order to understand the effect of temperature on the adsorption better, it is important to study the thermodynamic parameters such as standard Gibbs free energy change,  $\Delta G_o$ , standard enthalpy change  $\Delta H_o$ , and standard entropy change,  $\Delta S_o$ . The magnitude of the change in free energy can be used to determine the type of adsorption. The summary of thermodynamic parameters is given in the Table 3.2.

Table 3.2. Thermodynamic parameter of CeO<sub>2</sub> and ZrO<sub>2</sub>.

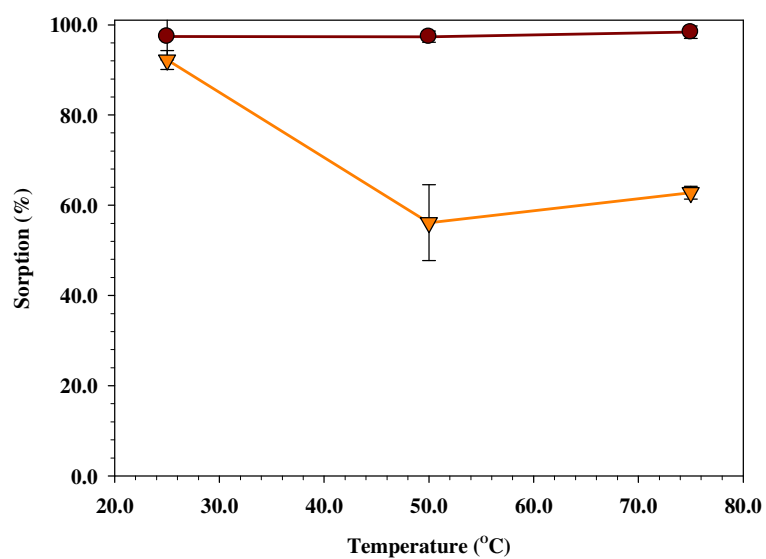
Se (IV)	$\Delta G$ (kJ/mol)		$\Delta H$ (kJ/mol)	$\Delta S$ (J/molK)	
	298 K	323 K		298 K	323 K
CeO <sub>2</sub>	-21.1	-25	-78.3	-175.2	-149.6
ZrO <sub>2</sub>	-23.8	-25.7	-1.24	75.7	82.1

Se(VI)	$\Delta G$ (kJ/mol)		$\Delta H$ (kJ/mol)	$\Delta S$ (kJ/molK)	
	298 K	323 K		298 K	323 K
CeO <sub>2</sub>	-25.1	-25.8	-15.9	30.8	30.8
ZrO <sub>2</sub>	-20.9	-16.7	-71.2	-168.5	-168.5



(a)



(b)

Figure 3.24. Effect of sorption temperature on the sorption of (●) Se(IV) and (▼) Se(VI) for (a) CeO<sub>2</sub> and (b) ZrO<sub>2</sub>. (20.0 mL and 100.0 μgL<sup>-1</sup> Se(IV) ,Se(VI) solution, at pH 2.0, 30 min shaking time, 50.0 mg sorbent)

### 3.3.1.5. Effect of Initial Concentration

The sorption efficiency of ceria and zirconia was tested as a function of initial concentration of Se(IV) and Se(VI) at the pH 2.0. As shown in table 3.2, with the increase in the initial concentration of Se(IV), a slight decrease in percentage sorption has first occurred for 10 mgL<sup>-1</sup> selenium for both sorbents and then for 100 mgL<sup>-1</sup> the efficiency of sorbents have only decreased almost to 75%. The sorption of Se(VI) has shown almost quantitative sorption at initial concentration of 1.0 mgL<sup>-1</sup> and decreased even for an initial concentration 10.0 mgL<sup>-1</sup> for both ceria and zirconia (Table 3.3). These findings show that, an initial concentration of 1.0 mgL<sup>-1</sup> for both selenium species can efficiently be retained by ceria and zirconia after which the sorption percentage starts to decrease gradually. The results also indicate the high sorption capacity of ZrO<sub>2</sub> and CeO<sub>2</sub>.

Table 3.3. Effect of initial Se(IV) concentration on the sorption efficiency for CeO<sub>2</sub> and ZrO<sub>2</sub>. (50.0 mg sorbent amount, at pH 2.0 in 20.0 mL Se(IV) solution, 30 min shaking time)

Se(IV)	CeO <sub>2</sub>	ZrO <sub>2</sub>
Concentration (mg L <sup>-1</sup> )	Sorption (%)	
<b>0.010</b>	99.8± 0.7	100±0.6
<b>0.10</b>	98.7± 0.1	97.2±0.2
<b>1.0</b>	99.2±0.1	99.0±0.1
<b>10.0</b>	87.3±0.9	88.1±0.8
<b>50.0</b>	75.0±8.3	76.2±4.2
<b>100.0</b>	73.8±3.5	74.9±2.0

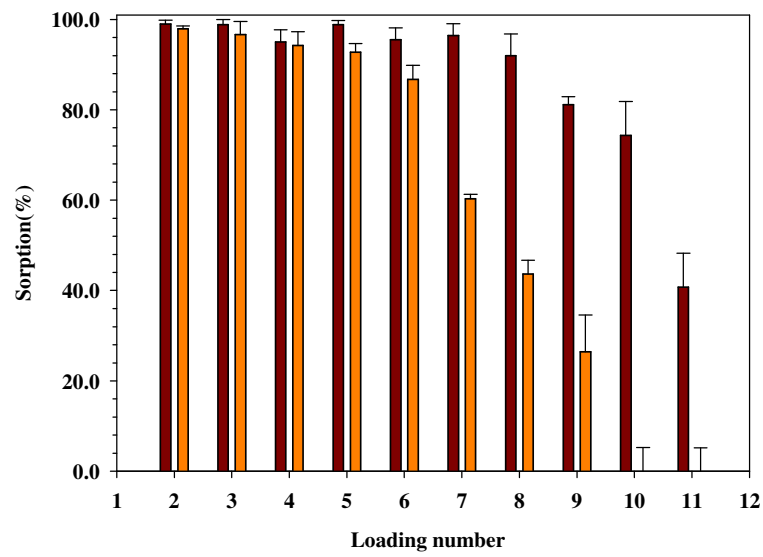
Table 3.4. Effect of initial Se(VI) concentration on the sorption efficiency for CeO<sub>2</sub> and ZrO<sub>2</sub>. (50.0 mg sorbent amount, at pH 2.0 in 20.0 mL Se(IV) solution, 30 min shaking time)

Se(VI)	CeO <sub>2</sub>	ZrO <sub>2</sub>
Concentration (mg L <sup>-1</sup> )	Sorption (%)	
<b>0.010</b>	100.0±0.4	93.8±0.7
<b>0.10</b>	98.8±0.1	96.2±0.1
<b>1.0</b>	92.3± 3.0	92.3±0.3
<b>10.0</b>	82.7±6.0	79.1±0.8
<b>50.0</b>	71.1±8.0	74.4±4.0
<b>100.0</b>	71.8±3.0	72.4±1.6

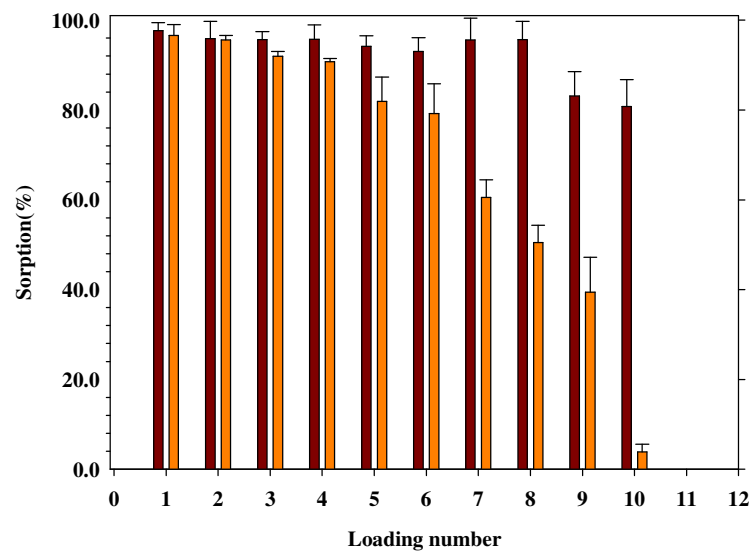
### 3.3.1.6. Repetitive Loading

Sequential sorption of Se(IV) and Se(VI) by CeO<sub>2</sub> and ZrO<sub>2</sub> were investigated and results were given in figure 3.25. As shown in Figure 3.25(a), for Se(IV), the sorption percentage of ceria has decreased slightly after eighth loading whereas the decline for Se(VI) was more noticeable after sixth loading and the sorption percentage reached zero values. It can be seen from Figure 3.25(b) that the sorption percentage of zirconia starts to without significant decrease with the ninth loading for Se(IV) and sorbed Se(VI) even starts to be released from zirconia surface after the fourth loading. The reason of decrease in sorption capacity can be the surface positive charge of zirconia and ceria after each loading could have been reduced which might also have changed the thickness of double layer around the particles. This might have resulted in a decrease in the sorption percentage after each step.





(a)



(b)

Figure 3.25. Percent sorption of (—) Se(IV) and (—) Se(VI) for (a) CeO<sub>2</sub> and (b) ZrO<sub>2</sub> ten loadings. (20.0 mL of 100.0 μgL<sup>-1</sup> at pH 2.0, 50.0 mg sorbent, 30 min at 25 °C, batch sorption)

### 3.3.1.7. Desorption Studies

Desorption studies were performed as described in section 2.5.1.7 for CeO<sub>2</sub> and ZrO<sub>2</sub>. The efficiency/feasibility of various eluents for the desorption of Se(IV) and Se(VI) was investigated. Table 3.5 and Table 3.6 summarizes the desorption percentage of various desorbing matrices for Se(IV) and Se(VI), respectively. At first, namely, HCl, HNO<sub>3</sub>, CH<sub>3</sub>COOH, 0.2% (m/v) KIO<sub>3</sub>, H<sub>2</sub>KO<sub>4</sub>P, NH<sub>4</sub>Cl, NH<sub>3</sub> and NaOH were used for the elution of the previously sorbed Se(IV) from CeO<sub>2</sub> and ZrO<sub>2</sub> by the batch method. As can be seen from Table 3.4, except for NH<sub>3</sub> and NaOH, other eluents did not give a quantitative desorption for Se(IV). In the case of Se (IV), following the sorption step with the optimized conditions, the sorbent was shaken for an hour in a solution of, 0.500 M NaOH and NH<sub>3</sub> solutions and then was removed from the mixture by filtration, respectively. The selenium concentration in the eluate was determined by HGAAS. The 90% release of previously-adsorbed selenite from the surface was obtained.. In the case of Se(VI), the desorption step was realized with the use of 0.1 M NH<sub>4</sub>Cl solution in a similar procedure and the 95% release of selenate ion was obtained by using 0.1 M NH<sub>4</sub>Cl. The sorption parameters were as follows; 100.0 µgL<sup>-1</sup> concentration of Se(IV) or Se(VI), shaking time of 30 min, solution volume of 20.0 mL, reaction temperature of 25.0 °C, solution pH of 2.0. The sorbents used were CeO<sub>2</sub> and ZrO<sub>2</sub>.

Table 3.5. Percent recovery of various desorbing matrices for Se(IV). (The sorption parameters; 100.0  $\mu\text{gL}^{-1}$  concentration of Se(IV) or Se(VI), shaking time of 30 min, 50.0 mg sorbent amount, solution volume of 20.0 mL, reaction temperature of 25.0  $^{\circ}\text{C}$ , solution pH of 2.0)

Eluent	Recovery %	
	ZrO <sub>2</sub>	CeO <sub>2</sub>
%0.2 (m/v) KIO <sub>3</sub> in 1.0 M HCl	36.6 ( $\pm 1.2$ )	20.6 ( $\pm 4.2$ )
1.0 M HCl	~ 0	~ 0
1.0 M HNO <sub>3</sub>	17.4 ( $\pm 3.1$ )	1.5 ( $\pm 0.8$ )
1.0 M CH <sub>3</sub> COOH	24.7 ( $\pm 0.9$ )	19.3 ( $\pm 2.7$ )
0.1 M KH <sub>2</sub> PO <sub>4</sub>	~ 0	4.5 ( $\pm 0.3$ )
0.1 M NH <sub>3</sub>	80.6 ( $\pm 0.1$ )	74.8 ( $\pm 1.1$ )
0.5 M NH <sub>3</sub>	85.8 ( $\pm 3.1$ )	89.8 ( $\pm 4.6$ )
0.1 NaOH	90.8 ( $\pm 2.7$ )	89.8 ( $\pm 1.1$ )
0.5 M NaOH	98.3 ( $\pm 4.2$ )	97.8 ( $\pm 7.1$ )
0.1 M NH <sub>4</sub> Cl	20.4 ( $\pm 1.8$ )	16.8 ( $\pm 2.1$ )

Table 3.6. Percent recovery of various desorbing matrices for Se(VI). (The sorption parameters; 100.0  $\mu\text{gL}^{-1}$  concentration of Se(IV) or Se(VI), shaking time of 30 min, 50.0 mg sorbent amount, solution volume of 20.0 mL, reaction temperature of 25.0 °C, solution pH of 2.0)

Eluent	Recovery%	
	ZrO <sub>2</sub>	CeO <sub>2</sub>
0.1 M NH <sub>3</sub>	88.4 ( $\pm 1.9$ )	85.1 ( $\pm 2.2$ )
0.5 M NH <sub>3</sub>	87.8 ( $\pm 3.1$ )	84.8 ( $\pm 1.1$ )
0.1 NaOH	83.5 ( $\pm 4.8$ )	88.5 ( $\pm 3.8$ )
0.5 NaOH	87.3 ( $\pm 2.7$ )	89.3 ( $\pm 5.7$ )
0.1 M NH <sub>4</sub> Cl	92.5 ( $\pm 0.1$ )	96.2 ( $\pm 0.8$ )

### 3.3.1.8. Method Validation

CeO<sub>2</sub> and ZrO<sub>2</sub> were used in sorption of selenite and selenate from three different type of water spiked samples as described in section 2.5.1.7. Firstly the sorption performance of the sorbents was checked. The results are summarized in Table 3.6 for CeO<sub>2</sub> and ZrO<sub>2</sub>, respectively. As seen from Table 3.7 the related sorbents displayed very efficient performances towards Se(IV) at the indicated pH for all water samples; the sorption percentages were above 99.6 % for CeO<sub>2</sub> and 96.2% for ZrO<sub>2</sub>. In contrast to Se(IV) the situation is more complicated for Se(VI). Selenate ion only could not be recovered from bottled and tap water spiked sample which means no sorption was obtained from these waters for both sorbents. This observation is in agreement with results obtained from effect of ionic strength of solution on sorption of selenate by CeO<sub>2</sub> and ZrO<sub>2</sub>. Especially, Tap water ionic content from salts other dissolved ions increase the ionic strength and tap water of Urla region indicate the presence of water hardness which explain the low percent sorption due to competitive ions.

Table 3.7. Percent sorption of spiked selenite and selenate in ultrapure, bottled and tap water for CeO<sub>2</sub> and ZrO<sub>2</sub>. (Sorption parameters; Se concentration: 100,0 µgL<sup>-1</sup>, pH: 2.0, shaking time: 30 min, amount of sorbent: 50.0 mg, temperature: 25.0 °C. Desorption parameters: eluent volume: 20.0 mL, shaking time: 60 min, eluent: 0.50 M NaOH)

	<b>Sorption (CeO<sub>2</sub>) %</b>		<b>Sorption (ZrO<sub>2</sub>) %</b>	
	Se(IV)	Se(VI)	Se(IV)	Se(VI)
U.P.W	99.6 (±0.3)	98.4 (±0.5)	97.4 (± 5.2)	98.4 (±0.5)
Bottled water	99.0 (±0.2)	18.2 (±1.1)	98.1 (±0.2)	18.2 (±1.1)
Tap water	98.5 (±0.9)	~0	96.2 (±0.6)	~0

To determine Se(VI) concentration in tap water and bottled water, Se(VI) and Se(IV) and only Se(IV) were spiked into water samples, respectively. Previous section showed that selenite ions were retained on sorbent for tap water and bottled water. So Se(VI) concentration was determined by HCl reduction of Se(VI) to Se(IV). For reduction process, 6.0 M HCl was added to certain amount of Se(IV) and Se(VI) spiked water samples and heated to 100 °C. After these steps, sorption procedure was applied to both ceria and zirconia. 0.1 M NaOH was used for desorption of selenite ions from the surface of sorbents. Prior to HGAAS determination of selenium in eluent, standards were prepared with in the same matrix of desorption solution. The recovery results obtained by addition of 10 µgL<sup>-1</sup> and 100 µgL<sup>-1</sup> to water samples, respectively, are given Table 3.8 and Table 3.9. The results show that it is possible to determine the total selenium concentration by using reduction process, on the other hand without reduction only Se(IV) concentration can be determined. The difference between the total selenium and Se(IV) concentration can give information about Se(VI). Also developed method seems very promising about enrichment of selenium or determination of selenium.

Table 3.8. Recovery of Se(IV) and Se(VI). (sorption parameters; Se concentration: 100,0 µgL<sup>-1</sup>, shaking time: 30 min, amount of sorbent: 50.0 mg, temperature: 25.0 °C. Desorption parameters: eluent volume: 20.0 mL, shaking time: 60 min, eluent: 0.50 M NaOH).

	<b>Recovery (µgL<sup>-1</sup>) (CeO<sub>2</sub>)</b>		<b>Recovery (µgL<sup>-1</sup>) (ZrO<sub>2</sub>)</b>	
	Se(IV)	Se(VI) +Se(IV)	Se(IV)	Se(IV) +Se(VI)
Bottled Water	110.8 (±1.6)	196.4 (±3.7)	107.8 (±3.1)	198.5 (±2.8)
Tap Water	102.7 (±2.2)	198.9 (±1.2)	113.0 (±2.6)	194.9 (±5.9)

Table 3.9. Recovery of Se (IV) and Se(VI). (Sorption parameters; Se concentration: 10,0  $\mu\text{gL}^{-1}$ , shaking time: 30 min, amount of sorbent: 50.0 mg, temperature: 25.0 °C. Desorption parameters: eluent volume: 20.0 mL, shaking time: 60 min, eluent: 0.50 M NaOH)

	Recovery ( $\mu\text{gL}^{-1}$ ) ( $\text{CeO}_2$ )		Recovery ( $\mu\text{gL}^{-1}$ ) ( $\text{ZrO}_2$ )	
	Se(IV)	Se(VI)+Se(IV)	Se(IV)	Se(IV)+Se(VI)
Bottled water	9.7 ( $\pm 0.6$ )	19.5 ( $\pm 1.7$ )	9.4 ( $\pm 3.1$ )	18.7 ( $\pm 0.8$ )
Tap water	9.4 ( $\pm 3.2$ )	18.9 ( $\pm 2.2$ )	9.1 ( $\pm 2.6$ )	19.4 ( $\pm 1.9$ )

### 3.3.2. Sorption Studies of Sol-gel and Hydrothermal Synthesized $\text{CeO}_2$ and $\text{ZrO}_2$

In the sorption of inorganic selenium studies besides the commercial available  $\text{CeO}_2$  and  $\text{ZrO}_2$  synthesized sorbents were investigated. Sorption studies were performed as described in section 2.5.2. These experiments provide to compare commercial available sorbents with synthesized sorbents. According to optimization results sorption studies were performed at pH 2.0 where the maximum sorptions were obtained for both inorganic selenium species. Commercially available and sol-gel synthesized  $\text{CeO}_2$  showed high sorption capacity (>95%) for Se(IV) and Se(VI) but when the hydrothermally synthesized ceria compared with the other sorbents, decreasing in sorption capacity was observed (Table 3.10). Sorption results obtained from  $\text{ZrO}_2$  was given in Table 3.10. All zirconia sorbents showed high sorption capacity for Se (IV). On the other hand, the sorption percentage of synthesized sorbents were decreased in comparison with commercial available zirconia for Se(VI). Low sorption behaviour of synthesized sorbents gave information about durability of sorbents. Especially, synthesized sorbents with hydrothermal method can be improved.

Table 3.10. Sorption results obtained with the commercial and the synthesized CeO<sub>2</sub> for Se(IV)/Se(VI). (●)Commercial available CeO<sub>2</sub> and ZrO<sub>2</sub>.(▲) Synthesized with Hydrothermal method CeO<sub>2</sub> and ZrO<sub>2</sub>.(■) Synthesized with sol-gel methodCeO<sub>2</sub> and ZrO<sub>2</sub>. Se concentration: 100.0 µgL<sup>-1</sup>. pH: 2.0. shaking time: 30 min. amount of sorbent: 50.0 mg).

pH		Sorption (CeO <sub>2</sub> ) %			Sorption (ZrO <sub>2</sub> ) %		
		●	▲	■	●	▲	■
2.0	Se(IV)	99.6 ±0.3	97.6±0.1	99.2±1.1	97.4 ±5.2	94.1±0.1	96.7±2.5
2.0	Se(VI)	98.4±0.5	73.3±3.8	98.2±2.0	92.2±2.1	80.8±3.8	89.3±3.5
8.0	Se(VI)	95.1 ±1.5	78.9±0.3	96.4±0.5	94.1 ±1.2	92.8±2.4	97.3±0.2

### 3.3.3.Sorption Studies Utilizing ZVI and nZVI-Modified ZrO<sub>2</sub>

In this study, The effect of pH on the sorption and desorption of Se(IV), Se(VI), Se-L-Cystine (SeCys) and Seleno-L-methionine (SeMet) was investigated. The sorption results of Fe<sup>0</sup> for selenium species depend on pH was given Figure 3.26. nZVI showed strong sorption capacity for both Se(IV) and Se(VI) from pH 4.0 to pH 9.0 (□ 90.0%). SeCys showed to reach maximum sorption at pHs 4.0 and 8.0 (□ 90.0%). Moreover, the sorption of SeMet was not observed at any pH worked. The sorption studies with ZrO<sub>2</sub> indicated that organic selenium species did not retain on the sorbent surface at any pH. the sorption of Se(VI) remained at low level and only Se(IV) was determined by quantitatively (Figure 3.27). Effect of pH on the sorption of selenium species for synthesized hybrid sorbent (nZVI-ZrO<sub>2</sub>) was illustrated in Figure 3.28. As mentioned hybrid sorbent represented similar feature like zero valent iron.

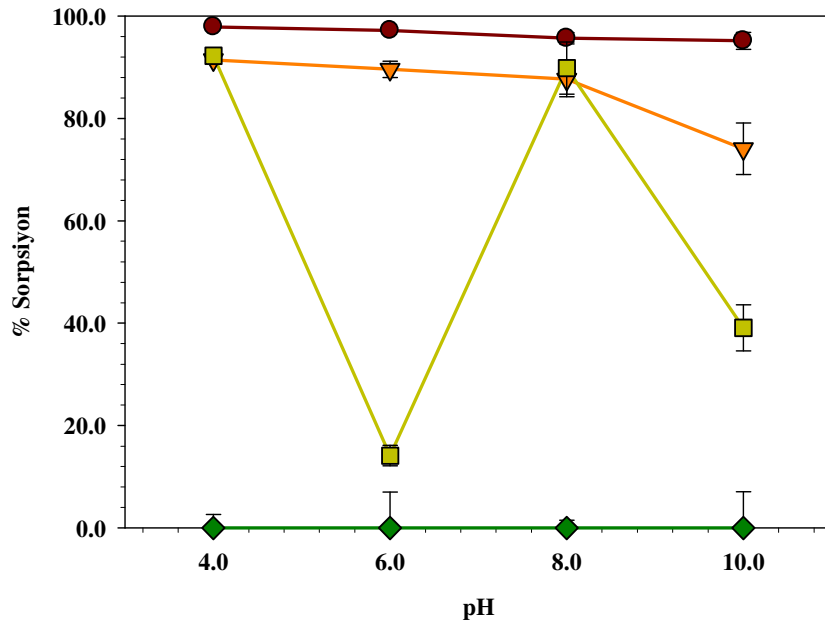


Figure.3.26.Effect of solution pH on the sorption of (●) Se(IV), (▼) Se(VI), (■)SeCys ve (◆) SeMet) from ZVI. (Se concentration:  $100.0 \mu\text{gL}^{-1}$ .shaking time 30 min.,amount of sorbent: 50.0 mg, 25 °C)

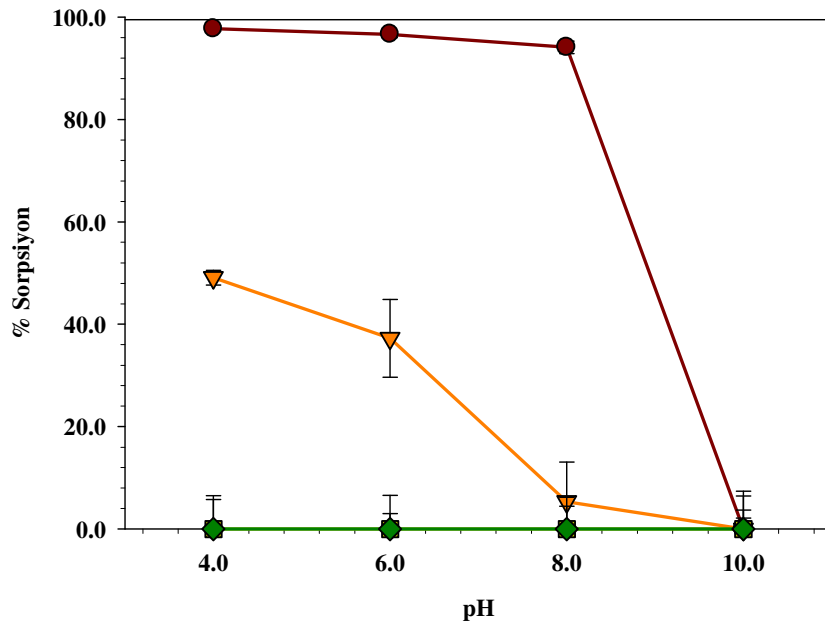


Figure 3.27.Effect of solution pH on the sorption of (●) Se(IV), (▼) Se(VI), (■) SeCys and (◆) SeMet for  $\text{ZrO}_2$ .(Se concentration:  $100.0 \mu\text{gL}^{-1}$ . shaking time 30 min. amount of sorbent: 50.0 mg, 25 °C)



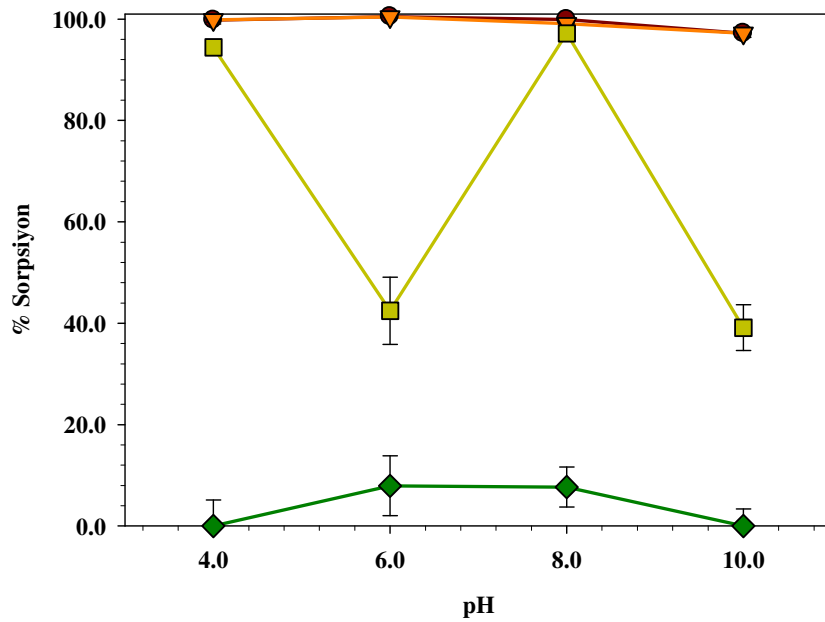


Figure 3.28. Effect of solution pH on the sorption of (●) Se(IV), (▼) Se(VI), (■) SeCys and (◆) SeMet on nZVI-ZrO<sub>2</sub>. (Se concentration: 100.0 μgL<sup>-1</sup>, shaking time 30 min, amount of sorbent: 50.0 mg, 25 °C)

As mentioned above, nZVI and nZVI-ZrO<sub>2</sub> indicate high sorption capacity for Se(IV), Se(VI) and SeCys. Following the sorption studies, 0.1 M NaOH was selected as eluent because the basic solutions are very effective to desorption of selenium species as remembered previous sections. The results of recovery for both sorbents are given Table 3.11. According to results, to obtain more quantitative results, molarity of eluent or reaction time can be changed.

Table 3.11. Percent Recovery of Se (IV), Se(VI) and SeCys. (Sorption parameters; Se concentration: 100,0 μgL<sup>-1</sup>, shaking time: 30 min, amount of sorbent: 50.0 mg, temperature: 25.0 °C. Desorption parameters: eluent volume: 20.0 mL, shaking time: 60 min, eluent: 0.50 M NaOH)

	Recovery (%)	
	nZVI	nZVI-ZrO <sub>2</sub>
Se(IV)	83.4 (±3.0)	85.4 (±0.2)
Se(VI)	76.8 (±4.3)	73.1 (±3.9)
SeCys	80.5 (±3.2)	79.6 (±4.1)

### 3.4. Sorption Studies Utilizing Cation Exchanger Resin (IR-120)

Selenium studies relevant to previous sections reveal that  $ZrO_2$  and  $CeO_2$  have only sorption of inorganic selenium species whereas the sorption of Se(IV), Se(VI) and SeCys was performed by nZVI and nZVI- $ZrO_2$ . The different strategy was required for seleno-DL-methionine because studied sorbents did not show any sorption to this organoselenium species. Looking at the structure of organoselenium compounds, it can be said that amino groups in structure can add to basic feature to these compounds. In this context, these analyte species can give sorption with the sorbents with acidic property. Application of developed strategy was tested with strong cation exchanger resin (IR-120). The resin in H form is composed of polystyrene with sulphonic functional groups. The sorption behaviour of this sorbent was realized for Se (IV), Se(VI), SeCys and SeMet. Sorption results given in figure indicates that due to the cation exchanger property, for Se(IV) and Se(VI) did not retain on sorbent, in the case of SeMet and SeCys, the sorption was obtained from pH 2.0 to 8.0. At pH 8.0, maximum sorption was observed for both organoselenium species (Figure 3.27).

Desorption studies were continued with SeMet and SeCys because of high sorption results. Sorption parameters; SeMet or SeCys concentration:  $100.0 \mu\text{gL}^{-1}$ . pH: 8.0. Solution volume: 20.0 mL, shaking time: 30 min. amount of sorbent: 50.0 mg. temperature:  $25^\circ\text{C}$ . Desorption of SeMet and SeCys was performed by using 0.1 M HCl solution with 60 min shaking time. The results obtained from desorption for SeCys and SeMet are 86.4% ( $\pm 4.6$ ) ve 80.8% ( $\pm 3.7$ ), respectively.

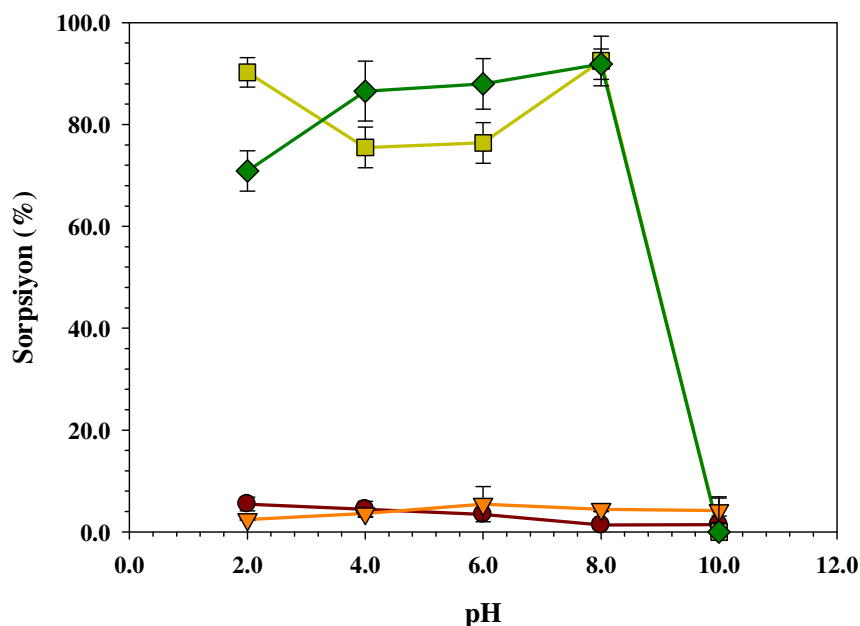


Figure 3.29. The effect of pH on the sorption of (●) Se(IV), (▼) Se(VI), (■)SeCys and (◆)SeMet with Amberlite IR-120 resin. (Sorption parameters; Se conc.: 100,0  $\mu\text{gL}^{-1}$ , shaking time: 30 min, amount of sorbent: 50.0 mg, temperature: 25 °C)

### 3.5. Sorption Studies $\text{CeO}_2$ and $\text{ZrO}_2$ Alginate Beads

In the column type sorption, 5.0-cm heights of glass pipettes were filled with ceria (or zirconia) entrapped in alginate matrix synthesized by three different methods as explained in Section 2.4.3. Standard solutions (50.0 mL) were passed through the columns in 5.0 mL portions with the help of a peristaltic pump at constant flow rate (1.0 mL/min). Selenium concentration in each fraction was determined by ICP-MS. Ceria (or zirconia) entrapped in calcium alginate beads prepared through Method A showed different behavior compared to bare ceria (or zirconia), on the sorption of Se(IV) and Se(VI). Sorption reached its maximum value at pH 2.0 and started to decrease with increasing pH (Figure 3.29). The reason for having different performances for column and batch type sorption studies can be ascribed to the entrapment of ceria (or zirconia) in the alginate matrix, which, therefore, results in the decrease of the possibility of interaction between the analyte species and the functional groups. The agglomeration of ceria (or zirconia) in the alginate matrix cannot be avoided and surface area of the functional groups is expected to reduce. When the solution passes through the column,

analyte species may not reach the interior of the alginate matrix and the sorption decreases. The other reason must be the insufficient interaction time for the analyte species with ceria (or zirconia) embedded in the matrix. When the solution pH is 2.0, the surface is protonated and the possibility of interaction between the analyte and the functional groups is increased. The sorption percentage can further be increased by decreasing the flow rate of the sample solution passed through the mini column.

In Method B, sodium alginate is mixed with Ca(II) ions and calcium alginate beads are formed through a cation exchange step. When these particles are mixed with Ce(III) (or Zr(IV)) solution, a similar cation exchange mechanism can be expected to occur between Ca(II) and Ce(III) or Zr(IV) ions with a low probability. Another possibility is the formation and more homogeneous distribution of ceria or zirconia on the surface of calcium alginate in a basic environment. Use of different strategies in the synthesis results in different sorption performances. The sorbent prepared through Method B demonstrates higher sorption efficiency compared to the sorbent prepared in Method A (Figure 3.30).

The preparation of ceria (or zirconia) through Method C is not similar to those of the other methods in a way that no calcium alginate is prepared at the intermediate stage. In this method, sodium alginate solution is added directly to Ce(III) or Zr(IV) solution dropwise. The beads formed are expected to contain more ceria (or zirconia). In addition, ceria or zirconia is more homogeneously distributed in the alginate matrix. The result of the improvement in the synthesis procedure can be seen in Figure 3.31. The sorbent prepared through Method C exhibits higher sorption percentages than the other sorbents towards Se(IV) and Se(VI) at a wider pH range.

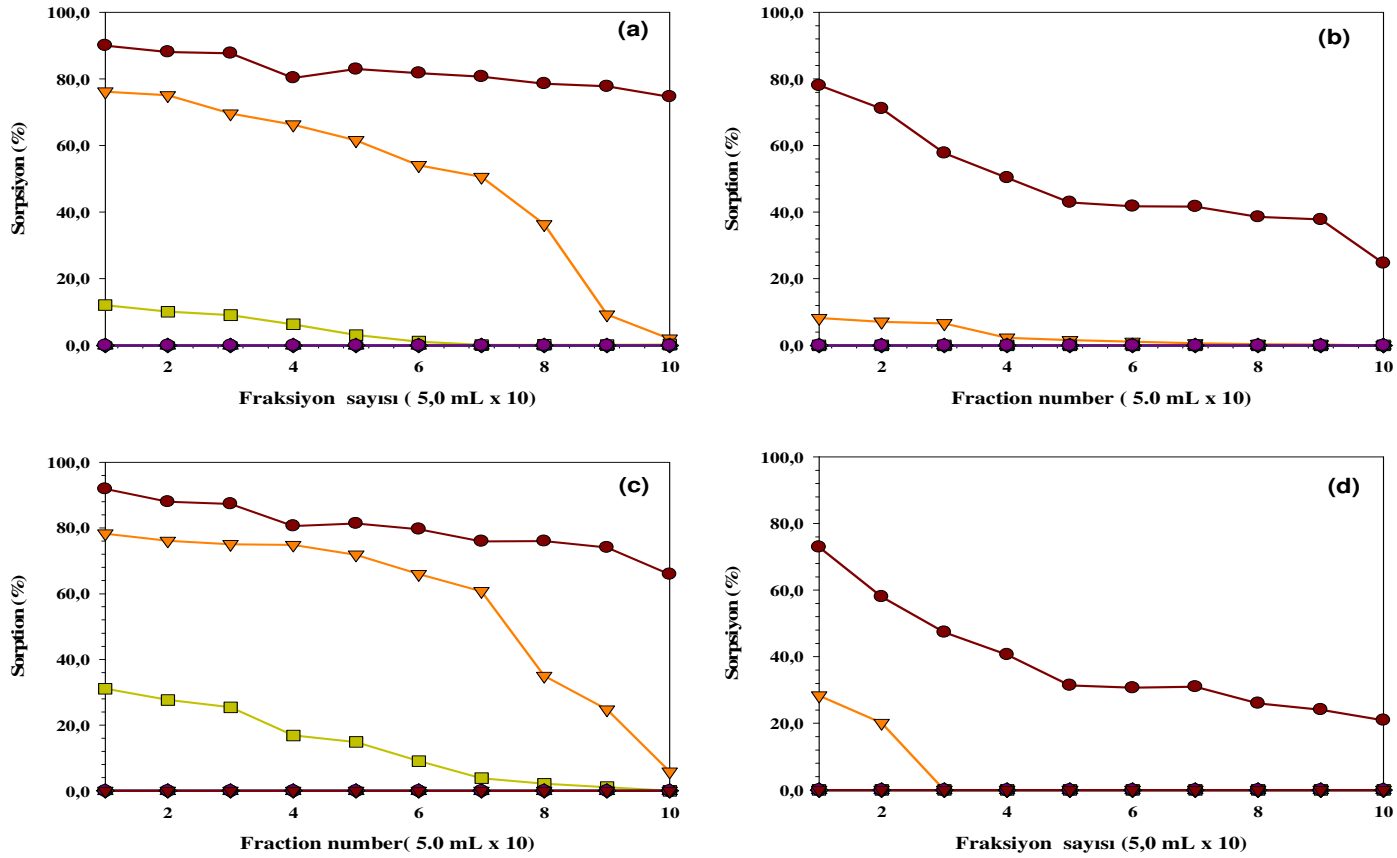


Figure 3.30. The effect of pH on (a) Se(IV) and (b) Se(VI) with CeO<sub>2</sub>-based-alginate sorbent and (c) Se(IV) and (d) Se(VI) with ZrO<sub>2</sub>-based-alginate sorbent obtained by Method A . pH 2.0 (●), pH 3.0 (▼), pH 4.0 (■), pH 5.0 (◆), pH 6.0(▲), pH 7.0 (●) pH 8.0 (●).

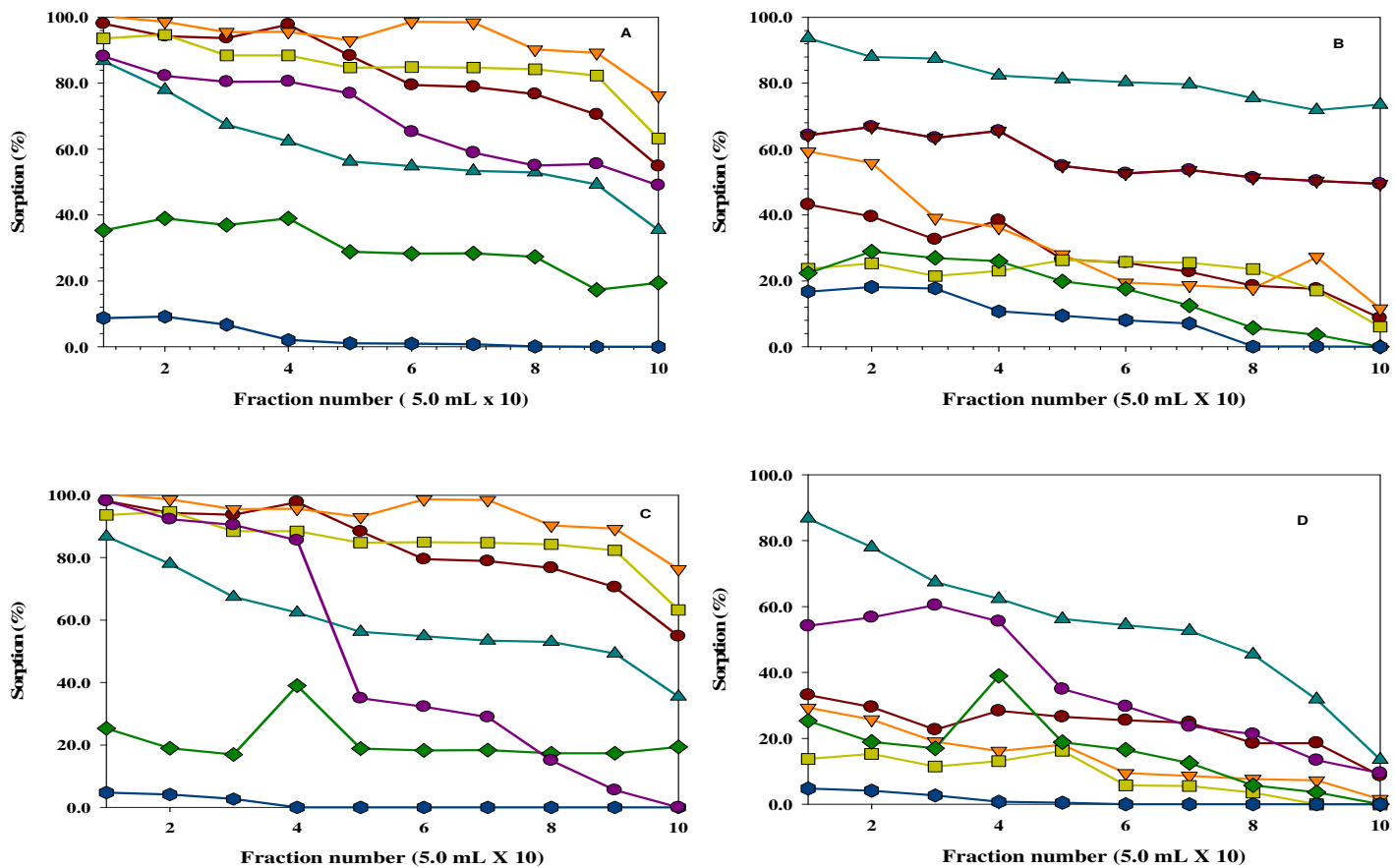


Figure 3.31. The effect of pH on (a) Se(IV) and (b) Se(VI) with CeO<sub>2</sub>-based-alginate sorbent and (c) Se(IV) and (d) Se(VI) with ZrO<sub>2</sub>-based-alginate sorbent obtained by Method B. pH 2.0 (●), pH 3.0 (▼), pH 4.0 (■), pH 5.0 (◆), pH 6.0 (▲), pH 7.0 (●) pH 8.0 (●).

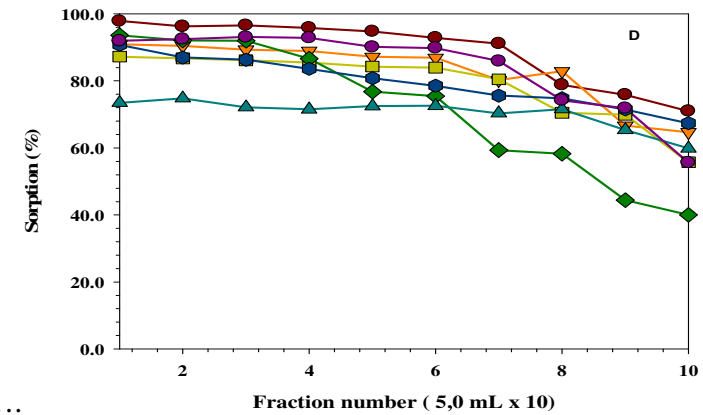
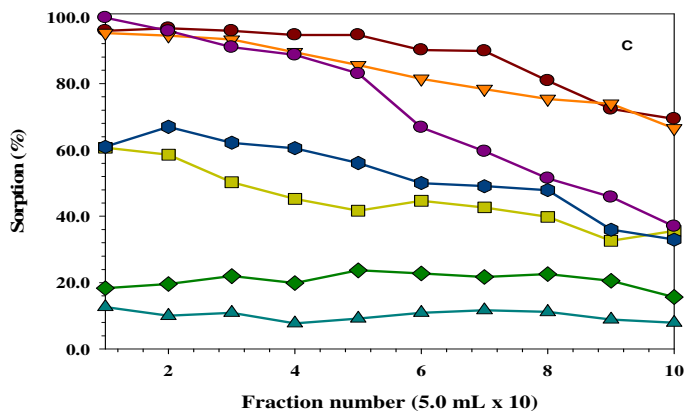
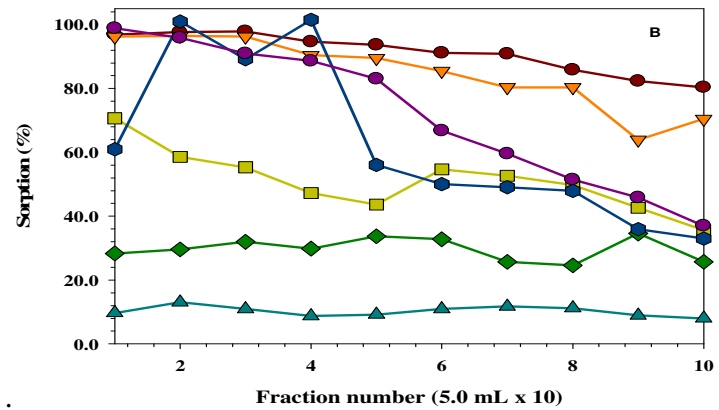
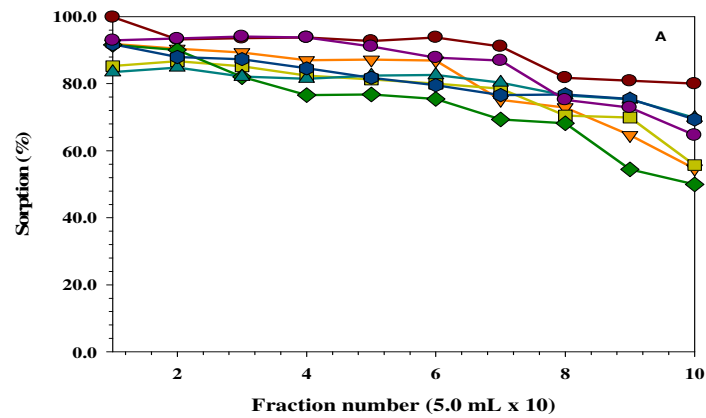


Figure 3.32. The effect of pH on (a) Se(IV) and (b) Se(VI) with CeO<sub>2</sub>-based-alginate sorbent and (c) Se(IV) and (d) Se(VI) with ZrO<sub>2</sub>-based-alginate sorbent obtained by Method B. pH 2.0 (●), pH 3.0 (▼), pH 4.0 (■), pH 5.0 (◆), pH 6.0 (▲), pH 7.0 (●) pH 8.0 (●).

## CHAPTER 4

### CONCLUSION

In this study, commercial and synthesized sorbents were used for the speciation of Se(IV), Se(VI), Seleno-L-Cystine and Seleno-L-Methionine prior to determination by atomic spectrometric techniques. Characterization of the sorbents was realized using SEM, XRD, TGA, and the results obtained have demonstrated the success of the synthesis procedure. Characterization studies were followed by the examination of the sorption performance of the commercial and the newly synthesized sorbents towards selenium species.

In the case of commercial cerium oxide and zirconium oxide, quantitative sorption (>95%) was obtained at pH 2.0 for both Se(IV) and Se(VI) species. On the other hand, both sorbents have also displayed higher than 95% sorption for Se(IV) at pH 8.0 while the sorption for Se(VI) was less than 10%. The commercial sorbents have shown slightly better results than the synthesized sorbents at pH 2.0 whereas the sorbents synthesized with sol-gel route have given better results at pH 8.0. Ceria and zirconia can be used in the speciation of inorganic selenium species. The validity of the method was checked via spike recovery experiments with different types of water (bottled-drinking, tap) and it was found that the method worked efficiently (> 90%) after the reduction of Se(VI) to Se(IV). Total selenium content was determined and Se(VI) was then calculated from the difference.

The other sorbents, namely, nZVI and nZVI-modified zirconia showed high sorption to both Se(IV) and Se(VI) in the pH range of 4.0-10.0; moreover, they sorbed seleno-L-cystine higher than 95% and seleno-L-methionine less than 10.0 % at pH 8.0. The results have shown that nZVI and nZVI-modified zirconia can be used in the speciation of organoselenium species. Also, commercial resin, Amberlite IR-120 can be used in the sorption of organoselenium species.

Finally, the novel alginate beads modified with cerium oxide and zirconium oxide have been shown to be efficient materials for column type sorption of inorganic selenium in waters.



## REFERENCES

- Ari U., Volkan M., Aras N.K. 1991. Determination of selenium in diet by Zeeman effect graphite furnace atomic absorption spectrometry for calculation of daily dietary intake. *J. Agric. Food Chem.* 39: 2180-2183.
- Bakir M.A., Yaseene T., Sarheel A., Othman I. 2004. The determination of selenium concentration in blood and tumour tissues of breast cancer patients in Syria using instrumental neutron activation analysis. 260: 607-612.
- Benemariya H., Robberecht H., Deelstra H. 1992. Zinc copper and selenium in milk and organs of cow and goat from Brundi, Africa. *The science of total environment.* 128: 83-98.
- Bezbaruaha A.N., Krajangpana S., Chisholmb B.J., Khana E., Bermudez J.J.E. 2008. Entrapment of iron nanoparticles in calcium alginate beads for groundwater remediation applications. *Journal of Hazardous Materials.* 166: 1339-1343.
- Biterna M., Arditoglou A., Tsikouras E., Voutsas D. 2007. Arsenate removal by zero valent iron: Batch and column tests. *Journal of Hazardous Materials.* 149: 548-552.
- Bortun A., Bortun M., Pardini J., Khainakov S.A., Garcí'a J.R. 2010. Synthesis and characterization of a mesoporous hydrous zirconium oxide used for arsenic removal from drinking water. *Material Research Bulletin.* 45: 142-148.
- Cabañero A.I., Madrid Y., Camara C. 2007. Mercury–selenium species ratio in representative fish samples and their bioaccessibility by an in vitro digestion method. *Biol. Trace Elem. Res.* 119: 195–211.
- Cao C.Y., Cui Z.M., Chen C.Q., Song W.G., Cai W. 2010. Ceria Hollow Nanospheres Produced by a Template-Free Microwave-Assisted Hydrothermal Method for Heavy Metal Ion Removal and Catalysis. *J. Phys. Chem. C.* 114: 9865-9870.
- Chand V., Prasad S. 2009. Trace determination and chemical speciation of selenium in environmental water samples using catalytic kinetic spectrophotometric method. *J. Hazard. Mat.* 165: 780-788.
- Chen L.P., Wang L. 2001. Characterization of a ca-alginate based ion-exchange resin and its applications in lead, copper, and zinc removal. *Separation Science and Technology.* 36: 16, 3617 — 3637.
- Cuvin-Aralar M.L., Furness R.W. 1991. Mercury and selenium interaction: a review. *Ecotoxicol. Environ. Saf.* 21: 348-364.
- Dauchy X., Gautier M.P., Astruc A., Astruc M. 1994. Analytical methods for the speciation of selenium compounds: a review. *Fresenius J. Anal. Chem.* 348: 792-805.

- Deng S., Zhijian L., Huang J., Yua G. 2010. Preparation, characterization and application of a Ce-Ti oxide adsorbent for enhanced removal of arsenate from water. *Journal of Hazardous Materials*.179: 1014-1021.
- Diaz J.P., Navarro M., Lopez H., Lopez M.C. 1997. Determination of selenium levels in dairy products and drinks by hydride generation atomic absorption spectrometry: correlation with daily dietary intake. *Food Addit. Contam.* 14: 109-114.
- Diaz-Alarcon J.P., Navarro-Alarcon M., Lopez-Ga de la Serrana H., Lopez-Martinez M.C. 1994. Determination of selenium in fresh fish from southeastern Spain for calculation of daily dietary intake. *J. Agric. Food Chem.* 42: 334-337.
- Duan J., Hu J. 2009. Speciation of selenomethionine and selenocystine using online micro-column containing Cu(II) loaded nanometer-sized Al<sub>2</sub>O<sub>3</sub> coupled with ICP-MS detection. *Talanta*. 79: 734-738
- Dumont E., Vanhaecke F., Cornelis R. 2006. Selenium speciation from food source to metabolites: a critical review. *Anal. Bioanal. Chem.* 385: 1304-23.
- Ellingsen D.G., Holland R.I., Thomassen Y., Landro-Olstad M., French W., Kjuus H. 1993. Mercury and selenium in workers previously exposed to mercury vapour at a chloroalkali plant. *Br. J. Ind. Med.* 50: 745-752.
- Escuderoa C., Fiol N., Villaescusa I., Bollinger J.C. 2009. Arsenic removal by a waste metal (hydr)oxide entrapped into calcium alginate beads. *Journal of Hazardous Materials*. 164: 533-541.
- Frost D.V. 1983. What do losses in selenium and arsenic bioavailability signify for health? *Sci. Total Environ.* 28: 455-466.
- Goessler W., Kuehnelt D., Schlagenhafen C., Kalcher K., Abegaz M., Irgolic K.J. 1997. Retention behavior of inorganic and organic selenium compounds on a silica-based strong-cation-exchange column with an inductively coupled plasma mass spectrometer as selenium-specific detector. *J. Chromatogr. A*.789: 233-245.
- Goldhaber S.B. 2003. Trace element assessment: essentially vs toxicity. *Regul. Toxicol. Pharmacol.* 38: 232-242
- Gondi F., Dauto G., Feher J., Bogye G., Alfthan G. 1992. Selenium in Hungary. The rock-soil-human system. *Biol. Trace Elem. Res.* 35: 299-306.
- Harwood J.J., Su W. 1997. Analysis of organic and inorganic selenium anions by ion chromatography-inductively coupled plasma atomic emission spectroscopy. *J. Chromatogr. A*. 788: 105-111.

- Hershey W., Oostdyk T.S., Keliher E.N. 1988. Determination of arsenic and selenium in environmental and agricultural samples by hydride generation atomic absorption spectrometry. *J. Assoc. Anal. Chem.* 71: 1090-1093.
- Ipolyi I., Stefánka Zs., Fodor P. 2001. Speciation of Se(IV) and the selenoamino acids by high-performance liquid chromatography–direct hydride generation–atomic fluorescence spectrometry. *Anal. Chim. Acta.* 435: 367-375.
- Izgi B., Gucer S., Jacimovic R. 2005. Determination of selenium in garlic (*Allium sativum*) and onion (*Allium cepa*) by electro thermal atomic absorption spectrometry. *Food chem.* 99: 630-637.
- Kápolna E., Shah M., Caruso J.A., Fodor P. 2007. Selenium speciation studies in Se-enriched chives (*Allium schoenoprasum*) by HPLC-ICP-MS. *Food chem.* 101: 1398-1406.
- Keshan Disease Research Group. 1979. Epidemiologic studies on the etiologic relationship of selenium and Keshan disease. *Chi. Med.* 92: 477-482.
- Kongwudthitia S., Prasertdama P., Silvestona P., Inoue M. 2003. Influence of synthesis conditions on the preparation of zirconia powder by the glycothermal method. *Ceramics International.* 29: 807–814
- Leggli C.V.S., Bohrer D., Noremberg S., Do Nascimento P.C., De Carvalho L.M., Vieira S.L., Reis R.N. 2009. Surfactant/oil/water system for the determination of selenium in eggs by graphitefurnace atomic absorption spectrometry. *Spectrochimica Acta Part B.* 64: 605-609
- Levander O.A., Burk R.F. 1994. *Selenium. In: Modern Nutrition in Health and Disease.* ed. Shils M.E., Olson J.A., Shike M. Philadelphia: Lea and Febiger : 242-251.
- Li, L., Fan, M., Brown, R.C., van Leeuwen, L. 2006. Synthesis, Properties, and Environmental Applications of Nanoscale Iron-Based Materials: A Review. *Critical Reviews in Environmental Science and Technology* 36:405-431.
- Li, X. and Zhang, W. 2006. Iron Nanoparticles: the Core-Shell Structure and Unique Properties for Ni(II) Sequestration. *Langmuir* 22:4638-4642.
- Li, X. and Zhang, W. 2007. Sequestration of Metal Cations with Zerovalent Iron Nanoparticles: A Study with High Resolution X-ray Photoelectron Spectroscopy (HR-XPS). *Journal of Physical Chemistry C* 111(19):6939-6946.
- Li, X., Brown, D.G., Zhang, W. 2007. Stabilization of biosolids with nanoscale zerovalent iron (nZVI). *Journal of Nanoparticle Research* 9:233-243.
- Lim S.F., Zheng Y.M., Zou S.W., Chen J.P. 2009. Removal of copper by calcium alginate encapsulated magnetic sorbent. *Chemical Engineering Journal.* 152: 509-513.

- Liu Q. 2009. Determination of ultra-trace amounts of inorganic selenium species in natural water by ion chromatography-inductively coupled plasma-mass spectrometry coupled with nano- $\text{Al}_2\text{O}_3$  solid phase extraction. *Cent. Eur. J. Chem.* 8(2): 326-330.
- Liu, Y., Choi, H., Dionysiou, D., Lowry, G.V. 2005a. Trichloroethene Hydrodechlorination in Water by Highly Disordered Monometallic Nanoiron. *Chemistry of Materials* 17:5315-5322.
- Liu, Y., Majetich, S.A., Tilton, R.D., Sholl, D.S., Lowry, G.V. 2005b. TCEDechlorination Rates, Pathways, and Efficiency of Nanoscale Iron Particles with Different Properties. *Environmental Science & Technology* 39:1338-1345.
- Macarovscha G.T., Bortoleto G.G., Cadore S. 2006. Silica modified with zirconium oxide for on-line determination of inorganic arsenic using a hydride generation-atomic absorption system. *Talanta*. 71: 1150-1154.
- Mai, H., Sun, L., Zhang, Y., Si, R., Feng, W., Zhang, H., Liu, H., Yan, C. 2005. Shape selective synthesis and oxygen storage behavior of ceria nanopolyhedra, nanorods and nanocubes. *Journal of Physical Chemistry B*. 109:24380-24385.
- Maleki N., Safavi A., Doroodmand M.M. 2005. Determination of selenium in water and soil by hydride generation atomic absorption spectrometry using solid reagents. *Talanta* 66: 858-862.
- Matos J.M.E., Júniora F.M.A., Cavalcanteb L.S., Santosb V., Júniora S.H., Lealc L.S.S. 2009. Reflux synthesis and hydrothermal processing of  $\text{ZrO}_2$  nanopowders at low temperature. *Material chemistry and physics*. 117: 455-459.
- Miekeley N., Pereira R.C., Casartelli E.A., Almedia A.C., Carvalho M.F.B. 2005. Inorganic speciation analysis of selenium by ion chromatography-inductively coupled plasma-mass spectrometry and its application to effluents from a petroleum refinery. *Spectrochimica Acta Part B*. 60: 633-641.
- Mondal K., Jegadeesen G., Lalvani S.B. 2004. Removal of Selenate by Fe and NiFe Nanosized Particles. *Ind. Eng. Chem. Res.* 43: 4922-4934.
- Najafi N.M., Seidi S., Alizadeh R., Tavakoli H. 2010. Inorganic selenium speciation in environmental samples using selective electrodeposition coupled with electrothermal atomic absorption spectrometry. *Spectrochimica Acta Part B* 65: 334-339.
- Navarro-Alarcon M., Lopez-Martinez M.C., 2000. Essentiality of selenium in human body: relationship with different diseases. *Sci. Total Environ.* 249: 347-371.
- Neve J., Henry M., Peretz A., Mareschi J.P. 1987. L'importance nutritionnelle du selenium. *Cah. Nut.r Diet.* 22: 145-162.

- Noubactep, C., Meinrath, G., Dietrich, P., Sauter, M., Merkel, B.J. 2005. „Testing the Suitability of Zerovalent Iron Materials for Reactive Walls. *Environmental Chemistry* 2:71-76.
- Nurmi, J.T., Tratnyek, P.G., Sarathy, G., Baer, D.R., Amonette, J.E., Pecher, K., Wang, C., Linehan, J.C., Matson, M.W., Penn, R.L., Driessen, M.D. 2005. Characterization and Properties of Metallic Iron Nanoparticles: Spectroscopy, Electrochemistry, and Kinetics. *Environmental Science & Technology* 39:1221, 1230.
- Ortuno J., Ros G., Periago M., Martinez C., Lopez G. 1996. Selenium bioavailability and methods of evaluation. *Food Sci. Technol. Int.* 2: 135-150.
- Ozturk N., Kavak D. 2008. Boron removal from aqueous solutions by batch adsorption on cerium oxide using full factorial design. *Desalination*. 223 : 106-112.
- Panigati M., Falciola L., Mussini P., Beretta G., Facino R.M. 2007. Determination of selenium in Italian rices by differential pulse cathodic stripping voltammetry. *Food Chem.* 105: 1091-1098.
- Pappa E., Pappas A., Surai P. 2006. Selenium content in selected foods from the Greek market and estimation of the daily intake. *Sci. Total Environ.* 372: 100–8.
- Pedersen G. A., Larsen E.H. 1997. Speciation of four selenium compounds using high performance liquid chromatography with on-line detection by inductively coupled plasma mass spectrometry or flame atomic absorption spectrometry. *Fresenius J. Anal. Chem.* 358: 591-598.
- Piticescu R.R., Monty C., Taloi D., Motoc A., Axinte S. 2001. Hydrothermal synthesis of zirconia nanomaterials. 21: 2057-2060
- Polatajko A., Jakubowski N., Szpunar J. 2006. State of the art report of selenium speciation in biological samples. *J. Anal. Atom Spectrom.* 21: 639-654.
- Pyrzynska K. 2008. Selenium speciation in enriched vegetables. *Food chemistry.* 114: 55-62.
- Recillas S., Colón J., Casals E., González E., Puentes V., Sánchez A., Font X. 2010. Chromium VI adsorption on cerium oxide nanoparticles and morphology changes during the process. *Journal of Hazardous Materials.* 184: 425-431.
- Sathyamurthy, S., Leonard, K.J., Dabestani, R.T., Paranthaman, M.P. 2005. Reverse micellar synthesis of cerium oxide nanoparticles. *Nanotechnology.* 16:1960-1964
- Saygi K.O., Melek E., Tüzen M., Soylak M. 2007. Speciation of selenium(IV) and selenium(VI) in environmental samples by the combination of graphite furnace atomic absorption spectrometric determination and solid phase extraction on Diaion HP-2MG. *Talanta* 71: 1375-1381.

- Seby F., Potin-Gautier M., Giffaut E., Borge G., Donard O.F.X. 2001. A critical review of thermodynamic data for selenium species at 25°C. *Chemical Geology*. 171: 173-194
- Shi K., Wang X., Guo Z., Wang S., Wu W. 2009. Se(IV) sorption on TiO<sub>2</sub>: Sorption kinetics and surface complexation modeling. *Colloid and Surface: Physicochem. Eng. Aspects*. 349: 90-95.
- Shunxing D.N. 2002. Separation and preconcentration of Se(IV)/Se(VI) species by selective adsorption onto nanometer-sized titanium dioxide and determination by graphite furnace atomic absorption spectrometry. *Anal. Bioanal. Chem.* 374: 1341-1345.
- Simonoff M., Simonoff G., ed. 1991. *Le sélénium et la vie*. Paris: Masson.
- Skoog D.A., Holler F.J. and Nieman T.A. 1998. *Principles of Instrumental Analysis*, Philadelphia: Saunders College Publishing.
- Srdić V.V., Omorjana P. 2005. Electrochemical performances of (La,Sr)CoO<sub>3</sub> cathode for zirconia-based solid oxide fuel cells. *Materials Science and Engineering B*. 116: 119-124
- Stripeikis J., Tudino M., Troccoli O., Wuilloud R., Olsina R., Martinez L. 2001. On-line copper and iron removal and selenium(VI) pre-reduction for the determination of total selenium by flow-injection hydride generation-inductively coupled plasma optical emission spectrometry. *Spectrochimica Acta Part B*. 56: 93-100.
- Su Y., Chen H., Gao Y., Li X., Hou X., Lv Y. 2008. A novel HPLC-UV/nano-TiO<sub>2</sub>-chemiluminescence system for the determination of selenocystine and selenomethionine. *Journal of Chromatography B*. 870: 216-221.
- Sun, Y., Li, X., Cao, J., Zhang, W., Wang, H.P. 2006. Characterization of zero-valent iron nanoparticles. *Advances in Colloid and Interface Science* 120:47-56.
- Suzuki T.M., Tanco M.L., Tanaka D.A., Pacheco M., Hideyuki T., Yokoyama T. 2001. Adsorption characteristics and removal of oxo-anions of arsenic and selenium on the porous polymers loaded with monoclinic hydrous zirconium oxide. *Separation science and technology*. 36: 1, 103-111.
- Tao Z., Yu-Xil G., Bail L., Yu-Feng L., Chun-Ying C., Gang W. 2008. Study of Selenium Speciation in Selenized Rice Using High-Performance Liquid Chromatography-Inductively Coupled Plasma Mass Spectrometer. *Chin. J. Anal. Chem.* 36: 206-210
- Valencia M.C., Nicolas E.A., Valley L.F. 1999. Speciation of selenium (IV) in natural waters by solid phase spectrophotometry. *Talanta* 49: 915-921.

- Vatansever S., Oksuzomer F., Koc S.N., Somer M., Deligoz H., Gurkaynak M.A. 2010. Fabrication of yttria stabilized zirconia nanoparticles by the reverse microemulsion method for SOFC applications. *Materials Science-Poland*. 18: 85-91.
- Vilano M., Padro A., Rubioa R., Raureta G. 1998. Organic and inorganic selenium speciation using high-performance liquid chromatography with UV irradiation and hydride generation quartz cell atomic absorption spectrometric detection. *J. Chromatogr. A*. 819: 211-220.
- Visual MINTEQ ver. 2.61.
- Wang, H., Zhu, J.J., Zhu, J.M., Liao, X.H., Xu, S., Ding, T., Chen, H.Y. 2002. Preparation of nanocrystalline ceria nanoparticles by sonochemical and microwave assisted heating methods. *Physical Chemistry Chemical Physics*. 4:3794-3799.
- Xiao H., Ai Z., Zhang L. 2009. Nonaqueous Sol-Gel Synthesized Hierarchical CeO<sub>2</sub> Nanocrystal Microspheres as Novel Adsorbents for Wastewater Treatment. *J. Phys. Chem. C*. 113: 16625-16630.
- Yeon K.H., Park H., Lee S.H., Park Y.M., Lee S.H., Iwamoto M. 2008. Zirconium mesostructures immobilized in calcium alginate for phosphate removal. *Korean J. Chem. Eng.* 25: 1040-1046.
- Yersel M., Erdem A., Eroğlu A.E., Shahwan T. 2005. Separation of trace antimony and arsenic prior to hydride generation atomic absorption spectrometric determination. *Analytica Chimica Acta* 534: 293–300.
- Zhao Q.X., Chen Y.W., Belzile N., Wang M. 2010. Low volume microwave digestion and direct determination of selenium in biological samples by hydride generation atomic fluorescence spectrometry. *Analytica Chimica Acta*. 665: 123–128.
- Zhang N., Fu N., Fang Z., Feng Y., Ke L. 2010. Simultaneous multi-channel hydride generation atomic fluorescence spectrometry determination of arsenic, bismuth, tellurium and selenium in tea leaves. *Food Chemistry*. 10.1016/j.foodchem.2010.07.033.
- Zhang L., Liu N., Yang L., Lin Q. 2009. Sorption behavior of nano-TiO<sub>2</sub> for the removal of selenium ions from aqueous solution. *J. Hazard. Mat.*, doi:10.1016/j.jhazmat.2009.05.098.
- Zhang Q., Li X., Shi H., Hongzhou, Yuan Z. 2010. Determination of trace selenium by differential pulse adsorptive stripping voltammetry at a bismuth film electrode. 55: 4717-4721.

Zhong L.S., Hu J.S., Cao A.M., Liu Q., Song W.G., Wan L.J. 2006. 3D Flowerlike Ceria Micro/Nanocomposite Structure and Its Application for Water Treatment and CO Removal. *Chem.Matter.* 19: 1648-1655.

Zhou, X.D., Huebner, W. and Anderson, H.U. 2002. Room temperature homogeneous nucleation synthesis and thermal stability of nanometer single crystal CeO<sub>2</sub>. *Applied Physics Letters.* 80:3814-3816.